universität wien

# DIPLOMARBEIT

Titel der Diplomarbeit

## Role of Histone Modifications in DNA Repair in *Candida albicans*

Verfasserin

Eva Stappler

angestrebter akademischer Grad

Magistra der Naturwissenschaften (Mag.rer.nat.)

Wien, 2011

| | |
|---|---|
| Studienkennzahl lt. Studienblatt: | A 490 |
| Studienrichtung lt. Studienblatt: | Diplomstudium Molekulare Biologie |
| Betreuer: | Ao. Univ.-Prof. Dipl.-Ing. Dr. Karl Kuchler |

# Summary

*Candida albicans* (*Ca*), an important human fungal pathogen, especially for immunocompromised patients, shows several distinct growth morphologies including yeast, pseudohyphal or true hyphae forms. Filamentation is considered a major virulence trait, since morphological transition from yeast to hyphae has been associated with *Ca* virulence. Various environmental or host stimuli can induce filamentous growth. For instance, treatment of *Ca* with genotoxic agents or depletion of components involved in the DNA damage response can trigger pseudohyphal growth. In the yeast *Saccharomyces cerevisiae,* the histone acetyltransferases Hat1, which forms a complex with the subunit Hat2, and Rtt109, which also interacts with Asf1, are implicated in DNA damage repair. We therefore analyzed the function of Hat1/Hat2 and Rtt109 in *Ca.* To investigate the function of *Ca*Hat1 and *Ca*Hat2, rabbit polyclonal antibodies were raised. The C-terminal region of Hat1 and Hat2, respectively, were expressed as soluble GST-fusion proteins, purified and used as antigens.

Moreover, to investigate the subcellular localization of Hat2, a YFP-tagged Hat2 fusion protein was constructed and integrated into the *Ca* genome. The functionality of Hat2-YFP was verified by testing the sensitivity to DNA-damaging agents. In the presence of Hat1, Hat2-YFP was mainly localized in the nucleus, whereas in a *hat1*Δ/Δ background the nuclear localization was lost. Treatment with DNA-damaging agent MMS led to an increase of the signal intensity in the nucleus.

Homozygous deletion of *RTT109* resulted in a hyperfilamentation phenotype, similar to what has been observed for *hat1*Δ/Δ as well as *hat2*Δ/Δ strains. *rtt109*Δ/Δ cells showed wrinkled colony morphology and pseudohyphal growth under yeast-promoting conditions. Furthermore, they were hypersensitive to DNA damaging agents.

A homozygous *asf1*Δ/Δ strain could not be obtained, suggesting that *ASF1* is essential in *Ca*. Placing *ASF1* under a conditional promoter was successful for the first allele, but the second allele could not be deleted.

Furthermore, various histone H4 mutants were constructed to study the effect of lysine acetylation. Mutations of lysine residues should mimic the acetylated or unacetylated state of Hat1 target residues. For this purpose, all but one histone H4 copies were deleted and the mutated H4 variant was integrated. A histone H4 variant mimicking the acetylated state of H4 was also introduced into the *hat1*Δ/Δ strain to see, if the *hat1*Δ/Δ phenotype could be rescued. Even when the acetylated state of both Hat1 acetylation sites was mimicked, cells still showed the *hat1*Δ/Δ phenotype of hypersensitivity to DNA damaging agents and filamentous growth.

# Zusammenfassung

*Candida albicans* (*Ca*), der häufigste human-pathogene Pilz, besonders bei immungeschwächte Patienten, zeigt mehrere unterschiedliche Wachstumsmorphologien, wie Hefe, Pseudohyphen und echte Hyphen. Filamentierung gilt als wichtiges Virulenzmerkmal, da der Wechsel zwischen Hefe- und Hyphenform mit Virulenz assoziiert ist. Verschiedene Umwelt- oder Wirtsstimuli können filamentöses Wachstum induzieren. Wachstum als Pseudohyphen kann zum Beispiel durch Behandlung mit genotoxischen Substanzen oder Depletion von Komponenten, die in die Antwort auf DNA-Schäden involviert sind, ausgelöst werden. In der Hefe *Saccharomyces cerevisiae* sind die Histonacetyltransferasen Hat1, die mit der Untereinheit Hat2 einen Komplex bildet, und Rtt109, die mit Asf1 interagiert, in die Reparatur von DNA-Schäden involviert. Daher haben wir die Rolle von Hat1/Hat2 und Rtt109 in *Ca* analysiert. Um die Funktion von *Ca*Hat1 und *Ca*Hat2 zu untersuchen wurden polyklonale Antikörper in Kaninchen produziert. Die C-terminale Region von Hat1 bzw. Hat2 wurde als lösliches GST-Fusionsprotein expremiert, aufgereinigt und als Antigen verwendet.

Weiters, um die subzelluläre Lokalisierung von Hat2 zu untersuchen, wurde ein YFP-markiertes Hat2 Fusionsprotein konstruiert und in das *Candida albicans* Genom integriert. Durch Testen der Sensitivität auf DNA-schädigende Substanzen wurde die Funktionalität von Hat2-YFP verifiziert. In der Anwesenheit von Hat1 ist Hat2-YFP hauptsächlich im Kern lokalisiert, wohingegen die Kernlokalisierung in einem *hat1*Δ/Δ Hintergrund verloren geht. Behandlung mit der DNA-schädigenden Substanz Methylmethansulfonat führte zu einer Steigerung der Signalintensität im Kern.

Deletion von *RTT109* führte zu Hyperfilamentierung, ähnlich zu dem, was schon in *hat1*Δ/Δ und *hat2*Δ/Δ Stämmen beobachtet wurde. *rtt109*Δ/Δ Zellen zeigten eine runzelige Koloniemorphologie und wuchsen als Pseudohyphen unter Bedingungen, die die Hefeform begünstigen. Außerdem waren sie hypersensitiv auf DNA-schädigende Substanzen.

Es war uns nicht möglich einen *asf1*Δ/Δ Stamm zu produzieren. Daher ist anzunehmen, dass *ASF1* in *Ca* essentiell ist. Ein Allel von *ASF1* konnte unter einen konditionellen Promotor gestellt werden, allerdings war es nicht möglich das zweite Allel zu deletieren.

Weiters wurden einige Histone H4 Mutanten konstruiert. Mutationen von Lysinen sollten die acetylierte oder unacetylierte Form von Hat1 Substraten nachahmen. Dazu wurden alle bis auf eine Kopie von Histon H4 deletiert und eine mutierte H4 Variante integriert. Eine Histon H4 Variante, die die acetylierte Form von H4 nachahmt, wurde auch in den *hat1*Δ/Δ Stamm integriert, um zu sehen, ob der *hat1*Δ/Δ Phänotyp wieder umgekehrt werden kann. Leider zeigten die Zellen, auch wenn die acetylierte Form von beiden Hat1 Acetylierungsstellen nachgeahmt wurde, weiter den *hat1*Δ/Δ Phänotyp von Hypersensitivität auf DNA-schädigende Substanzen und filamentöses Wachstum.

# 1. Introduction

## 1.1. *Candida albicans*

Several C*andida* species are normally harmless commensal colonizers of most human mucosal layers. They exist as colonizers as part of the microbiological flora in the gastrointestinal tract, the genitourinary tract and to a lesser extent on the skin. They can cause superficial, non-life threatening infections at these sites. About 75% of women suffer from vaginal infections caused by *Candida* species at least once in their life. In 85 to 90% the causative agent for those infections is *Candida albicans* (Fidel, 2007). Furthermore, depending on the immune status of the host, *Candida* can invade and colonize host tissue. Thus, in immunocompromised patients, for example due to cancer chemotherapy, HIV infection or immunosuppression after organ transplantation, *Candida* can also cause systemic infections.

There are over 200 *Candida* species but only few of them are of medical importance. Interestingly, 90% of invasive infections due to *Candida* species are attributed to *C. albicans*, *C. glabrata*, *C. parapsilosis*, *C. tropicalis* and *C. krusei* (Pfaller and Diekema, 2007). Furthermore, *Candida* species are the fourth-most common cause for nosocomial blood-stream infections in the United States with a mortality rate of 40% (Pfaller and Diekema, 2007). With the increased prevalence of immunosuppressive therapies and the use of broad-spectrum antibiotics incidences of infection have risen (Pfaller and Diekema, 2004).

The most frequent causative agent for candidasis is *Candida albicans*. It is rarely isolated from the environment and is therefore considered to be obligatorily associated with mammalian hosts. Although *C. albicans* is a diploid organism without a known haplophase, mating has been observed (Hull *et al.*, 2000; Magee and Magee, 2000). It is regulated by transcription factors encoded at the mating type locus (MTL). Only cells homozygous at the MTL are able to undergo phenotypic switching from white to opaque cells which are the mating competent form of *C. albicans*. After mating the resulting cells can remain tetraploid or return to the diploid state by non-meiotic chromosome loss (Bennett and Johnson, 2003).

### 1.1.1. Morphology of *Candida albicans*

*Candida albicans* can grow in three distinct morphological forms: yeast, pseudohyphae and true hyphae (Figure 1). Yeast form cells are ellipsoid and appear similar to *Saccharomyces cerevisiae* cells. They divide by budding and separate easily from each other (Berman and Sudbery, 2002). True hyphae have parallel sides along their entire length and no constrictions between cells. The shape of pseudohyphae can vary enormously, ranging from cells resembling yeast cells with elongated buds to cells with the length of hyphae. Pseudohyphal cells remain attached to each other after completion of the cell cycle. The cells cycle in a unipolar pattern of budding and therefore grow in a highly branched pattern. Pseudohyphae have a width greater than the one of true hyphae and have constrictions at every septal junction (Sudbery *et al.*, 2004).

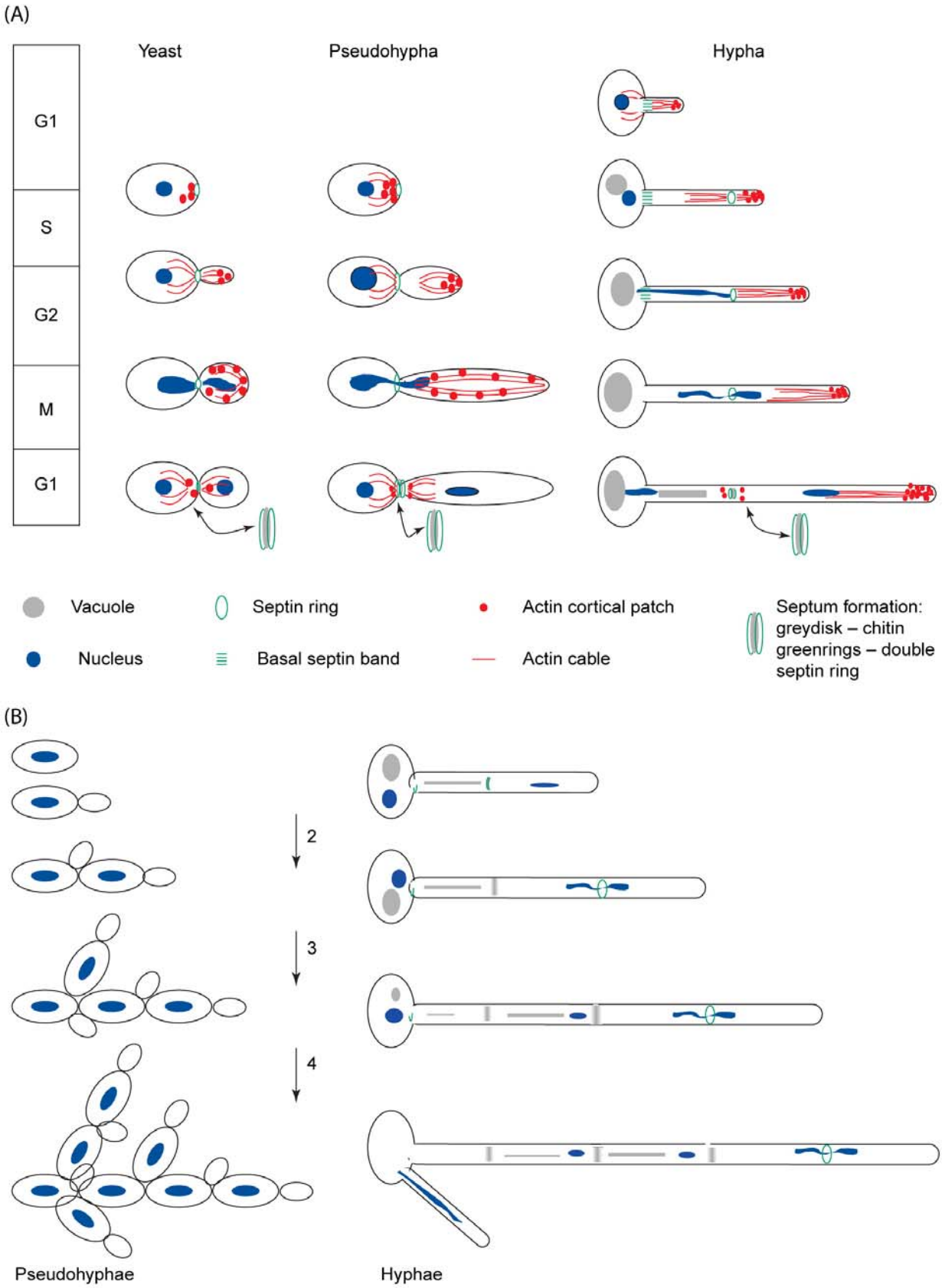


**Figure 1: The three distinct morphological forms of *Candida albicans*.** (A) Cell cycle of the yeast form and the first cell cycle of hyphae and pseudohyphae induced from unbudded yeast cells. (B) Pseudohyphae form a highly branched structure while the branching pattern of true hyphae is less regular. Adapted from Sudbery et al., 2004.

Switching from one growth form to another can be induced by several environmental stimuli. A range of conditions that more or less mimic certain host conditions like serum, neutral pH, hypoxia, higher temperature, certain amino acids and sugars, like N-acetylglucosamine (GlcNAc), or some synthetic growth media can trigger filamentous growth (Ernst, 2000; Shepherd *et al.*, 1980). Furthermore filamentous growth can be induced by perturbations of cell-cycle progression. For example, treatment with the DNA-replication inhibitor hydroxyurea causes filamentous growth (Bachewich *et al.*, 2005; Shi *et al.*, 2007). In addition, UV-radiation and the DNA-alkylating agent methyl methane sulfonate (MMS) have a similar effect. Thus, DNA replication stress, as well as DNA damage causes *Candida albicans* to switch to filamentous growth.

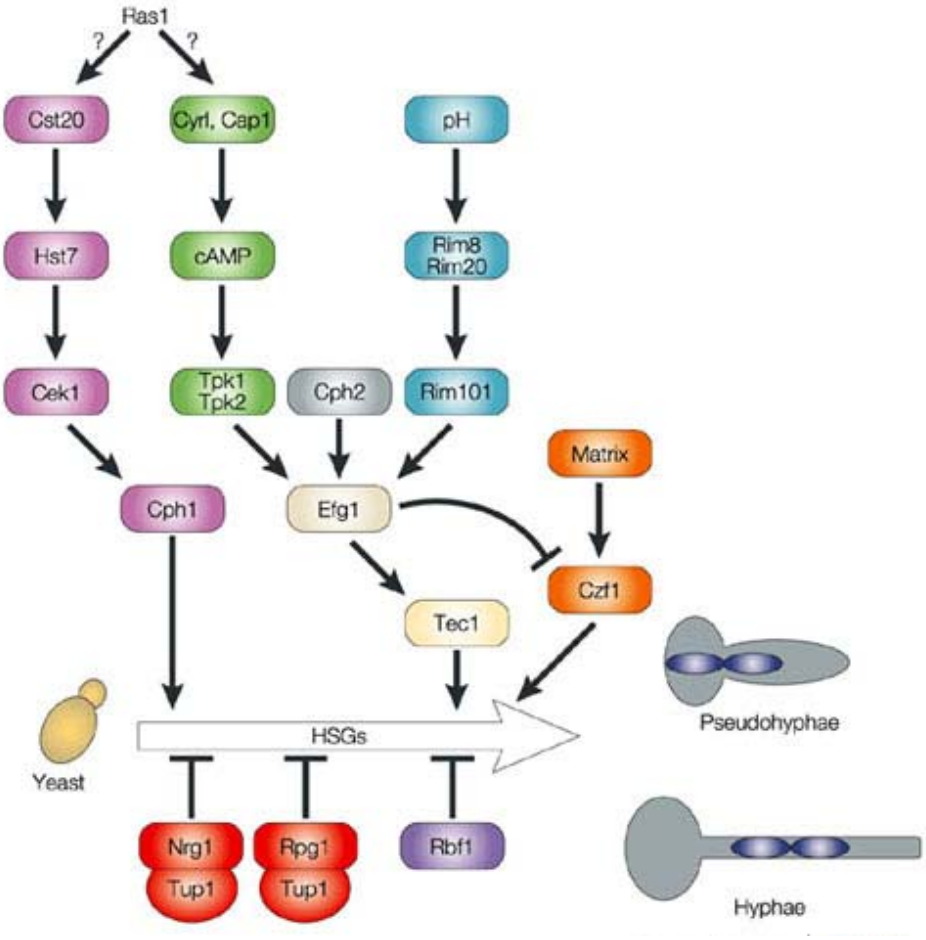


**Figure 2: Several signaling pathways regulate the yeast-hyphae transition.** Adapted from Berman and Sudbery, 2002.

Many positive and negative regulators of filamentous growth have been identified by now. Signals are transmitted by several conserved signaling pathways (Figure 2). A very important role plays the cAMP-PKA pathway, which includes the adenylate cyclase Cyr1, cAMP-dependent protein kinases Tpk1 and Tpk2 and the transcription factor Efg1. Cells with defects in this pathway fail to grow in the hyphal form. Negative regulators of

filamentous growth include Tup1, Rfg1, Nrg1 and Rbf1. Deletion of these repressors leads to constitutive filamentous growth even under yeast promoting conditions (Biswas *et al.*, 2007; Liu, 2001). Other pathways regulating filamentous growth include the mitogen-acitvated protein kinase (MAPK) pathway, the Rim101 pathway induced by alkaline pH, and the HOG MAPK pathway, in response to osmostress (Biswas *et al.*, 2007; Liu, 2001).
The ability of *Candida albicans* to switch between different growth forms seems to be important for pathogenicity. Notably, cells that are locked in either yeast or the hyphal growth form show decreased virulence (Gow *et al.*, 2002; Sudbery *et al.*, 2004).

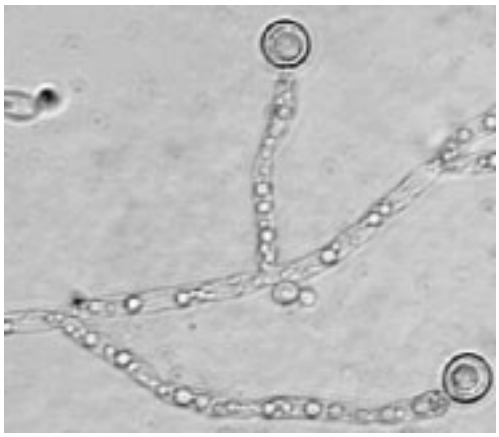

**Figure 3: *Candida albicans* chlamydospores.** Adapted from Staib and Morschhauser, 2007.

Chlamydospores are another growth form of *Candida albicans* (Figure 3). They are thick-walled, round cells that form at the end of branched filaments or suspensor cells in environments that are hypoxic, varying temperature and nutrients (Berman and Sudbery, 2002; Whiteway and Bachewich, 2007). The biological function of these chlamydospores is unknown, although they have been proposed to allow survival in harsh environments. The ability to form chlamydospores has served as an important diagnostic tool for the identification of *Candida albicans* for a long time (Staib and Morschhauser, 2007; Whiteway and Bachewich, 2007).

## 1.2. Chromatin

In eukaryotic cells, DNA is packaged and condensed into the nucleus in the form of chromatin. The basic unit of chromatin is the nucleosome. It consists of 147 base pairs (bp) of DNA wrapped 1.7 times around an octamer complex of histone proteins containing two copies of each of the four core histones (Figure 4 (A)). Two histone H3 and histone H4 proteins form a heterotetramer. Together with two heterodimers of H2A and H2B they constitute the histone octamer. Neighboring nucleosomes are connected by 10 to 80 bp of so called linker DNA. Histone H1 is known as the linker histone, since it binds to the linker DNA between two nucleosomes (Figure 4 (B)). In contrast to the four core histones, histone H1 is not essential for viability in *Saccharomyces cerevisiae* (He and Lehming, 2003), although in mice and *Drosophila* severe depletion of histone H1 is fatal (Fan *et al.*, 2003; Lu *et al.*, 2009).

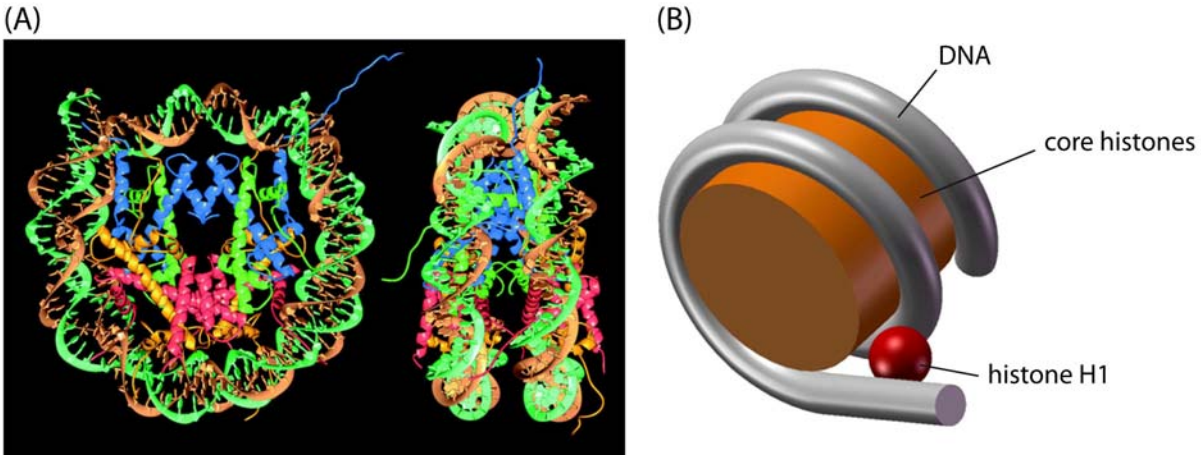


**Figure 4: Nucleosomes** (A) DNA wrapped around the histone octamer. Histone H3 is depicted in blue, H4 in green, H2A in yellow and H2B in red. Adapted from Luger et al., 1997. (B) Histone H1 binds to the nucleosome and the linker DNA. Adapted from Happel and Doenecke, 2009.

The nucleosomes form a “beads-on-a-string” fibre of about 11nm in diameter, with nucleosomes as beads and the DNA linking them together as the string. Nucleosomes are packaged further into so-called 30nm chromatin fibres which are stabilized by binding of histone H1 (Figure 5).

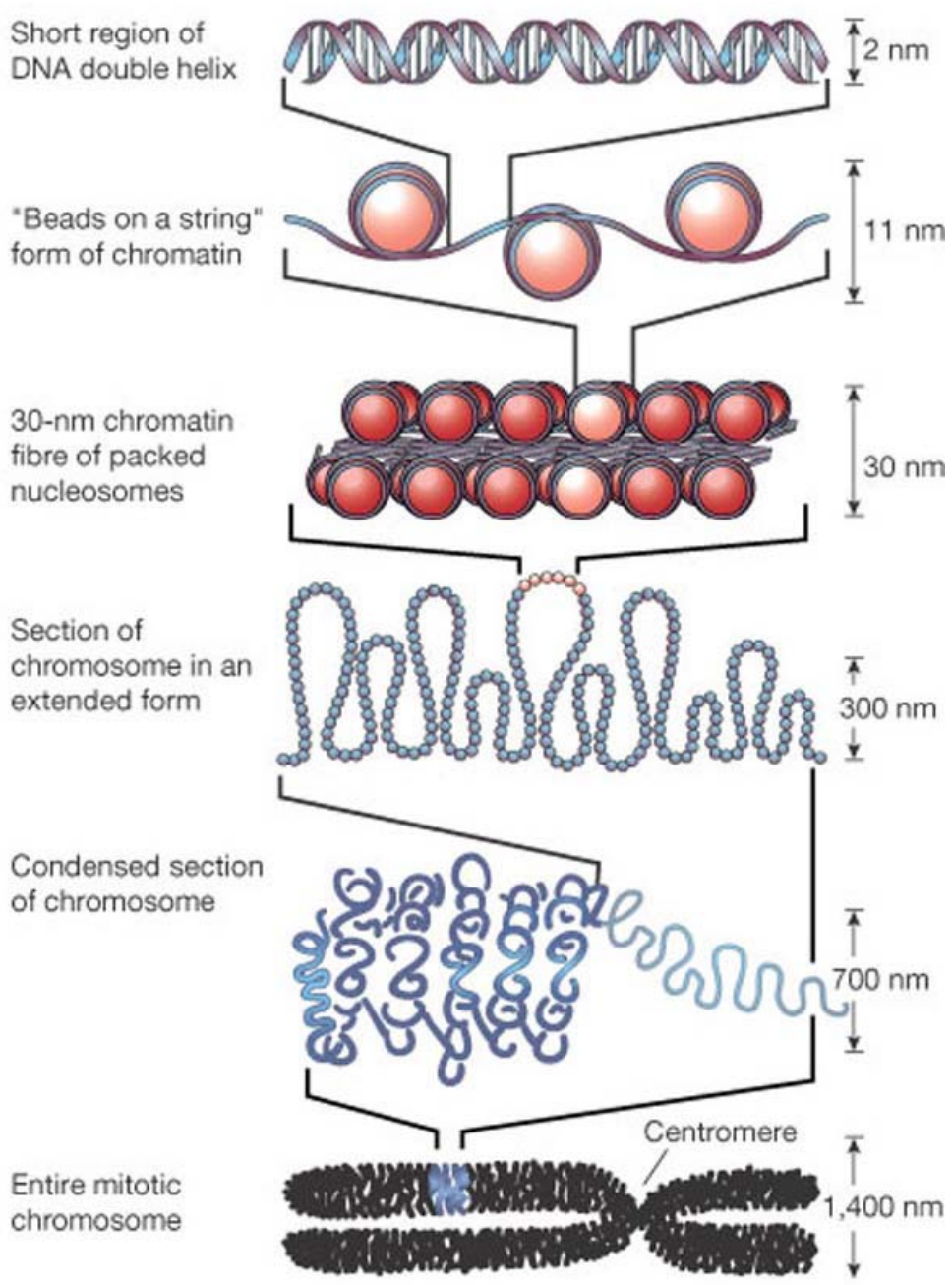


**Figure 5: Chromatin organization.** The smallest unit in chromatin is the nucleosome in which DNA is wrapped twice around a histone octamer. Nucleosomes are linked together by short stretches of DNA. They are packed into 30nm fibres which are further folded into higher order structures. Adapted from Felsenfeld and Groudine, 2003.

Core histones are among the most highly conserved eukaryotic proteins known. Histone equivalent proteins have even been found in some Archeabacteria (Sandman *et al.*, 1998). Originally, it was thought that the main purpose of histones was compacting DNA to fit into the nucleus. Today, it is known that histones play fundamentally important roles. Nucleosomes compact the genome. However, in doing so, also restrict access of other proteins to the DNA and thus gene promoters and therefore are general repressors of transcription (Grunstein, 1990).

Core histones have a structured globular domain and highly basic flexible tails. The globular domain interacts with other histones and the DNA wrapped around it, while the unstructured N-terminal tails extend outward from the nucleosome. Each tail is the substrate for several post-translational modifications, which can alter chromatin structure, compaction and accessibility.

Chromatin can be broadly divided into two categories depending on its condensation state. Heterochromatic regions are highly condensed regions that stay condensed throughout the cell cycle and are transcriptionally silent. Lesser condensed regions are called euchromatin. The majority of actively expressed genes is located there. In addition to hetero- and euchromatin, there are several other chromatin domains displaying distinctive chromatin structures, including centromers, Hda1-affected subtelomeric (HAST) domains and Htz1-activated domains (HAZDs) (Figure 6). Each chromosomal domain is characterized by a typical set of distinct histone modifications (Millar and Grunstein, 2006).

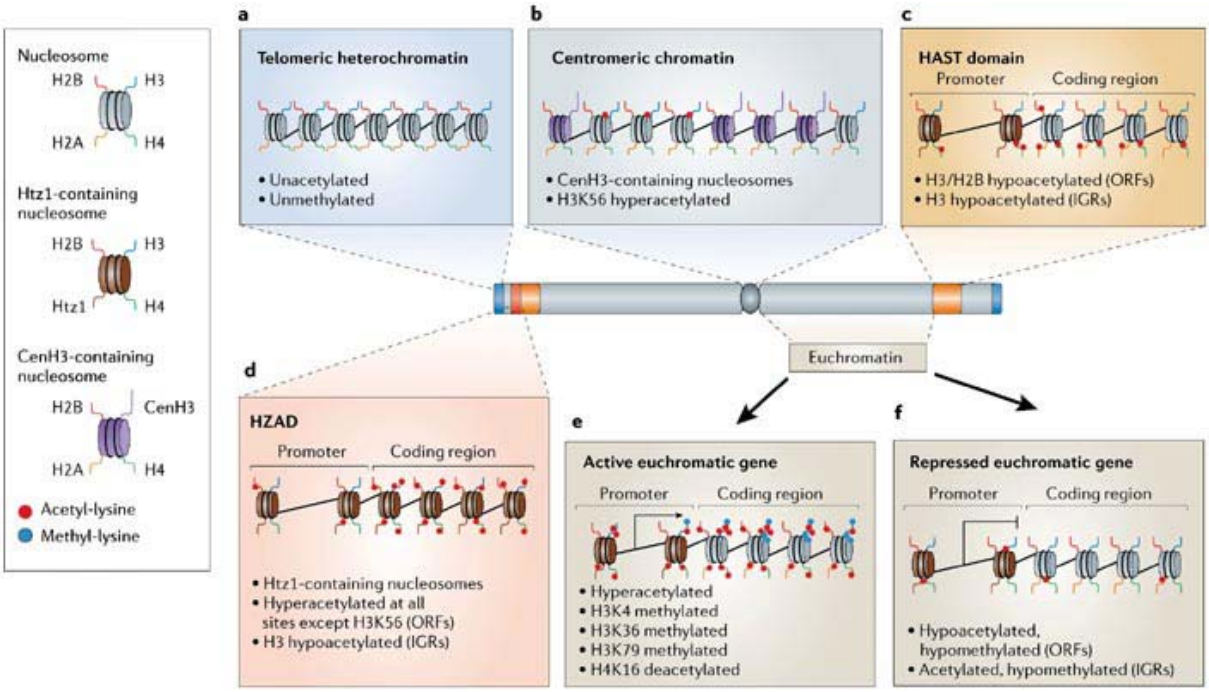


**Figure 6: Chromatin domains of a *Saccharomyces cerevisiae* chromosome:** (a) Telomeric heterochromatin is unacetylated and unmethylated. (b) Centromeric chromatin is hyperacetylated on H3K56. Centromeric nucleosomes contain the histone variant CenH3. (c) In Hda1-affected subtelomeric (HAST) domains histones H3 and H2A are hypoacetylated at open reading frames (ORFs) and histone H3 also at intergenic regions (IGRs). (d) In Htz1-activated domains (HZADs), the H2A variant Htz1 is highly enriched in promoter and coding regions. In coding regions, H3K56 is hyperacetylated, while at promoters histone H3 is hypoacetylated. (e) Active euchromatic genes are methylated at H3K4, H3K36 and H3K79. The 5' end is hyperacetylated, but not on H4K16. (f) Repressed euchromatic genes are hypoacetylated and hypomethylated. Their promoters are often more acetylated than the coding regions. Adapted from Millar and Grunstein, 2006.

Even within euchromatin, different features, such as promoters and the coding sequences of genes, have different patterns of histone modifications. Hence, genes can be divided into groups based on their acetylation pattern (Millar and Grunstein, 2006).

Two classes of enzymes are able to modify chromatin structure: the histone modifiers and the ATP-dependent remodelers. Post-translational histone modifications by modifiers can lead to an altered interaction with DNA and other histones changing the chromatin structure. ATP-dependent remodelers use the energy of ATP hydrolysis to move nucleosomes along the DNA, to exchange histones or insert other histone variants (Escargueil *et al.*, 2008).

## 1.3. Histone Modifications

Histones are substrates for at least 8 types of known post-translational modifications: acetylation, methylation, phosphorylation, ubiquitylation, sumoylation, ADP ribosylation, deimination and proline isomerization (Table 1).

**Table 1: Different classes of modifications identified on histones.** The functions associated with each modification are shown. Adapted from Kouzarides, 2007.

| Chromatin Modifications | Residues Modified | Functions Regulated |
|---|---|---|
| Acetylation | **K**-ac | Transcription, Repair, Replication, Condensation |
| Methylation (lysines) | **K**-me1 **K**-me2 **K**-me3 | Transcription, Repair |
| Methylation (arginines) | **R**-me1 **R**-me2a **R**-me2s | Transcription |
| Phosphorylation | **S**-ph **T**-ph | Transcription, Repair, Condensation |
| Ubiquitylation | **K**-ub | Transcription, Repair |
| Sumoylation | **K**-su | Transcription |
| ADP ribosylation | **E**-ar | Transcription |
| Deimination | **R > Cit** | Transcription |
| Proline Isomerization | **P-cis > P-trans** | Transcription |

Over 60 different residues of histone proteins are known to be modified (Table 2). Most modifications are located on the N-terminal tails of histones, but some can also be found on the globular core domain. Of course, not all modifications are present at the same histone at the same time, rather a combination of some of the possible modifications will determine the function. This concept is referred to as the histone code (Jenuwein and Allis, 2001; Strahl and Allis, 2000). Although the histone code has been widely accepted in the last decade, it is now heavily disputed. Histone modifications may be only one signal in a signal transduction pathway or regulate DNA accessibility (Henikoff and Shilatifard, 2011).

**Table 2: Modified histone residues.** h.s.: *Homo sapiens*; s.c.: *Saccharomyces cerevisiae*; NI: modification reported but residues not identified. Adapted from Escargueil et al., 2008.

| Histones | Acetylated residues | Methylated residues | Ubiquitylated residues | Phosphorylated residues | Sumoylated residues | Isomerized prolines |
|---|---|---|---|---|---|---|
| H2A | K5 | – | K119 | S1, T120 | K126 (s.c.) | – |
| H2AX | – | – | – | T136, S139 (h.s.) | – | – |
| H2B | K5, K12, K15, K20 | – | K120 | S14 | K6, K7, K16, K17 (s.c.) | – |
| H3 | K9, K14, K18, K23, K27, K56 | R2, K4, R8, K9, R17, R26, K27, K36, K79 | NI | T3, S10, T11, S28 | NI | P30, P38 |
| H4 | K5, K8, K12, K16, K91 (Ye *et al.*, 2005) | | NI | S1 | K5, K8, K12, K16, K20 (s.c.) | – |

Histone modifications function by two mechanisms. They alter the interaction between histones and DNA, thereby changing chromatin structure and they regulate recruitment of other proteins to the nucleosome. These proteins carry enzymatic activities which can further modify histones or recruit proteins involved in transcription, replication or DNA repair (Kouzarides, 2007).

### 1.3.1. Acetylation

Histone acetylation is almost always associated with transcriptionally active regions of chromatin. Histone acetyltransferases (HATs) enzymatically transfer an acetyl group from acetyl-CoA to the amino-group of a lysine residue. Most HATs acetylate more than one lysine but some specificity has been observed. Acetylation of lysine neutralizes its positive charge, thereby weakening its interaction with negatively charged DNA and making the DNA more accessible for other proteins (Woodcock and Ghosh, 2010).

There exist three main families of HATs: the GNAT-superfamily, including Gcn5, PCAF, Hat1, Elp3 and Hpa2, the MYST-family, named after its founding members MOZ, Ybf2/Sas3, Sas2, and Tip60, and CBP/p300 (Kouzarides, 2007; Sterner and Berger, 2000). Furthermore, HATs have been divided into two categories: type A and type B HATs. Type A HATs are localized in the nucleus and acetylate histones within chromatin. Type B HATs are found in the cytoplasmic fraction of cells and are able to acetylate free but not nucleosomal histones. They are believed to acetylate newly synthesized histones before their transport into the nucleus (Brownell and Allis, 1996; Garcea and Alberts, 1980).

As most histone modifications, acetylation is a reversible process. Deacetylation of histones is carried out by histone deacetylases (HDACs). There are three families of HDACs: class I and class II histone deacetylases and class III NAD-dependent enzymes of the Sir family.

They are not specific to certain lysine residues, although some HDACs show specificity towards certain histones (Kouzarides, 2007). HDACs often are found in repressive chromatin complexes and are involved in several signaling pathways (Kouzarides, 2007). They are not only involved in transcriptional regulation, but also in DNA replication, repair and heterochromatin formation (Kurdistani and Grunstein, 2003).

### 1.3.2. Methylation

Histones can be methylated on lysine and arginine residues. Each lysine can be mono-, di- or trimethylated, arginine can be mono- or dimetyhlated (symmetric or asymmetric). Lysine methyltransferases are usually very specific and modify only one specific lysine residue. Lysine methylation is implicated in both activation and repression of transcription depending on the modified residue. H3K4, H3K36 and H3K79 methylation is connected to activation of transcription, while H3K9, H3K27 and H4K20 methylation is implicated in repression of transcription (Kouzarides, 2007).

For a long time histone methylation was considered as a permanent mark until the first histone demethylase *LSD1* (lysine-specific demetylase 1) was discovered (Shi *et al.*, 2004). Specificities of histone demethylases are influenced by other proteins with which they form complexes, but also depends on the methylation state (Kouzarides, 2007; Shi and Whetstine, 2007).

Finally, the methylation of arginine residues, like lysine methylation, can activate or repress transcription depending on the modified residues. Reversal of arginine methylation can either be carried out by demethylases or methylarginine can be converted to citrulline by deiminases (Chang *et al.*, 2007; Cuthbert *et al.*, 2004; Kouzarides, 2007).

### 1.3.3. Phosphorylation

Histone phosphorylation plays an important role in the chromatin condensation and cell cycle progression. Furthermore, phosphorylation of histone H2A in budding yeast and H2AX in mammalian cells is involved in DNA damage repair. It is one of the first responses observed after DNA double strand breaks. Regulation of transcription is influenced by phosphorylation as well. Phosphorylation of histone H3S10 can enhance H3K12 acetylation and thereby influence transcriptional activity (Ito, 2007; Kouzarides, 2007).

### 1.3.4. Ubiquitination

Ubiquitin is a 76 amino acid protein, which can be conjugated via its C-terminal glycine to lysine residues of any protein. Polyubiquitination marks a protein for degradation by the proteasome (Chau et al., 1989; Thrower et al., 2000), whereas monoubiqitylated proteins are usually stable (Hicke, 2001). Ubiquitination is involved in endocytosis (Hicke and Riezman, 1996; Kolling and Hollenberg, 1994), signaling (Geetha et al., 2005; Gupta-Rossi et al., 2004), replication and transcription (Bienko et al., 2005; Kannouche et al., 2004; Mukhopadhyay and Riezman, 2007).

Addition of ubiquitin to histone residues has been linked to regulation of transcription and DNA repair. In yeast, ubiquitination of H2BK120 is an activator of transcription, but it has also been shown that some enzymes responsible for deubiquitination of histones are required for transcriptional activation. Furthermore, ubiquitination of histone H3 and H4 is implicated in DNA repair of UV-induced damage (Higashi *et al.*, 2010; Kouzarides, 2007).

### 1.3.5. Sumoylation

SUMO (small ubiquitin-like modifier) is a small protein of about 100 amino acids. Its structure is similar to ubiquitin even though it shares only ~18% sequence identity (Johnson, 2004). Like ubiquitin, it is linked via its C-terminus to a lysine residue of target proteins. Sumoylation has been detected on lysine residues of all four core histones. It competes with acetylation and ubiquitination, both of which are implicated in the activation of transcription, for the same lysine residues and is connected to repression of transcription. Desumoylation is carried out by specific SUMO-cleaving enzymes (Kouzarides, 2007).

### 1.3.6. ADP Ribosylation

Histones can be mono- or poly-ADP ribosylated on lysine residues by mono-ADP-ribosyltransferases (MARTs) and poly-ADP-ribose polymerases (PARPs), respectively. All four core histones can be modified in this way at their N-terminal tails. Addition of ADP-ribosyl to histones does not only neutralize the positive charge of lysine, it also adds a negative charge, and blocks the residue for other kinds of modifications (Messner *et al.*, 2010). ADP ribosylation has also been linked to regulation of transcription (Kouzarides, 2007).

### 1.3.7. Deimination

Arginine residues in histones H3 and H4 can be converted to citrulline by the peptidyl arginine deiminase 4 (PADI4). Citrulline can no longer be methylated. Therefore, deimination counteracts arginine methylation and its activating effect. Additionally, mono-methylated arginine can be deiminated as well, thereby removing the methylation mark (Cuthbert *et al.*, 2004; Kouzarides, 2007).

### 1.3.8. Proline Isomerization

Proline can exist in two conformations: *cis* and *trans*. Changing from one conformation to the other dramatically affects the structure of a polypeptide backbone. The *Saccharomyces cerevisiae* proline isomerase Fpr4 isomerizes H3P30 and H3P38 from *cis* to *trans in vitro*. Since the appropriate proline isomer is necessary for recognition by the Set2 methyltransferase, Fpr4 activity regulates the amount of H3K36 methylation, thereby affecting transcription (Kouzarides, 2007; Nelson *et al.*, 2006).

## 1.4. Histone Modification and Processing after Synthesis

Histones are not only modified after their incorporation into chromatin. Newly synthesized histones are also processed before their assembly into nucleosomes. Both histones H3 and H4 are acetylated after synthesis, a modification that is removed during chromatin maturation (Annunziato and Hansen, 2000; Jackson *et al.*, 1976). The ability of type B HATs to acetylate free histones makes them the most likely enzyme to carry out this task.

### 1.4.1. Hat1, the Only Type B Histone Acetyltransferase

Hat1 was the first histone acetyltransferase identified, and remains the only type B HAT known. Hat1 was isolated from cytoplasm and found to acetylate free histone H4, but not nucleosomal histones. Lysine 5 and 12 in the N-terminal tail of histone H4 are acetylated on newly synthesized histones, a pattern that is highly conserved in eukaryotes (Sobel *et al.*, 1995). Native Hat1 isolated from yeast acetylates histone H4 lysine 12, while recombinant Hat1 is capable of acetylating H4K5 and H4K12 (Parthun *et al.*, 1996). Although lysines 8 and 16 are not acetylated themselves, it seems their positive charge is important for substrate binding to Hat1 (Benson *et al.*, 2007).

In yeast, Hat1 co-purifies with another protein, Hat2. Hat2 is a WD40 repeat protein and a homologue to mammalian Rbap46/48 proteins. *In vitro* experiments showed that association of Hat2 with Hat1 increases its catalytic activity ten-fold (Parthun *et al.*, 1996). This complex composition is evolutionary conserved, as purification of type B histone acetyltransferase complexes from human, *Xenopus laevis*, chicken and maize all contain a catalytic subunit similar to Hat1, as well as a second subunit similar to Hat2 (Ahmad *et al.*, 2000; Chang *et al.*, 1997; Eberharter *et al.*, 1996; Imhof and Wolffe, 1999; Verreault *et al.*, 1998). This complex is often referred to as the HAT-B complex.

In *Saccharomyces cerevisiae*, it was shown that Hat1, despite being classified as a type B HAT, is not only found in the cytoplasm but also in the nucleus (Ai and Parthun, 2004; Poveda *et al.*, 2004). Deletion of *HAT1* leads to the loss of the histone H4-specific acetyltransferase activity in cytoplasmic, as well as nuclear fractions (Ruiz-Garcia *et al.*, 1998). Epitope-tagging and immunofluorescent labeling show that Hat1 and Hat2 are mainly localized in the nucleus (Poveda *et al.*, 2004).

The *Saccharomyces cerevisiae* nuclear HAT-B complex, referred to as NuB4 complex, contains Hif1 (Hat1 Interacting Factor 1) in addition to Hat1 and Hat2. Hif1 is a histone

chaperone specific for histone H3 and H4 and functions in chromatin assembly (Ai and Parthun, 2004). Interaction of Hif1 with Hat1 is mediated by Hat2, as in the absence of Hat2, the Hat1 and Hif1 interaction is lost (Poveda *et al.*, 2004). Furthermore, the nuclear localization of Hat1 depends on Hat2, but not on Hif1 (Poveda *et al.*, 2004). In contrast, localization of Hat2 and Hif1 are independent of Hat1 and of each other (Poveda *et al.*, 2004).

Surprisingly, even though acetylation of H4K5 and H4K12 is highly conserved in eukaryotes, it is not essential in *Saccharomyces cerevisiae* (Ma *et al.*, 1998). Neither mutating lysines 5 and 12 to arginine to mimic the unacetylated state, nor deleting *HAT1* results in a significant phenotype. Only in combination with the deletion of the N-terminal tail of histone H3 or mutation of specific lysine residues in it, an effect can be seen. Deletion of the H3 N-terminus together with altering the histone H4 N-terminal lysines causes a loss of nucleosome assembly and cell death. Deletion of *HAT1* together with specific substitutions of lysines in the histone H3 N-terminal tail causes a defect in telomeric silencing and in the repair of DNA double-strand breaks (Kelly *et al.*, 2000; Qin and Parthun, 2002). A similar phenotype is observed when the histone H3 mutations are combined with deletions of *HAT2* or *HIF1* (Kelly *et al.*, 2000; Poveda *et al.*, 2004). The *in vivo* acetylation level of H4K12 is not affected by deletion of *HAT1*, *HAT2* or *HIF1* (Poveda *et al.*, 2004). This can be explained by the fact that the acetylation of H4K12 by Hat1 is only a transient modification and therefore does not contribute to a significant extend to the total steady-state level of H4K12 acetylation.

In response to DNA double strand breaks (DSB), Hat1 is recruited to the site of DNA damage, and H4K12 acetylation levels in the regions surrounding the DSB increase (Qin and Parthun, 2006). Since Hat1 is unable to acetylate nucleosomal histones, it may participate in a histone exchange process, in which histone H3/H4 tetramers are replaced. Interestingly, recruitment of Hat1 to the site of DNA damage does not require repair of the DSB, suggesting that Hat1 may be directly involved in the DNA repair process rather than only in the restoration of chromatin structure after repair is complete (Qin and Parthun, 2006). However, deletion of *HAT1* also causes a significant defect in the repair-linked chromatin reassembly. Surprisingly, loss of Hat2 results only in a minor defect. It is possible that in this process Hat1 does not depend strongly on its catalytic activity or that the influence of Hat2 *in vivo* is not that strong. Alternatively, Hat1 may have the ability to modify other substrates for which Hat2 is not required (Ge *et al.*, 2011).

### 1.4.2. Rtt109, a Histone H3 Specific Histone Acetyltransferase

Histone H3, just like histone H4, is acetylated after synthesis (Masumoto *et al.*, 2005). Unlike histone H4 with its highly conserved pattern of modifications, acetylation sites of histone H3 vary between different organisms. In *Drosophila* and *Tetrahymena*, deposition-related acetylation is associated with H3K14/23 and H3K9/14, respectively (Sobel *et al.*, 1995). In *Saccharomyces cerevisiae*, newly synthesized histone H3 is acetylated on lysine 9 (Kuo *et al.*, 1996). But not only residues on the N-terminal tail can be modified. Lysine residues in the globular domain can be acetylated as well. In *Saccharomyces cerevisiae* and *Schizosaccharomyces pombe*, newly synthesized histones H3 are abundantly acetylated on lysine 56 (Han *et al.*, 2007; Xhemalce *et al.*, 2007). This acetylation mark persists after incorporation into chromatin until the $G_2$/M-phase when lysine 56 is deacetylated by HDACs Hst3 and Hst4 (Celic *et al.*, 2006).

The *Saccharomyces cerevisiae* histone acetyltransferase Rtt109 acetylates several lysines on histone H3. Its specificity is controlled by the histone chaperones Asf1 and Vps75. Rtt109-Asf1 has strong site specificity for H3K56, while Rtt109 in a complex with Vps75 acetylates H3K56 and H3K9. Further addition of Asf1 to this complex enhances the acetylation activity of Rtt109 (Fillingham *et al.*, 2008). Deletion of *RTT109* leads to a complete loss of H3K56 acetylation, suggesting that Rtt109 is the only H3K56 HAT in *Saccharomyces cerevisiae*. Similarly, deletion of *ASF1* results in complete loss of H3K56 acetylation, whereas the acetylation level of H3K56 in cells lacking Vps75 remains normal. The acetylation level of H3K9 in cells lacking Rtt109, Asf1 or Vps75 is reduced. H3K9 is not only acetylated by Rtt109 but also by the HAT Gcn5. Deleting *GCN5* in combination with either *RTT109*, *ASF1* or *VPS75* results in a complete loss of H3K9 acetylation, suggesting that Rtt109, Asf1 and Vps75 function together in a Gcn5-independent pathway (Fillingham *et al.*, 2008).

Acetylation of H3K56 by Rtt109 is required for genome stability, resistance to DNA-damaging agents, chromatin reassembly after DNA damage repair and deposition of newly synthesized histones into chromatin (Chen *et al.*, 2008; Driscoll *et al.*, 2007; Han *et al.*, 2007; Li *et al.*, 2008; Masumoto *et al.*, 2005; Tsubota *et al.*, 2007). Cells depleted for Rtt109 or Asf1 are highly sensitive to DSBs causing agents, and exhibit an elevated level of spontaneous chromosome breaks (Driscoll *et al.*, 2007; Fillingham *et al.*, 2008; Han *et al.*, 2007).

### 1.4.3. Histone Processing by Hat1 and Rtt109

Newly synthesized histones are modified, transported into the nucleus and finally deposited into chromatin. Even though many proteins involved in this process have been identified, the mechanism as a whole remains poorly understood. A working model of histone H3 and H4 processing in *Saccharomyces cerevisiae* is depicted in Figure 7. First, histone H4 is bound and acetylated at lysine 5 and 12 by the Hat1/Hat2 complex in the cytoplasm. Histone H4 is not released after acetylation but remains bound to the Hat1/Hat2 complex. At some point during this process histone H3 becomes associated. The Hat1/Hat2/H3/H4 complex is then imported into the nucleus by karyopherins such as Kap123. In the nucleus, Hif1 becomes associated forming the NuB4 complex. Histones H3 and H4 are then transferred from Hif1 to the histone chaperone Asf1. After that, Asf1 can recruit Rtt109 or Rtt109/Vps75, which in turn acetylates histone H3 on lysine 9 and 56. In the last step, histones H3 and H4 are deposited into chromatin (Campos *et al.*, 2010; Fillingham *et al.*, 2008; Parthun, 2007).

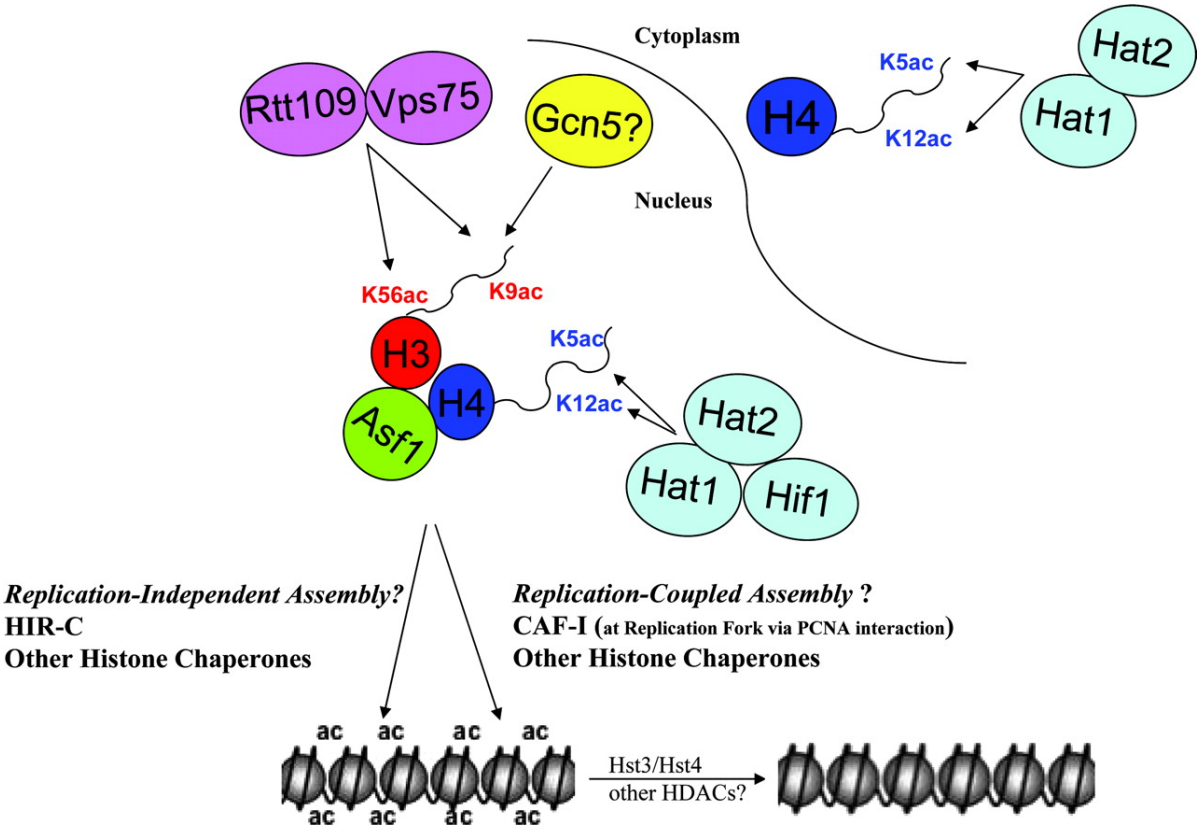


**Figure 7: Model illustrating the roles of histone chaperones and HATs during chromatin assembly.** Adapted from Fillingham *et al.*, 2008.

## 1.5. Aims of this Diploma Thesis

*Candida albicans* is an important human fungal pathogen with several distinct growth forms. Filamentation is considered a major virulence trait and can be induced by various environmental or host stimuli. For instance, treatment of *Candida albicans* with genotoxic agents or depletion of components involved in the DNA damage response can trigger pseudohyphal growth. In the yeast *Saccharomyces cerevisiae,* the histone acetyltransferases Hat1, which forms a complex with the subunit Hat2, and Rtt109, which interacts with Asf1, are both implicated in DNA damage repair. We therefore analyzed the roles of Hat1/Hat2 and Rtt109/Asf1 in *Candida albicans*.

The major aims of this thesis were:

- To raise antibodies as a tool for the characterization of Hat1 and Hat2 function.

- Moreover, Hat2 should be epitope-tagged with a fluorescent protein to investigate its intracellular localization, its dependence on Hat1 and the influence of DNA-damaging agents.

- Furthermore, deletion strains of *RTT109* and *ASF1* should be constructed to investigate their function in *Candida albicans*.

- Finally, strains with mutated histone H4 variants that would mimic the acetylated or unacetylated state of Hat1-targeted lysine residues should be constructed.

# 2. Material & Methods

## 2.1. Basic Bacteriological Methods

### 2.1.1. Media for *E. coli*

1x LB:

10g/l Tryptone

5g/l Yeast extract

10g/l NaCl

For LB-plates, add bacteriological agar (BD) at a final concentration of 2% (w/v).

For LB+Amp medium, add ampicillin after autoclaving at a final concentration of 120µg/ml.

For LB+chloramphenicol medium, add chloramphenicol after autoclaving at a final concentration of 40µg/ml in plates and 50µg/ml in liquid culture.

### 2.1.2. Competent *E. coli*

- Grow o/n culture *E. coli* in 500ml S.O.B. medium at 18°C or room temperature to $OD_{600}$=1.
- Chill culture on ice for 20min.
- Spin down at 2500rpm 10min 4°C (50ml falcons).
- Gently resuspend pellet in 10ml ice-cold TB.
- Put on ice for 10min.
- Spin down at 2500rpm 10min 4°C in a microfuge.
- Resuspend in 35ml ice-cold TB.
- Add DMSO (Sigma, tissue culture grade) to a final concentration of 7% (v/v).
- Put on ice for 10min.
- Freeze 500µl aliquots in liquid nitrogen and store at -80°C.

S.O.B. medium:

| | |
|---|---|
| 2% | Tryptone (w/v) |
| 0.5% | Yeast extract |
| 10mM | NaCl |
| 2.5mM | KCl |
| 20mM | $MgCl_2$ |

Dissolve tryptone yeast extract and NaCl in $dH_2O$, add KCl, adjust pH to 7.5 with NaOH, autoclave and add sterile $MgCl_2$.

| | | |
|---|---|---|
| TB: | 10mM | Pipes |
| | 55mM | $MnCl_2$ |
| | 15mM | $CaCl_2$ |
| | 250mM | KCl |

Mix all components except $MnCl_2$ in $dH_2O$, adjust to pH 6.7 with KOH, add $MnCl_2$, sterilize by filtration through a 0.45µm Millipore filter and store at 4°C.

### 2.1.3. *E. coli* Transformation

- Slowly thaw competent cells on ice.
- Gently mix 1-10µl DNA with 100µl competent cells.
- Incubate on ice for 30min.
- Heat shock cells at 42°C for 45sec.
- Cool on ice for 2min.
- Add 900µl S.O.C. medium.
- Incubate at 37°C for 1 hour.
- Plate cells on a selective LB plate and incubate at 37°C overnight.

| | | |
|---|---|---|
| S.O.C. medium: | 2% | Tryptone |
| | 0.5% | Yeast extract |
| | 2.5mM | KCl |
| | 10mM | $MgSO_4$ |
| | 20mM | Glucose |
| | 10mM | NaCl |
| | 10mM | $MgCl_2$ |

## 2.2. Basic Yeast Methods

### 2.2.1. Media for Yeast

<u>1x YPD</u>:

10g/l Yeast extract (BD)

20g/l Peptone (BD)

2% Glucose (w/v)

For YPD-plates, add bacteriological agar (BD) at a final concentration of 2% (w/v).

For YPD+NAT medium, add nourseothricin after autoclaving at a final concentration of 300µg/ml in plates and 150µg/ml in liquid culture.

1x SC:

6.7g/l Bacto-YNB w/o amino acids and $(NH_4)_2SO_4$ (DIFCO)

5g/l Ammonium sulfate

2% Glucose

1.43g/l Amino acid mix

If required add uracil, histidine and leucine at a final concentration of 4mg/l uracil, 6mg/l histidine and 26mg/l leucine. For SC-plates, add bacteriological agar at a final concentration of 2% (w/v).

| | | |
|---|---|---|
| Amino acid mix (Sigma; g/29g): | 0.4g | Arginine |
| | 0.6g | Tyrosine |
| | 0.6g | Isoleucine |
| | 0.8g | Adenine |
| | 1.0g | Phenylalanine |
| | 2.0g | Glutamic acid |
| | 2.0g | Aspartic acid |
| | 3.0g | Valine |
| | 3.0g | Methionine |
| | 3.6g | Lysine |
| | 4.0g | Threonine |
| | 8.0g | Serine |

1x MM (minimal medium):

6.7g/l Bacto-YNB w/o amino acids and $(NH_4)_2SO_4$ (DIFCO)

5g/l Ammonium sulfate

2% Glucose

For MM-plates add bacteriological agar (BD) at a final concentration of 2% (w/v).

### 2.2.2. Preparation of Yeast TCA Extracts for Immunoblotting

- Dilute o/n culture in 5ml YPD.
- Harvest cells with $OD_{600}$=0.8-1 by spinning 5min at 3000rpm.
- Resuspend cells in 1ml $H_2O$.
- Add 150µl Yex-lysis buffer and vortex.
- Incubate 10min on ice.
- Add 150µl cold 50% (w/V) TCA (trichloracetic acid).
- Incubate at least 10min on ice.

- Spin 5min 13000rpm 4°C.
- Discard supernatant.
- Spin again.
- Carefully take off supernatant.
- Resuspend pellet in protein sample buffer (20µl/$OD_{600}$).
- Incubate 15min at 37°C on shaker (700rpm).
- Spin down cell debris 5min at 13000rpm.
- Load 10µl (0.5 $OD_{600}$) of supernatant on SDS-PAGE gel.

| | | |
|---|---|---|
| Yex-lysis buffer: | 1.85M | NaOH |
| | 7.5% | β-mercaptoethanol (v/v) (freshly added) |

| | | |
|---|---|---|
| Protein sample buffer: | 40mM | Tris-HCl pH 6.8 |
| | 8M | Urea |
| | 5% | SDS (w/v) |
| | 0.1mM | EDTA |
| | 1% | β-mercaptoethanol (v/v) (freshly added) |
| | 0.1g/l | Bromophenol blue |
| | 0.1M | Tris base (Trizma® base) |

### 2.2.3. Preparation of Genomic Yeast DNA

- Grow 5ml yeast cultures overnight to saturation in appropriate media at 30°C.
- Sediment cells for 5min at 1500rpm (Beckmann).
- Resuspend cells in 0.5ml sterile distilled water.
- Transfer the cells to 1.5ml tube.
- Spin down cells for 5sec in the Eppendorf centrifuge at the maximum speed (14000rpm).
- Decant the supernatant and briefly vortex the pellet in 200µl Yeast Lysis Buffer.
- Add 200µl PCI and 0.3g of acid-washed glass beads (Sigma).
- Disrupt cells in FastPrep (FastPrep®-24, MP Biomedicals) for 45sec, 6m/sec.
- Add 200µl TE pH 8.
- Spin for 5min and transfer aqueous phase to a new tube.
- Add 1ml 100% EtOH, mix by inversion and incubate at -20°C for 20min.
- Spin for 10min at 4°C, and aspirate the supernatant.
- Resuspend the pellet in 400µl TE and 4µl RNase A (Boerhinger Mannheim).

- Incubate at 37°C until the pellet is dissolved.
- Add 10µl 4M ammonium acetate and 1ml 100% EtOH. Incubate 20min at -20°C.
- Spin for 10min at 4°C and discard the supernatant. Wash with 1ml 70% EtOH.
- Air-dry the pellet and resuspend in 50µl TE or water.

PCI: Phenol:chloroform:isoamyl alcohol (25:24:1)

1x TE:

| | |
|---|---|
| 10mM | Tris-HCl pH 8.0 |
| 1mM | EDTA |

Yeast Lysis Buffer (Winston Lysis Buffer):

| | |
|---|---|
| 100mM | NaCl |
| 10mM | Tris-HCl pH 8 |
| 1mM | EDTA |
| 2% | Triton X-100 |
| 1% | SDS |

### 2.2.4. Transformation by Electroporation

- Dilute overnight culture in 50ml YPD and grow at 30°C to $OD_{600}$=~1.5.
- Harvest at 2500rpm (1000g Eppendorf) for 5min.
- Wash with 25ml $H_2O$ (vortex).
- Resuspend in 8ml $H_2O$, 1ml 10x TE and 1ml 1M lithium acetate.
- Incubate 60min at 30°C, 150rpm.
- Add 250µl 1M DTT (keep DTT on 4°C).
- Incubate 30min at 30°C, 150rpm.
- Add 40ml $H_2O$ (cold).
- Centrifuge at 2500rpm (1000g) 5min 4°C.
- Resuspend in 25ml cold $H_2O$ by gentle shaking.
- Centrifuge at 2900rpm (1000g) 5min 4°C.
- Wash pellet in 5ml cold 1M Sorbitol.
- Resuspend pellet in 550µl 1M Sorbitol.
- Sterilize clean electroporation cuvettes by 3x autocrosslink in Stratagene crosslinker.
- Cool electroporation cuvettes on ice.
- Transfer 10µl DNA deletion construct into electroporation cuvette.
- Transfer 100µl of competent cells into electroporation cuvette.
- Leave on ice for 5-10min.

- Electroporator settings: BioRad gene pulser (200Ω, 1.5kV, 25µF)
  Time constant should be ~4.6ms.
- Add 950µl YPD.
- Transfer to 15ml tube and shake at 30°C for 4 hours.
- Plate on YPD-Nat.
- Incubate at 30°C for 1-2 days.

| | | |
|---|---|---|
| 10x TE: | 100mM | Tris-HCl pH 8.0 |
| | 10mM | EDTA |

### 2.2.5. Colony PCR

- Pick cells with a sterile toothpick and resuspend in 40µl PCR-mix 1:
  5µl 10x PCR buffer
  3µl 50mM $MgCl_2$
  32µl $dH_2O$
- Break cells by incubating at 93°C for 10min.
- Add 10µl PCR-mix 2:
  4µl dNTPs (2.5mM each)
  2.5µl Forward primer (10µM)
  2.5µl Reverse primer (10µM)
  1µl Taq polymerase
- PCR-program:

| | | | | |
|---|---|---|---|---|
| 93°C | 3’ 00’’ | denaturation | | |
| 93°C | 30’’ | denaturation | 35 cycles | $T_M$: melting temperature primers |
| $T_M$ | 30’’ | primer annealing | | |
| 72°C | x’’ | extension | | 2’ for 1kb |
| 72°C | 10’ 00’’ | final extension | | |
| 10°C | | hold | | |

| | | |
|---|---|---|
| 10x PCR buffer: | 500mM | KCl |
| | 100mM | Tris-HCl pH 9.0 |
| | 1% | TritionX-100 |
| | 15mM | $MgCl_2$ |

### 2.2.6. Spotting Assay on Agar Plates

- Dilute overnight cultures to $OD_{600}$=0.1 and grow for several hours at 30°C.
- Prepare agar plates (2% bact. agar (BD)) containing substances for sensitivity testing.
- Dilute culture to $OD_{600}$=0.1 in 200µl $dH_2O$.
- Make 1:5 serial dilutions by adding 40µl of one dilution to 160µl $H_2O$.
- Spot 3µl of each dilution on plates and incubate for 2 to 5 days at 30°C.

### 2.2.7. Microscopy

Single cell pictures:

- Dilute o/n culture in fresh YPD and grow cells at 30°C for several hours.
- For nuclear staining add Hoechst33342 to a final concentration of 2µg/ml for 1 hour.
- Spin down cells.
- Wash with PBS.
- Take up cells in PBS.
- Cells are examined using an Olympus cell$^R$ - Imaging Station. Pictures were taken with a Hamamatsu ORCA-ER digital camera.

Colony pictures:

- Plate cells on YPD and let grow for 2-3 days at 30°C.
- Colony pictures are taken with a Discovery.V12 Stereomicroscope and an AxioCam MRc5 (Zeiss).

## 2.3. DNA Methods

### 2.3.1. Agarose Gel Electrophoresis

- Mix DNA samples (5-50µl) with an appropriate amount of 6x DNA loading buffer.
- Load samples on a gel containing 0.7-2% agarose in 1x TBE buffer and 0.5µg/ml ethidium bromide, in electrophoresis chamber filled with 1x TBE buffer.
- Load 3µl molecular weight standard on the gel (Bioline Hyperladder I or Fermentas GeneRuler™ 1kb Plus DNA Ladder).
- Separate DNA fragments in an electric field with 90V.
- Visualize nucleic acid fragments under UV-light.

| | | |
|---|---|---|
| 1x TBE: | 89mM | Tris base |
| | 89mM | Boric acid |
| | 2mM | EDTA |
| 6x DNA loading buffer: | 0.25% | Bromophenol blue (w/v) |
| | 0.25% | Xylenecyanol FF (w/v) |
| | 30% | Glycerol (v/v) |

### 2.3.2. Molecular Biology Cloning Procedures

Restriction enzyme digest:

- Digest DNA in a total volume of 100µl using the proper buffer supplied with the enzyme using conditions recommended by the manufacturer (Fermentas or NEB).

Phosphatase treatment:

- After restriction digest add 2µl FastAP™ Thermosensitive Alkaline Phosphatase (1U/µl, Fermentas) to the reaction mix.
- Incubate 60min at 37°C.

Gel elution:

- Load reaction mix on a gel to elute the fragment.
- Cut the desired DNA fragment out of the gel.
- Elute DNA from gel using the peqGOLD Gel Extraction Kit (peqlab) according to manufacturer's instructions.

Ligation of DNA fragments:

- Vector and insert are ligated with T4 DNA ligase (1U/µl, Roche) at a molar ratio of 1:3 or 1:5.
- Ligation mix: 10µl total
  50ng Vector DNA
  x µl Insert
  1µl 10x ligation buffer
  1µl T4 DNA ligase
- Incubate ligation mix for 60min at room temperature before transforming 5µl into competent *E. coli* cells.

### 2.3.3. Plasmid Mini Preparation

- Grow *E. coli* cells containing the plasmid in 5ml LB+antibotic at 37°C overnight.
- Harvest cells in 2ml tube.
- Resuspend pellet in 250µl buffer P1 (QUIAGEN).
- Add 250µl buffer P2 (QUIAGEN) and mix by inverting.
- Add 350µl buffer P3 (QUIAGEN) and mix by inverting.
- Incubate 5min on ice.
- Centrifuge 5min at 13000rpm 4°C.
- Transfer supernatant to new tube.
- Add 0.7x volume isopropanol (-20°C).
- Incubate 15min on ice.
- Centrifuge 10min at 13000rpm 4°C.
- Discard supernatant.
- Wash with 1ml 70% EtOH (-20°C).
- Dry at 55°C.
- Resuspend in 100µl $dH_2O$.

| | | |
|---|---|---|
| Buffer P1 (resuspension buffer): | 50mM | Tris-HCl pH 8.0 |
| | 10mM | EDTA |
| | 100µg/ml | RNase A |
| Buffer P2 (lysis buffer): | 200mM | NaOH |
| | 1% | SDS (w/v) |
| Buffer P3 (neutralization buffer): | 3M | Potassium acetate pH 5.5 |

### 2.3.4. DNA Precipitation

- Add $^1/_{10}$ of the original volume of 3M Na-acetate pH 5.3 and 3 times the volume of EtOH.
- Incubate at -20°C for 1 hour.
- Spin down for 15min at 4°C.
- Wash with 70°C.
- Dry pellet at 50°C.
- Resuspend pellet in appropriate amount of $dH_2O$.

### 2.3.5. DNA-Sequencing

DNA sequencing was carried out by the I.M.P. Sequencing Service.

### 2.3.6. PCR

Reaction mix: 50µl total volume

| | |
|---|---|
| 10ng | Template |
| 10µl | 5x Phusion® HF Buffer (Finnzymes) |
| 4µl | dNTPs (2.5mM each) |
| 2.5µl | Forward primer (10µM) |
| 2.5µl | Reverse primer (10µM) |
| 0.3µl | Phusion® High-Fidelity DNA Polymerase (2U/µl) (Finnzymes) |

PCR-program:

| | | | | |
|---|---|---|---|---|
| 98°C | 30'' | denaturation | | |
| 98°C | 10'' | denaturation | 35 cycles | $T_M$: melting temperature primers |
| $T_M$+3°C | 30'' | primer annealing | | |
| 72°C | x'' | extension | | 30'' for 1kb |
| 72°C | 3' 00'' | final extension | | |
| 10°C | | hold | | |

### 2.3.7. Fusion PCR

To obtain tagging cassettes purified overlapping PCR-fragments were mixed at a molar ratio of 1:1 and amplified using appropriate primers.

Reaction mix: 50µl total volume

overlapping PCR-fragments as template

| | |
|---|---|
| 5µl | 10x Ex Taq™ Buffer ($Mg^{2+}$ plus) (TaKaRa) |
| 4µl | dNTPs (2.5mM each) |
| 2.5µl | Forward primer (10µM) |
| 2.5µl | Reverse primer (10µM) |
| 0.5µl | Ex Taq™ Polymerase (5U/µl) (TaKaRa) |

PCR-program:

| | | | | |
|---|---|---|---|---|
| 93°C | 3’ 00’’ | denaturation | | |
| 93°C | 30’’ | denaturation | 30 cycles | $T_M$: melting temperature primers |
| $T_M$ | 30’’ | primer annealing | | |
| 72°C | x’’ | extension | | 1’ for 1kb |
| 72°C | 10’ 00’’ | final extension | | |
| 10°C | | hold | | |

### 2.3.8. Site-Directed Mutagenesis

- Set up two separate primer extension reactions, one for the forward and one for the reverse primer.

Reaction mix: 50µl total volume

| | |
|---|---|
| 100ng | Plasmid template |
| 10µl | 5x Phusion® HF Buffer (Finnzymes) |
| 4µl | dNTPs (2.5mM each) |
| 2.5µl | Forward or reverse primer (10µM) |
| 0.3µl | Phusion® High-Fidelity DNA Polymerase (2U/µl) (Finnzymes) |

PCR-program:

| | | | | |
|---|---|---|---|---|
| 98°C | 30’’ | denaturation | | |
| 98°C | 10’’ | denaturation | 4 cycles | |
| 60°C | 30’’ | primer annealing | | |
| 72°C | x’’ | extension | | 30’’ for 1kb |
| 72°C | 3’ 00’’ | final extension | | |
| 10°C | | hold | | |

- Combine 25µl from each extension reaction above.
- Incubate as above, except repeat a total of 18 cycles.
- Transfer 25µl of the reaction to a microcentrifuge tube.
- Add 1µl DpnI restriction enzyme (Fermentas, 10 U/µl).
- Mix well and incubate at 37°C for 1-2 hours.
- After the first incubation step add again 1µl DpnI and incubate another 1-2 hours.
- Transform 1-5µl of the reaction into competent *E. coli*.

### 2.3.9. Quantitative PCR

Quantitative PCR was performed in triplicates on a Realplex Mastercycler (Eppendorf) using the KAPA SYBR® FAST qPCR Kit (Kapa Biosystems).

Reaction mix: 20µl total volume

| | |
|---|---|
| 3µl | Template (2.5ng/µl genomic DNA) |
| 0.3µl | Primer mix (25µM each) |
| 10µl | KAPA SYBR® FAST qPCR MasterMix 2x |
| 0.4µl | KAPA SYBR® FAST ROX Low 50x |

PCR-program:

| | | | |
|---|---|---|---|
| 95°C | 5’ 00’’ | denaturation | |
| 95°C | 10’’ | denaturation | 40 cycles |
| 62°C | 10’’ | primer annealing | |
| 72°C | 15’’ | extension | |
| 95°C | 20’’ | denaturation | |
| 62°C-95°C | 30’ 00’’ | melting curve | |
| 25°C | | hold | |

For analysis the Realplex 2.0 program (Eppendorf) was used. Data analysis was done according to Pfaffl, 2001.

### 2.3.10. Southern Blot

- Isolate genomic DNA.
- Measure concentration of genomic DNA.
- Digest 25µg genomic DNA overnight using conditions recommended by the manufacturer.

Agarose gel for electrophoresis of genomic DNA:

- Pour a big gel containing 0.7% agarose in 1xTBE.
- Load genomic DNA samples and molecular weight standard.
- Apply electric field of 60-80 volts.
- Take a photo of the gel.
- Mark bands of molecular weight standard on the gel with a sterile glass pipette.

Denaturation and neutralization of agarose gel:

- Soak agarose gel for 1h in 0.5M NaOH, 1.5M NaCl.
- Soak agarose gel for 1h in 0.5M Tris-HCl pH 7.5, 1.5M NaCl.

Capillary blotting:

- Prepare blotting stock in a glass tray as follows:
  - Gel tray upside down
  - 1 Long piece of Whatman-3MM paper soaked in 20xSSC
  - 1 Piece of Whatman-3MM paper soaked in 20xSSC
  - Agarose gel (upside down)
  - Nylon membrane (Nylon Membranes, positively charged from Roche) soaked in 20xSSC
  - Put pieces of Parafilm at the sides to seal blot
  - 1 Piece of Whatman-3MM paper
  - Stack of green towels
  - Put a 1kg weight on top.
- Fill glass tray with 20xSSC.
- Transfer overnight.
- Mark bands of molecular weight standard on the membrane with a pencil.
- Crosslink DNA on the membrane using Stratagene UV Crosslinker (auto-crosslink).
- Rinse membrane briefly with $dH_2O$ and allow to air-dry.

Detection:

Detect DNA fragments using DIG High Prime DNA Labeling and Detection Starter Kit II (Roche) according to the manufacturer's instructions.

| | | |
|---|---|---|
| 20xSSC: | 3M | NaCl pH 7.0 |
| | 300mM | Sodium citrate |

## 2.4. Protein Methods

### 2.4.1. SDS-Polyacrylamide Gel Electrophoresis (SDS-PAGE)

- Load samples and 5µl PageRuler™ Plus Prestained Protein Ladder (Fermentas).
- Run gel at 180V in 1x running buffer.

| | stacking gel | separation gel | | |
|---|---|---|---|---|
| | 4.5% | 12% | 15% | 16% |
| $dH_2O$ | 1.500ml | 1.750ml | 1.250ml | 1.100ml |
| 1.5M Tris HCl (pH 8.8) | - | 1.250ml | 1.250ml | 1.250ml |
| 0.5M Tris HCl (pH 6.8) | 0.625ml | - | - | - |
| 30% Acrylamide (Bio-Rad) | 0.375ml | 2.000ml | 2.500ml | 2.650ml |
| 10% SDS | 0.050ml | 0.050ml | 0.050ml | 0.050ml |
| 10% APS | 0.025ml | 0.050ml | 0.050ml | 0.050ml |
| TEMED | 0.003ml | 0.005ml | 0.005ml | 0.005ml |

| | | |
|---|---|---|
| Running buffer: | 25mM | Tris |
| | 192mM | Glycine |
| | 0.1% | SDS |

### 2.4.2. Coomassie-Staining of Protein Gels

- Stain protein gel by shaking for 30min in Coomassie-staining solution.
- Replace staining solution with $dH_2O$ and heat in the microwave oven for a few seconds.
- Shake for 15min.
- Repeat until background is destained.

| | | |
|---|---|---|
| Coomassie staining solution: | 10% | Acetic acid |
| | 25% | Isopropanol |
| | 0.031% | Coomassie Brilliant Blue G-250 |

### 2.4.3. Silver-Staining of Protein Gels

- Fix gel by shaking in fixing solution for 1h.
- Wash three times for 20min with 50% EtOH.
- Incubate the gel in pre-treatment solution for 1min.
- Wash three times for 20sec with $dH_2O$.
- Stain gel by shaking in staining solution for 20min in the dark.

- Wash twice for 20sec with $dH_2O$.
- Incubate gel in developing solution until bands appear.
- Wash twice for 2min with $dH_2O$.
- Stop the developing with stopping solution.
- Wash with 50% MeOH.

| | | |
|---|---|---|
| Fixing solution: | 50% | MeOH |
| | 12% | $CH_3COOH$ |
| | 0.5ml/l | 37% HCOH |
| Pre-treatment solution: | 0.2g/l | $Na_2S_2O_3.5H_2O$ |
| Staining solution: | 2g/l | $AgNO_3$ |
| | 0.5ml/l | 37% HCOH |
| Developing solution: | 60g/l | $Na_2CO_3$ |
| | 0.5ml/l | 37% HCOH |
| | 4mg/l | $Na_2S_2O_3.5H_2O$ |
| Stopping solution: | 50% | MeOH |
| | 12% | $CH_3COOH$ |

### 2.4.4. Western Blot

- Prepare blotting stock as follows:
  - Anode
  - Whatman-paper soaked in transfer buffer
  - Membrane (Whatman® Protran® Nitrocellulose Membrane) moisturized with transfer buffer
  - Gel
  - Whatman-paper soaked in transfer buffer
  - Cathode
- Blot for 1h at 200mA with the Mini Trans-Blot cell (Bio-Rad) in transfer buffer.
- Detect proteins on membrane with Ponceau S (SIGMA).
- Destain the membrane by washing in $H_2O$.
- Block unspecific binding by shaking in blocking solution.
- Incubate overnight at 4°C with the primary antibody diluted in TBS-T.

- Wash three times for 15min with TBS-T.
- Incubate 1h with the secondary antibody diluted in TBS-T.
- Wash three times for 15min with TBS-T.
- Wash with 1x PBS.
- Scan membrane using the Odyssey® Infrared Imaging System.

| | | |
|---|---|---|
| Transfer buffer: | 25mM | Tris |
| | 192mM | Glycine |
| | 20% | MeOH |
| Blocking solution: | 5% | BSA |
| | 1x | TBS |
| TBS: | 140mM | NaCl |
| | 2.5mM | KCl |
| | 25mM | Tris pH 7.5 |
| TBS-T: | 1x | TBS |
| | 0.1% | Tween-20 |
| PBS: | 140mM | NaCl |
| | 2.5mM | KCl |
| | 8.1mM | $Na_2HPO_4$ |
| | 1.5mM | $KH_2PO_4$ pH 7.3 |

### 2.4.5. Purification of GST-Fusion Protein from *E. coli*

Induction in total extracts:

- Dilute overnight culture in fresh 20ml LB+Amp to $OD_{600}$=0.25-0.5.
- Incubate for 30min at 30°C to equilibrate.
- Take a 1.5ml control sample at t=0min as the uninduced control.
- Induce protein expression by adding IPTG at a final concentration of 0.2-1mM.
- Incubate at 30°C for 4 hours.
- Take 1.5ml samples at different time points (20-240min).
- Spin down samples and discard supernatant.
- Resuspend pellet in protein sample buffer.
- Boil for 10min on heat block (95°C).

- Spin down at 13000rpm for 15min.
- Run 0.2-1 $OD_{600}$ equivalents of the total extract on SDS-PAGE gel.
- Stain with Coomassie Blue.

Determine if GST fusion-protein is soluble or not:

- Dilute overnight culture in fresh 20ml LB+Amp to $OD_{600}$=0.25-0.5.
- Incubate for 30min at 30°C to equilibrate.
- Take a 1.5ml control sample at t=0min as the uninduced control.
- Induce protein expression by adding IPTG at a final concentration of 0.2-1mM.
- Incubate at 30°C for the optimal time.
- Spin down cells (15ml) for 15min at full speed and wash once with cold PBS.
- Suspend cells in 1ml cold PBS.
- Lyse cell suspension by sonicating 3 times for 15 imp, cycle 70% (sonicator: Bandelin electronics, UW70, tip SH70).
- Transfer to 1.5ml Eppendorf tube.
- Spin homogenate for 10 min at 6700g at 4°C to pellet insoluble inclusion bodies (IB).
- Take sample from supernatant (soluble fraction) and add sample buffer (same volume).
- Resuspend insoluble fraction in sample buffer (10µl/$OD_{600}$).
- Boil all samples for 10min at 95°C.
- Run 5µl of total extracts (0.2 $OD_{600}$) and insoluble fraction (0.5 $OD_{600}$) and 8µl of supernatant on SDS-PAGE gel.
- Stain with Coomassie Blue.

Binding of GST fusion-protein to glutathione sepharose beads (large scale):

- Dilute overnight culture in 500ml LB+Amp to $OD_{600}$=0.5.
- Incubate for 60min at 30°C to equilibrate.
- Take a 1.5ml control sample at t=0min as the uninduced control.
- Induce protein expression by adding IPTG at a final concentration of 0.2-1mM.
- Incubate at 30°C for 2 hours.
- Harvest cells by centrifugation at 4000rpm for 5min in a GS3 rotor in a Sorvall centrifuge.
- Resuspend pellet in 3.5ml TpG buffer and add protease inhibitor cocktail (Roche).
- Lyse cells by sonication (5x 10imp, cycle 70%).
- Spin down cell debris at 4°C 10min at 13000rpm.
- Equilibrate 150µl Glutathione Sepharose™ 4B beads (GE Healthcare) per ml cell lysate in TpG buffer.

- Add 150µl 50% glutathione sepharose beads to 1ml cell lysate.
- Incubate overnight on a rotation mixer.
- Centrifuge at 2000rpm 2min at 4°C and wash beads three times with TpG buffer.
- Elute GST fusion-protein by shaking beads 10min at room temperature in 125µl elution buffer.
- Spin down beads 2min at 2000rpm and repeat elution twice.
- Repeat elution with 40mM glutathione.
- Run 0.25 $OD_{600}$ equivalents of each step on SDS-PAGE gel.
- Stain with Coomassie Blue.

| | | |
|---|---|---|
| TpG buffer: | 20mM | Tris-HCl pH 8 |
| | 100mM | NaCl |
| | 1mM | EDTA |
| | 0.1mM | $ZnCl_2$ |
| | 0.5% | NP40 (v/v) |
| Elution buffer: | 50mM | Tris-HCl pH 8 |
| | 5mM | Reduced glutathione |

### 2.4.6. Inclusion Body Preparation

- Dilute overnight culture in 200ml LB+Amp to $OD_{600}$=0.5.
- Incubate for 60min at 30°C to equilibrate.
- Induce protein expression by adding IPTG to a final concentration of 0.2-1mM.
- Incubate at 30°C for 4h.
- Harvest cells at 5000rpm 10min in a Sorvall centrifuge (GS3 rotor).
- Resuspend pellet in 10ml lysis buffer.
- Add 1ml freshly made lysozyme (20mg/ml stock solution) at a final concentration of 1mg/ml.
- Leave on ice for 60min.
- Add directly to the suspension from stocks:
  300µl 10% NP-40 (final 0.1%)
  200µl DNaseI (Fermentas)
  300µl 1M $MgCl_2$ (final 10mM)
  adjust volume to 30ml with Lysis Buffer.
- Mix thoroughly with a glass pipette.
- Leave on ice for at least 60min.

- Lyse remaining cells by sonicating 3 times for 15 imp, cycle 70% (sonicator: Bandelin electronics, UW70, tip SH70).
- Spin down 10min at 7000rpm 4°C (Sorvall HB4), pellet should be whitish (complete lysis).
- Wash IB by resuspending pellet in 30ml Lysis Buffer + 1% NP-40 detergent.
- Wash IB by resuspending pellet in 30ml Lysis Buffer + 2M Urea.
- Wash IB by resuspending pellet in 30ml Lysis Buffer and respinning.
- Repeat washing steps until the pellet loses all the brownish color and is completely white/grey.
- Resuspend pellet in approximately 4ml Lysis Buffer and freeze in 1ml aliquots.
- Run 0.15 $OD_{600}$ equivalents on SDS-PAGE gel.
- Stain with Coomassie Blue.

| | | |
|---|---|---|
| Lysis buffer: | 50mM | Tris-HCl pH 7.8 |
| | 100mM | NaCl |
| | 10mM | EDTA |

### 2.4.7. Rabbit Antibody Production

New Zealand White Rabbits (Charles River Canada) were injected with the indicated amount of purified antigen (2µg/ml in PBS) (Table 3). Rabbit #129 was injected with GST-Hat1 and rabbit #128 was injected with GST-Hat2. Blood was drawn at the indicated time points to test for antibody specificity.

**Table 3: Antibody production schedule.**

| day | amount antigen | |
|---|---|---|
| 0 | | preimmune |
| 6 | 400µg | 1st injection |
| 28 | 250µg | 2nd injection |
| 49 | | 1st bleed |
| 53 | 125µg | 3rd injection |
| 67 | | 2nd bleed |
| 75 | 125µg | 4th injection |
| 90 | | 3rd bleed |
| 96 | 125µg | 5th injection |
| 103 | | 4th bleed |
| 110 | | 5th bleed |
| 126 | | 6th bleed |
| 131 | | final bleed |

Testing of antiserum:

- Leave blood at room temperature for several hours to coagulate.
- Spin down 20min at 4000rpm 4°C.
- Add $NaN_3$ to the supernatant at a final concentration of 0.02%.
- Sterile filter through a 0.45µm filter.
- Test different dilutions of the antiserum in a Western blot.

### 2.4.8. IgG Purification with Ammonium Sulfate

- Centrifuge serum for 20-30min at 10000g 4°C.
- Transfer supernatant to a fresh tube and add saturated ammonium sulfate solution dropwise to produce 35-45% final saturation.
- Incubate on rotation shaker at 4°C overnight.
- Spin down 2min at 13000rpm 4°C.
- Discard the supernatant and dissolve the precipitate in 10-20% of the original volume in PBS.
- Load on Amicon Ultra 10k (Millipore) for buffer exchange to PBS.

### 2.4.9. Affinity Purification of Polyclonal Antibodies

- Spot 100µg Hat1-GST onto nitrocellulose membrane and let dry.
- Place membrane in 15ml tube.
- Block membrane with 5% milk in PBS for 1h at room temperature.
- Wash three times with PBS-T for 5min.
- Incubate with 5ml antiserum overnight at 4°C.
- Remove depleted fraction and store (→ control).
- Wash three times with PBS-T for 5min.
- Elute with 5ml 100mM glycine-HCl pH 2.5 for 2, 5, 10 and 15min.
- Remove liquid and immediately adjust to pH 7 by adding 0.1ml 1M Tris-HCl pH 8 per ml glycine.
- Load on Amicon Ultra 10k (Millipore) for buffer exchange to PBS.
- Add $NaN_3$ at a final concentration of 0.02% and store at 4°C.
- Store membrane in PBS with 0.02% $NaN_3$ – can be reused.

| | | |
|---|---|---|
| PBS-T: | 1x | PBS |
| | 0.1% | Tween-20 |

### 2.4.10. Immunoprecipitation

- Dilute overnight culture in 100ml YPD to an $OD_{600}$ of 0.3.
- Grow at 30°C to an $OD_{600}$ of ~2.0.
- Harvest cells by centrifugation for 5min at 3000rpm 4°C.
- Wash cells with 20ml cold $H_2O$, centrifuge again.
- Resuspend cells in breaking buffer (Buffer A or PBS) (250µl Buffer/50 OD units), transfer 50 $OD_{600}$ units to 2ml screw cap tubes and add equal volume glass beads.
- Break up cells with FastPrep (FastPrep®-24, MP Biomedicals), 5x 30sec at 6m/sec with 5min on ice between the runs.
- Spin down beads and cell debris for 5min at 13000rpm and 4°C and pool supernatants.
- Spin supernatant again for 15min at 13000rpm and 4°C.
- Determine protein concentration by measuring absorption at 280nm (1:200 dilution).
- Add 2µg antibody to the supernatant and incubate o/n at 4°C on a rotary shaker.
- Prepare 50µl Dynabeads® Protein G (Invitrogen) according to the manual (Step 2.1).
- Resuspend beads in 50µl breaking buffer (Buffer A or PBS) and add to the extract.
- Incubate for 4h at 4°C.
- Wash the beads three times using 200µl breaking buffer.
- Resuspend beads in 100µl breaking buffer and transfer to a new tube.
- Place tubes on the magnet, remove the supernatant and resuspend in 20µl 2x Lämmli buffer.
- Incubate at 70°C for 10min and run SDS-PAGE.

| | | |
|---|---|---|
| Buffer A: | 50mM | HEPES pH 8 |
| | 400mM | $(NH_4)_2SO_4$ |
| | 5% | Glycerol (v/v) |
| | 0.5mM | EDTA |
| | protease inhibitor cocktail, EDTA-free (Roche) | |
| 2x Lämmli Buffer: | 0.125M | Tris-HCl pH 6.8 |
| | 4% | SDS |
| | 10% | β-mercaptoethanol (freshly added) |
| | 20% | Glycerol |
| | 0.004% | Bromophenol blue |

### 2.4.11. Determination of Protein Concentration – Bradford Method

- Prepare BSA standard solutions (25, 125, 250, 500, 750, 1000, 1500, 2000µg/ml).
- Add 35µl sample to 1ml Bio-Rad Protein Assay Dye Reagent Concentrate, vortex-mix.
- Let stand for 10min at room temperature.
- Measure absorbance at 595nm.
- Draw standard curve and calculate protein concentrations of samples from the graph.

### 2.4.12. Determination of Protein Concentration – BCA Assay

- Prepare BSA standard solutions (25, 125, 250, 500, 750, 1000, 1500, 2000µg/ml).
- Add 25µl sample and 25µl 10%SDS to 1ml BCA reagent (bicinchoninic acid (Sigma) containing 0.08% $CuSO_4$) and vortex-mix.
- Incubate 30min at 37°C.
- Measure absorbance at 562nm.
- Draw standard curve and calculate protein concentrations of samples from the graph.

## 2.5. Oligonucleotides, Strains, Plasmids and Antibodies

### 2.5.1. Oligonucleotides

| Name | Sequence 5' – 3' |
|---|---|
| HAT1-antig2_fwd | ATCGGATCCCCGGAGCGGGTGATGATAACACCAAGAAAG |
| HAT1-antig2_rev | ATCGAATTCGCTAATAATACAAATATACTTAC |
| HAT2-antig2_fwd | ATCGGATCCCCGGAGCGGGTGGAGTGAGTGATTTAAGTTG |
| HAT2-antig2_rev | ATCGAATTCTAGGGCCAGTTTTACTC |
| SATflipp_5C | TTTGGAACTAACGATGCATACGAC |
| SATflipp_3C | CCTAACATATGTGAAGTGTGAAGGG |
| heukan2 | CGTCAAGACTGTCAAGGAGGG |
| heukan3 | CATCATCTGCCCAGATGCGAAG |
| 5C_HAT2_FPTag | GACACTGAAACCAGGTACTCAC |
| 55_CA2146_FPTag | GTCAGAGGATAGTCATGTCTACTTG |
| 53_HAT2-FPTag | CTTCACCTTTAGAACCTGCGGCCTCTAAAATCGACACATCTACTTC |
| 35_HAT2-pFA | GCTGCTGCAGGTCGACCGGTGTCGGAACTGGCCCTAGCTAGAG |
| 35_HAT2-pSFS | GCGCTTGGCGTAATCATGGAACTGGCCCTAGCTAGAG |
| 33_Ca2146 | ATCGGAGCTCTCGAGCGATCGCCTAGTCTAAATGTTTAGCTGTGTGG |
| 55_2_Ca2146_FPTag | AATACTATGCCGAGTCCTCC |
| 33_2_Ca2146 | CCAATACCAAACCACAAAGCC |
| FPoe_fwd | GCCGCAGGTTCTAAAGGTGAAGAATTATTCAC |
| pFA6a-backb_rev | CCGACACCGGTCGACCTGCAGCAGCAGGTTAACCTGGCTTATCG |
| SATflipp_oe_rev | CCATGATTACGCCAAGCGC |
| YEPoe_rev | CCGGGCTCTAGAACTAGTGGATC |
| FP_KpnISmaI_fwd | ATGCCCGGGTACCATGTCTAAAGGTGAAGAATTATTCAC |
| FP_AscI_rev | ATCGGCGCGCCTTATTTGTACAATTCATCCATACCATG |
| FPTag_5C | GCATCACCTTCACCTTCACC |

| Name | Sequence 5' – 3' |
|---|---|
| RFP_KpnISmaI_fwd | ATCGGTACCCGGGATGGATAACACTGAAGATGTTATTAAAG |
| RFP_ApaIAscI_rev | ATCGGGCCCGGCGCGCCTTATTGAGAACCAGAGTGTCTAG |
| 55_Ca2146_XmaI_RFP | ACTCCCGGGTCAGAGGATAGTCATGTCTACTTG |
| 53_Ca2146_XmaI_RFP | ACTCCCGGGAGCACCCTCTAAAATCGACACATCTACTTCAG |
| 53_CaHAT2oe_mCherry | CTTCTTCACCTTTTGAAACACCTGCGGCCTCTAAAATCGACACATCTACTTC |
| RFPoe_ATG_fwd | GCCGCAGGTATGGATAACACTGAAGATGTTATTAAAG |
| RFPoe_fwd | GCCGCAGGTGATAACACTGAAGATGTTATTAAAGAATTC |
| RFP_5C_rev | TTGAGTACCTTCATATGGTTTACC |
| mCherry_KpnISmaI_fwd | ATCGGTACCCGGGATGGTTTCAAAAGGTGAAGAAG |
| mCherry_ApaIAscI_rev | ATCGGGCCCGGCGCGCCTTATTTATATAATTCATCCATACCACC |
| mCherry_ATG_fwd | ATGGTTTCAAAAGGTGAAGAAG |
| mCherry_oe_fwd | GCCGCAGGTGTTTCAAAAGGTGAAGAAGATAATATGG |
| mCherry_5C_rev | GAGTACCTTCATATGGTCTACCTTC |
| 5C_CaACT1 | GAAGCAAGTATATCTGGCAAAC |
| 55_CaACT1 | CAGTACAACGAATATTTCAGCG |
| 53_CaACT1oe_RFP | CATCTTCAGTGTTATCCATACCTGCGGCTACCACCGTCCATTTTGAATG |
| 53_CaACT1oe_mCherry | CTTCACCTTTTGAAACCATTTTGAATGATTATATTTTTTTAATATTAATATCG |
| 35_CaACT1oe | GCTGCAGGTCGACCGGTGTCGGGAGTGAAATTCTGGAAATCTGG |
| 33_CaACT1 | CATAAAACAACGAGATTTACTAATACAAG |
| 3C_CaACT1 | CAACAACAACAATTTCAATCCATC |
| 5C_Ca2146 | TTACATTCACCAACTGCAGTGACC |
| 55_Ca2146 | ACGTGGGCCCGATCGGAAACGAAGCCGAGACATAGGC |
| 53_Ca2146 | ATCGCTCGAGGGCTGGTGTTGAAAAGAAAAAGTGAC |
| 35_Ca2146 | ACGTCCGCGGTAAAACTGGCCCTAGCTAGAGAC |
| 33_Ca2146 | ATCGGAGCTCTCGAGCGATCGCCTAGTCTAAATGTTTAGCTGTGTGG |
| 3C_Ca2146 | GTTTTGGCTGTAAGTGACAAGTGC |
| INT5_Ca2146 | GTACGGTCTTTCATGGAACCC |
| INT3_Ca2146 | TCGGCATAGTATTGGCTAACC |
| 5c_ASF1 | CCATTTTAAACTAGCAATAACCAAG |
| 55_ASF1_KpnI | CATGGTACCTAAAACCGCACTATCTACCG |
| 53_ASF1_ApaI_rev | TCAGGGCCCATGGAGTTTGGGTCTTGAG |
| 35_ASF1_BglII | AGTAGATCTCCAAAAGACTAGCTAAACATAAC |
| 33_ASF1_NotIApaI_rev | ATCGGGCCCGCGGCCGCGAATTTGCTGAGAGATGATGATAATC |
| 3c_ASF1_rev | TGGGGACGAAGATGATGATG |
| INT5_ASF1 | CCTGCTAGTGAATTAGTTAGTGTC |
| INT3_ASF1 | TCATCTTCATCTTCTTCCTCCTC |
| ASF1_oe_fwd | AAATACCCTCCCCAGAAAACATGTCGATAGTATCATTAACAGGAATTG |
| ASF1_AscI_rev | ATCGGCGCGCCTCTACTTCACTTTCACTAGC |
| MET3-P_SmaI_fwd | AGTCCCGGGAATGACTATTGGTAGCGTGTTC |
| MET3-P_oe_rev | GTTAATGATACTATCGACATGTTTTCTGGGGAGGGTATTTAC |
| ASF1_2_AscI_rev | ATCGGCGCGCCGAACAACTTAATATTATCACGGTGAC |
| ASF1_int_fwd | ATTAGATCATGATCAAGAATTAGATAG |
| ASF1_int_rev | GAATCTGATGATCCAACATAAG |
| ur_ASF1_fwd | ACTGGTACCTGATATACCATTAGTTATACTATGC |
| ur_ASF1_rev | ACTGGTACCACTCACATTTCAGTACCATATC |
| MET3-P_KpnI_fwd | ACTGGTACCAATGACTATTGGTAGCGTGTTC |
| 5C_ur_ASF1_fwd | ATAATGTGCTCCAACGAGTATTC |
| MET3-P_5C_rev | GCTTGGAATAGACAATTGTTCG |
| 5c_RTT109 | TTTAAGTTTATAGGTGGTGTATTTGG |
| 55_RTT109_KpnI | CATGGTACCATCCCAGTTAATTGTTTACCATCTG |
| 53_RTT109_ApaI_rev | TCAGGGCCCTAAAACAACAAGATCTTGATGTAG |
| 35_RTT109_BglII | AGTAGATCTATCGACGATAACCTCACAC |

| Name | Sequence 5' – 3' |
|---|---|
| 33_RTT109_NotIApaI_rev | ATCGGGCCCGCGGCCGCGTTATCTTGCAGCATGATAG |
| 3c_RTT109_rev | CTAGAAGTTGTAGTCTCTTGTGATG |
| INT5_RTT109 | GCATTGAGTACCGAACTTTACC |
| INT3_RTT109 | CGACACTCTACAATTACCAATTCC |
| 5C_CaHHF1 | GTATTGTTTTGTTTGTGCCTGG |
| 55_CaHHF1 | ATCCGATCGGTACCCTCTTTTATTCTTCCCCATC |
| 53_CaHHF1 | ATCGGGCCCGATTAATTGATTTATTTGTAGATG |
| 35_CaHHF1 | ATCAGATCTACTGGGTTGTATTTCTAATTGTC |
| 33_CaHHF1 | ATCGGGCCCGCGGCCGCAAACTCAGTGAGCTGTTACG |
| 3C_CaHHF1 | CCTCCATCAATTGCTTCAAACC |
| 5C_CaHHF22 | CGTCTTTCTCTCTCTTGTGTAC |
| 55_CaHHF22 | ATCGGTACCCCAAGATGAGAATAGATGGAAC |
| 53_CaHHF22 | ATCGGGCCCAAAGGAGAATATTAAAGCTTCAATG |
| 35_CaHHF22 | ATCAGATCTCTTCTTTTCTTTATGTTTTTCGATTC |
| 33_CaHHF22 | ATCGCGGCCGCTTTTCAGGCTACTTCAAAGG |
| 33_CaHHF22_ApaINotI | ATCGGGCCCGCGGCCGCTTTTCAGGCTACTTCAAAGG |
| 3C_CaHHF22 | CTCAAAGTCATACAGTCAAGCTAAC |
| 5C_CaHHT2 | TCTTCCCTTGAATATGCCCAG |
| 55_CaHHT2 | ATCCGATCGGTACCCCATCATACATCATCCATGC |
| 53_CaHHT2 | ATCGGGCCCTCTTAGGTTTTATTTCCTTGATGG |
| INT5_HHT2 | CAACAGTACCTGGCTTATATCTG |
| INT3_HHT2 | CGTTCCATCTATTCTCATCTTGG |
| HHF1 K5Q_fwd | GGTACCGGTAGAGGACAAGGTGGTAAAGGTTT |
| HHF1 K5Q_rev | AAACCTTTACCACCTTGTCCTCTACCGGTACC |
| HHF1 K5R_fwd | GGTACCGGTAGAGGAAGAGGTGGTAAAGGTTT |
| HHF1 K5R_rev | AAACCTTTACCACCTCTTCCTCTACCGGTACC |
| HHF1 K12Q_fwd | GGTAAAGGTTTAGGACAAGGTGGTGCTAAACG |
| HHF1 K12Q_rev | CGTTTAGCACCACCTTGTCCTAAACCTTTACC |
| HHF1 K12R_fwd | GGTAAAGGTTTAGGAAGAGGTGGTGCTAAACG |
| HHF1 K12R_rev | CGTTTAGCACCACCTCTTCCTAAACCTTTACC |
| RT5_CaH4 | GAGGTGGTGTTAAACGTATTTCTG |
| RT3_CaH4 | CAACATCCAATGAAGTGACGG |
| RT5_CaASF1 | TGAATATCCTCCTGAACAACCA |
| RT3_CaASF1 | ATCACCATTAAGGTCTTCATCGTC |
| RT5_CaMET3 | CTATGAGAATGGGTGGTGATAGAG |
| RT3_CaMET3 | GGACCATAGAAATCCACTCCT |

### 2.5.2. Bacterial Strains

| Name | Genotype | Source |
|---|---|---|
| DH5α | $F^-$ φ80*lacZ*ΔM15 Δ(*lacZYA-argF*)U169 *recA1 endA1 hsd*R17($r_k^-$, $m_k^+$) *pho*A *sup*E44 *thi*-1 *gyr*A96 *rel*A1 $\lambda^-$ | Invitrogen |
| TOP10 | $F^-$ *mcr*A Δ(*mrr-hsd*RMS-*mcr*BC) φ80*lacZ*ΔM15 Δ*lac*X74 *rec*A1 *ara*D139 Δ(*ara-leu*) 7697 *gal*U *gal*K *rps*L ($Str^R$) *end*A1 *nup*G $\lambda^-$ | Invitrogen |
| BL21 (DE3) | $F^-$ *omp*T *hsd*$S_B$ ($r_B^-$, $m_B^-$) *gal dcm rne*131 | Invitrogen |

### 2.5.3. Candida albicans Strains

| Name | Genotype | Parent strain |
|---|---|---|
| SC5314 | clinical isolate | |
| MT007 | *hat1*Δ::FRT/*HAT1* | |
| MT014 | *hat1*Δ::FRT/*hat1*Δ::FRT | |
| MT031 | *hat2*Δ::FRT/*HAT2* | |
| MT039 | *hat2*Δ::FRT/*hat2*Δ::FRT | |
| MT088 | *hat1*Δ::FRT/*hat1*Δ::FRT *hat2*Δ::FRT/*HAT2* | |
| CaES002 | *asf1*Δ::FRT/*ASF1* | SC5314 |
| CaES079 | *asf1*Δ::$P_{MET3}$-*ASF1*-FRT/*ASF1* | CaES002 |
| CaES004 | *rtt109*Δ::FRT/*RTT109* | SC5314 |
| CaES008 | *rtt109*Δ::FRT/*rtt109*Δ::FRT | CaES004 |
| CaES024 | *rtt109*Δ::FRT/*rtt109*Δ::*RTT109* | CaES008 |
| CaES068 | *hat1*Δ::FRT/*hat1*Δ::FRT *rtt109*Δ::FRT/*RTT109* | MT014 |
| CaES070 | *hat1*Δ::FRT/*HAT1 rtt109*Δ::FRT/*rtt109*Δ::FRT | CaES008 |
| CaES076 | *hat1*Δ::FRT/*hat1*Δ::FRT *rtt109*Δ::FRT/*rtt109*Δ::FRT | CaES070 |
| CaES005 | *HAT2*-YFP-NAT1/ *hat2*Δ::FRT | MT031 |
| CaES012 | *hat1*Δ::FRT/*hat1*Δ::FRT *HAT2*-YFP-NAT1/*HAT2* | MT014 |
| CaES031 | *hat1*Δ::FRT/*hat1*Δ::FRT *hat2*Δ/*HAT2*-YFP-FRT | MT088 |
| CaES037 | *hat1*Δ::FRT/*hat1*Δ::*HAT1*-FRT *hat2*Δ/*HAT2*-YFP | CaES031 |
| CaES039 | *hat1*Δ::FRT/*HAT1 hat2*Δ::FRT/*HAT2* | MT007 |
| CaES016 | *hhf1*Δ::FRT/*HHF1* | SC5314 |
| CaES020 | *hhf1*Δ::FRT/*hhf1*Δ::FRT | CaES016 |
| CaES030 | *hhf1*Δ::FRT/*hhf1*Δ::FRT *hhf22*Δ::FRT/*HHF22* | CaES028 |
| CaES116 | *hhf1*Δ::FRT/*HHF1 hht2-hhf22*Δ::FRT/*HHT2-HHF22* | CaES016 |
| CaES050 | *hhf1*Δ::FRT/*hhf1*Δ::*HHF1 hhf22*Δ::FRT/*HHF22* | CaES030 |
| CaES065 | *hhf1*Δ::FRT/*hhf1*Δ::*HHF1 hhf22*Δ::FRT/*HHF22* | CaES030 |
| CaES096 | *hhf1*Δ::FRT/*hhf1*Δ::*HHF1 hhf22*Δ::FRT/*HHF22* | CaES030 |
| CaES097 | *hhf1*Δ::FRT/*hhf1*Δ::*HHF1 hhf22*Δ::FRT/*HHF22* | CaES030 |
| CaES045 | *hhf1*Δ::FRT/*hhf1*Δ::*HHF1* K12Q *hhf22*Δ::FRT/*HHF22* | CaES030 |
| CaES063 | *hhf1*Δ::FRT/*hhf1*Δ::*HHF1* K12Q *hhf22*Δ::FRT/*HHF22* | CaES030 |
| CaES092 | *hhf1*Δ::FRT/*hhf1*Δ::*HHF1* K12Q *hhf22*Δ::FRT/*HHF22* | CaES030 |
| CaES047 | *hhf1*Δ::FRT/*hhf1*Δ::*HHF1* K12R *hhf22*Δ::FRT/*HHF22* | CaES030 |
| CaES048 | *hhf1*Δ::FRT/*hhf1*Δ::*HHF1* K12R *hhf22*Δ::FRT/*HHF22* | CaES030 |
| CaES064 | *hhf1*Δ::FRT/*hhf1*Δ::*HHF1* K12R *hhf22*Δ::FRT/*HHF22* | CaES030 |
| CaES093 | *hhf1*Δ::FRT/*hhf1*Δ::*HHF1* K12R *hhf22*Δ::FRT/*HHF22* | CaES030 |
| CaES094 | *hhf1*Δ::FRT/*hhf1*Δ::*HHF1* K12R *hhf22*Δ::FRT/*HHF22* | CaES030 |
| CaES095 | *hhf1*Δ::FRT/*hhf1*Δ::*HHF1* K12R *hhf22*Δ::FRT/*HHF22* | CaES030 |
| CaES083 | *hhf1*Δ::FRT/*HHF1 hat1*Δ::FRT/*hat1*Δ::FRT | MT014 |
| CaES107 | *HHF1*/*hhf1*Δ::*HHF1*-FRT *hat1*Δ::FRT/*hat1*Δ::FRT | CaES083 |

| Name | Genotype | Parent strain |
|---|---|---|
| CaES108 | *HHF1*/*hhf1*Δ::*HHF1*-FRT *hat1*Δ::FRT/*hat1*Δ::FRT | CaES083 |
| CaES143 | *HHF1*/*hhf1*Δ::*HHF1* K5Q-FRT *hat1*Δ::FRT/*hat1*Δ::FRT | CaES083 |
| CaES144 | *HHF1*/*hhf1*Δ::*HHF1* K5Q-FRT *hat1*Δ::FRT/*hat1*Δ::FRT | CaES083 |
| CaES145 | *HHF1*/*hhf1*Δ::*HHF1* K5Q-FRT *hat1*Δ::FRT/*hat1*Δ::FRT | CaES083 |
| CaES146 | *HHF1*/*hhf1*Δ::*HHF1* K5Q-FRT *hat1*Δ::FRT/*hat1*Δ::FRT | CaES083 |
| CaES147 | *hhf1*Δ/*hhf1*Δ::*HHF1* K5Q-FRT *hat1*Δ::FRT/*hat1*Δ::FRT | CaES083 |
| CaES148 | *hhf1*Δ/*hhf1*Δ::*HHF1* K5Q-FRT *hat1*Δ::FRT/*hat1*Δ::FRT | CaES083 |
| CaES149 | *hhf1*Δ/*hhf1*Δ::*HHF1* K5Q-FRT *hat1*Δ::FRT/*hat1*Δ::FRT | CaES083 |
| CaES150 | *hhf1*Δ/*hhf1*Δ::*HHF1* K5Q K12Q-FRT *hat1*Δ::FRT/*hat1*Δ::FRT | CaES083 |
| CaES151 | *hhf1*Δ/*hhf1*Δ::*HHF1* K5Q K12Q-FRT *hat1*Δ::FRT/*hat1*Δ::FRT | CaES083 |
| CaES105 | *HHF1*/*hhf1*Δ::HHF1 K12Q-FRT *hat1*Δ::FRT/*hat1*Δ::FRT | CaES083 |
| CaES106 | *HHF1*/*hhf1*Δ::*HHF1* K12Q-FRT *hat1*Δ::FRT/*hat1*Δ::FRT | CaES083 |
| CaES109 | *hhf1*Δ/*hhf1*Δ::*HHF1* K12Q-FRT *hat1*Δ::FRT/*hat1*Δ::FRT | CaES083 |
| CaES152 | *hhf1*Δ/*hhf1*Δ::*HHF1* K12Q-FRT *hat1*Δ::FRT/*hat1*Δ::FRT | CaES083 |
| CaES153 | *hhf1*Δ/*hhf1*Δ::*HHF1* K12Q-FRT *hat1*Δ::FRT/*hat1*Δ::FRT | CaES083 |
| CaES154 | *hhf1*Δ/*hhf1*Δ::*HHF1* K12Q-FRT *hat1*Δ::FRT/*hat1*Δ::FRT | CaES083 |
| CaES155 | *hhf1*Δ/*hhf1*Δ::*HHF1* K12Q-FRT *hat1*Δ::FRT/*hat1*Δ::FRT | CaES083 |
| CaES072 | *hat1*Δ::FRT/*HAT1 hhf1*Δ/Δ::*HHF1* K12Q *hhf22*Δ::FRT/*HHF22* | CaES045 |

### 2.5.4. Plasmids

| Name | DNA-insert (nucleotide position) | Parental plasmid / reference |
|---|---|---|
| pGEX-5X-2 (gb_U13857) | | GE Healthcare |
| pGEX-5X-2_Hat1 Antigen | *HAT1* (+4 to +243) | pGEX-5X-2 |
| pGEX-5X-2_Hat2 Antigen | *HAT1* (+4 to +156) | pGEX-5X-2 |
| pGEX-5X-2_Hat1 Antigen2 | *HAT2* (+1093 to +1261) | pGEX-5X-2 |
| pGEX-5X-2_Hat2 Antigen2 | *HAT2* (+1006 to +1161) | pGEX-5X-2 |
| YEp352-GFP | | Ingrid Frohner |
| YEp352-CFP | | Ingrid Frohner |
| YEp352-YFP | | Ingrid Frohner |
| pSFS3b | | Michael Tscherner |
| pSFS3b-GFP | GFP | pSFS3b |
| pSFS3b-YFP | YFP | pSFS3b |
| pSFS3b-CFP | CFP | pSFS3b |
| pFA6a-GFP | | Michael Tscherner |
| pFA6a-YFP | YFP | pFA6a-GFP |
| pFA6a-CFP | CFP | pFA6a-GFP |

| Name | DNA-insert (nucleotide position) | Parental plasmid / reference |
|---|---|---|
| pMG2169-RFP-URA3 | | FGSC (Gerami-Nejad et al., 2009) |
| pFA6a-RFP | RFP | pFA6a |
| pSFS3b-RFP | RFP | pSFS3b |
| pMG2254-mCherry-URA3 | | FGSC (Gerami-Nejad et al., 2009) |
| pFA6a-mCherry | mCherry | pFA6a |
| pSFS3b-mCherry | mCherry | pSFS3b |
| pSFS3b-3'HAT2_RFP | downstream region *HAT2* | pSFS3b-RFP |
| pSFS3b-HAT2_RFP | *HAT2* (+615 to +1146) | pSFS3b-HAT2_RFP |
| pSFS3b-3'ASF1 | downstream region *ASF1* | pSFS3b |
| pSFS3b-ASF1 urdr | upstream region *ASF1* | pSFS3b-3'ASF1 |
| pFA6a-MET3-P_ASF1 | $P_{MET3}$-*ASF1* (+1 to +697) | pFA6a |
| pFA6a-MET3-P_ASF1_2 | $P_{MET3}$-*ASF1* (+1 to +299) | pFA6a |
| pSFS3b-MET3P-ASF1-drASF1 | $P_{MET3}$-*ASF1* (+1 to +1235) | pSFS3b-3'ASF1 |
| pSFS3b-urASF1-MET3P-ASF1-drASF1 | upstream region $P_{ASF1}$ | pSFS3b-MET3P-ASF1-drASF1 |
| pSFS3b-3'RTT109 | downstream region *RTT109* | pSFS3b |
| pSFS3b-RTT109 urdr | upstream region *RTT109* | pSFS3b-3'RTT109 |
| pSFS3b-CaRTT109-Rev | *RTT109* (-348 to +1653) | pSFS3b-3'RTT109 |
| pSFS3b-3'HHF1 | downstream region *HHF1* | pSFS3b |
| pSFS3b-HHF1 urdr | upstream region *HHF1* | pSFS3b-3'HHF1 |
| pSFS3b-CaHHF1-Rev | *HHF1* (-521 to +803) | pSFS3b-3'HHF1 |
| pSFS3b-CaHHF1 K5Q | *HHF1* K5Q | pSFS3b-CaHHF1-Rev |
| pSFS3b-CaHHF1 K5Q K12Q | *HHF1* K5Q K12Q | pSFS3b-CaHHF1 K12Q |
| pSFS3b-CaHHF1 K12Q | *HHF1* K12Q | pSFS3b-CaHHF1-Rev |
| pSFS3b-CaHHF1 K12R | *HHF1* K12R | pSFS3b-CaHHF1-Rev |
| pSFS3b-3'HHF22 | downstream region *HHF22* | pSFS3b |
| pSFS3b-HHF22 urdr | upstream region *HHF22* | pSFS3b-3'HHF22 |
| pSFS3b-5'HHT2-3'HHF22 | upstream region *HHT2* | pSFS3b-3'HHF22 |

### 2.5.5. Antibodies

| Antibody | Dilution | Type | Source |
|---|---|---|---|
| α-H4 | 1:1000 | rabbit, polyclonal | Abcam, ab10158 |
| α-H4K12 | 1:3000 | rabbit, polyclonal | Upstate, cat.#: 07-595 |
| α-H3 | 1:1000 | rabbit, polyclonal | Abcam, ab46765 |
| α-GFP | 1:1000 | mouse, mixture of 2 monoclonal ab | Roche, cat.#: 11814460001 |
| α-RFP | 1:1000 | rabbit, polyclonal | BioVision, cat.#: 3993-100 |
| α-Hat1 | 1:500 | rabbit, polyclonal | rabbit #129 |

| Antibody | Dilution | Type | Source |
|---|---|---|---|
| α-Hat2 | 1:4000 | rabbit, polyclonal | rabbit #128 |
| α-rabbit IRDye 800CW | 1:14000 | goat | LI-COR, cat.#: 926-32211 |
| α-rabbit IRDye 680 | 1:14000 | goat | LI-COR, cat.#: 926-32221 |
| α-mouse IRDye 800CW | 1:14000 | goat | LI-COR, cat.#: 926-32210 |
| α-mouse IRDye 680 | 1:14000 | goat | LI-COR, cat.#: 926-32220 |

# 3. Results

## 3.1. α-Hat1 and α-Hat2 Antibodies

Polyclonal antibodies against *Ca*Hat1 and *Ca*Hat2 should be raised to obtain a tool for further characterization of the function of these two proteins in *Candida albicans*. The antibodies should allow the determination of protein levels via immunoblotting. Furthermore, they should be used in immunoprecipitation experiments to identify binding partners of *Ca*Hat1 and *Ca*Hat2.

### 3.1.1. N-terminal Antigen

The first step for raising antibodies against *Ca*Hat1 and *Ca*Hat2 was to select antigenic regions for both proteins, which were then used for immunization of two rabbits. The plasmids pGEX-5X-2_Hat1-Antigen and pGEX-5X-2_Hat2-Antigen (Figure 8) were constructed by Michael Tscherner for this purpose. The N-terminal regions of Hat1 and Hat2 were chosen (amino acids 2 – 81 and 2 – 52 respectively). The sequence was PCR-amplified from genomic DNA and cloned into the pGEX-5X-2 vector. pGEX-5X-2 contains the glutathione-S-transferase ORF after the Ptac promoter. This promoter is repressed by *LacI* which can be inactivated by addition of IPTG. The antigenic regions of Hat1 and Hat2 were cloned into pGEX-5X-2 in frame with GST to create a GST-Hat1 and GST-Hat2 fusion protein, respectively.

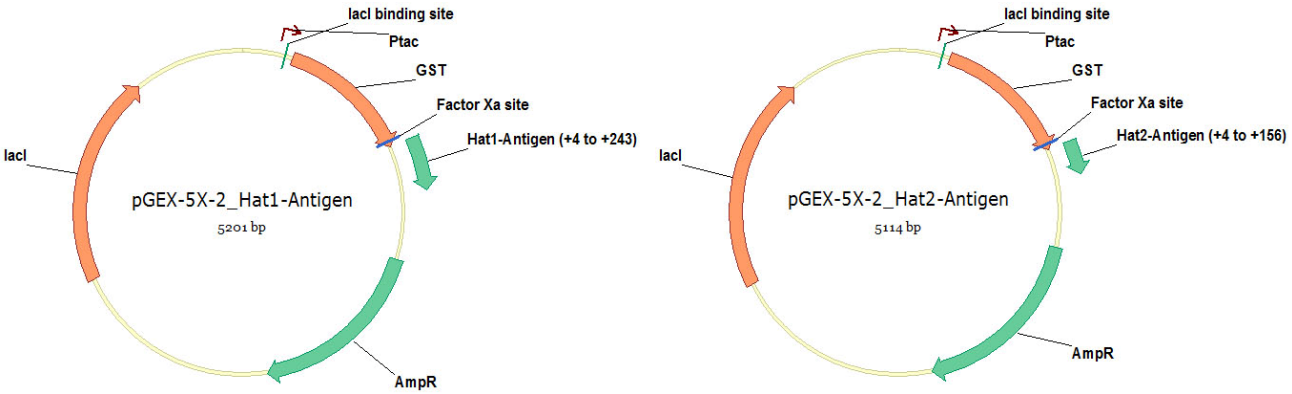


**Figure 8: Plasmids to express the N-terminal antigen of Hat1 and Hat2.** The N-terminal part of the coding sequence of Hat1 and Hat2 was cloned in frame after GST into pGEX-5X-2.

The expression of GST-Hat1 in bacterial DH5α cells after induction with IPTG was examined as described in section 2.4.5. Expression was induced by addition of IPTG to a final concentration of 0.2mM. Aliquots were taken at several time points to determine the optimal induction time. Furthermore, 0.32 $OD_{600}$ equivalents were separated trough a 12%

SDS-PAGE gel and stained with Coomassie Blue. Hardly any expression could be detected. Thus, the experiment was repeated with a final concentration of 1mM IPTG. This time 0.2 $OD_{600}$ equivalents taken from several time points were separated through a 12% SDS-PAGE gel and stained with Coomassie Blue. Since expression levels were still relatively low, even after induction with 1mM IPTG and incubation for 4 hours, pGEX-5X-2_Hat1-Antigen, as well as pGEX-5X-2_Hat2-Antigen were transformed into protease deficient BL21 (DE3) cells. Expression of GST-Hat1 and GST-Hat2 in BL21 cells was examined after induction with 1mM, 5mM and 10mM IPTG for 3 hours. Again, 0.2 $OD_{600}$ equivalents were separated through a 12% SDS-PAGE gel and stained with Coomassie Blue. A concentration of 1mM IPTG was found to be sufficient to induce expression of GST-Hat1 and GST-Hat2 (Figure 9).

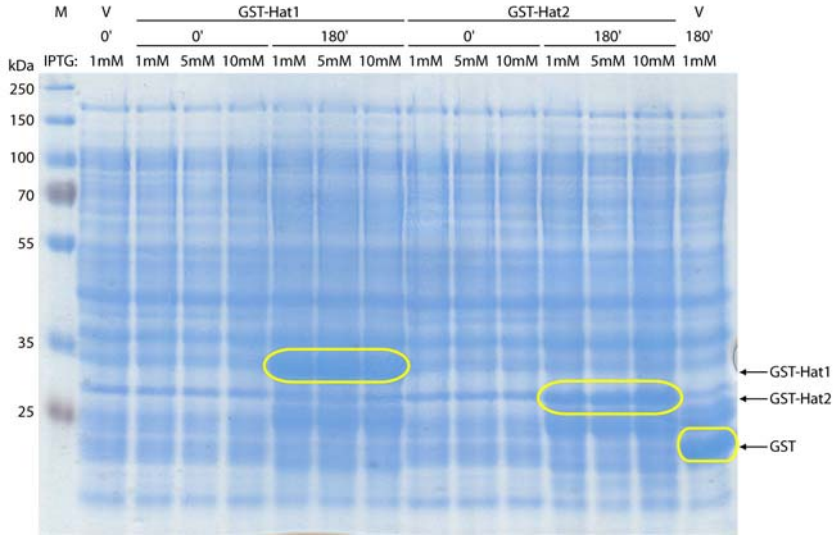


**Figure 9: Induction of GST-Hat1 and GST-Hat2 expression.** BL21 cells harboring pGEX-5X-2 (V), pGEX-5X-2_Hat1-Antigen or pGEX-5X-2_Hat2-Antigen were induced to express the GST-fusion proteins (GST 27.5kDa, GST-Hat1 36.2kDa, GST-Hat2 33.3kDa) by addition of 1mM, 5mM and 10mM IPTG and incubated at 30°C for 180 minutes. 0.2 $OD_{600}$ equivalents before (0') and after (180') induction were separated through a 12% SDS-PAGE gel and stained with Coomassie Blue.

The next step was to determine the solubility of the GST-Hat1 and GST-Hat2 fusion proteins. Solubility was tested as described in section 2.4.5. Expression of the fusion proteins was induced by addition of IPTG to a final concentration of 1mM. Cells were grown at 30°C for 3 hours before they were lysed by sonication. The soluble fraction was separated from the insoluble fraction by centrifugation. Aliquots of total extracts, the insoluble fractions and the soluble fractions were separated through a 12% SDS-PAGE gel and stained with Coomassie Blue. Unfortunately the majority of the fusion proteins were detected in the insoluble fractions, which are so-called inclusion bodies (Figure 10).

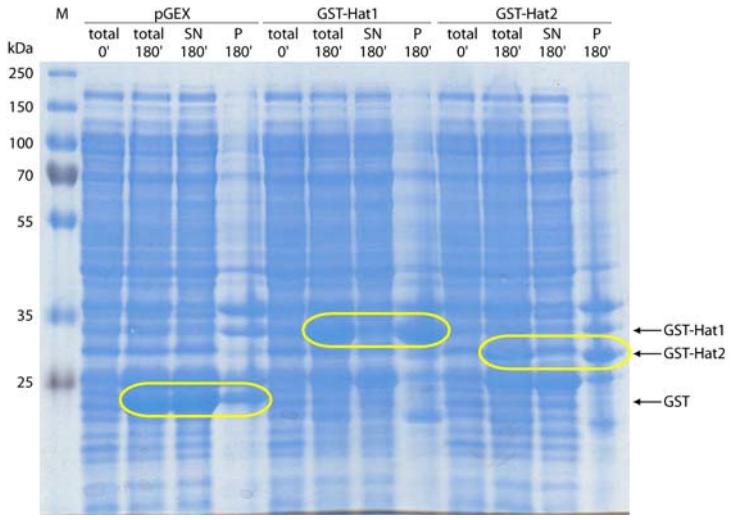


**Figure 10: Solubility of GST-Hat1 and GST-Hat2.** BL21 cells harboring pGEX-5X-2, pGEX-5X-2_Hat1-Antigen or pGEX-5X-2_Hat2-Antigen were induced to express the GST-fusion proteins (GST 27.5kDa, GST-Hat1 36.2kDa, GST-Hat2 33.3kDa) by addition of 1mM IPTG and incubated at 30°C for 180 minutes. 0.2 $OD_{600}$ equivalents of total extracts, 0.5 $OD_{600}$ equivalents of the insoluble fraction and 8µl of the soluble fraction were separated through a 12% SDS-PAGE gel and stained with Coomassie Blue.

To increase the solubility of fusion proteins, bacterial cells were grown at a lower temperature. First, induction with 1mM IPTG at 25°C was checked. Aliquots were taken at several time points and 0.2 $OD_{600}$ equivalents were separated through a 12% SDS-PAGE gel and stained with Coomassie Blue. Even though the expression was not very strong, solubility of GST-Hat1 was tested. Expression was induced with 1mM IPTG and cells were grown at 25°C for 2 hours. Cells were lysed by sonication. Soluble and insoluble fractions were separated by centrifugation. Aliquots of total extracts, the insoluble fraction and the soluble fraction were separated through a 12% SDS-PAGE gel and stained with Coomassie Blue. Still the majority of GST-Hat1 was found in the insoluble fraction (Figure 11).

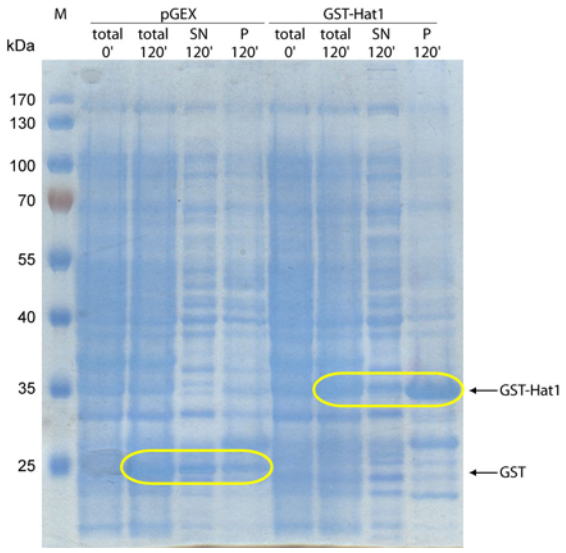


**Figure 11: Solubility of GST-Hat1 at 25°C.** BL21 cells harboring pGEX-5X-2 or pGEX-5X-2_Hat1-Antigen were induced to express the GST-fusion protein (GST 27.5kDa, GST-Hat1 36.2kDa) by addition of 1mM IPTG and incubated at 25°C for 120 minutes. 0.2 $OD_{600}$ equivalents of total extracts, 0.5 $OD_{600}$ equivalents of the insoluble fraction and 8µl of the soluble fraction were separated through a 12% SDS-PAGE gel and stained with Coomassie Blue.

To purify the antigen from the insoluble fraction, inclusion bodies were prepared as described in section 2.4.6. Expression of the fusion proteins was induced with 1mM IPTG. Cells were grown at 30°C for 4 hours. Cells were lysed using lysozyme and sonication. The insoluble fraction was washed with different buffers to obtain a cleaner inclusion body pellet. Samples were taken at every step and were separated through a 12% SDS-PAGE gel. Coomassie Blue-staining revealed that there were still other proteins, as well as degraded fusion proteins present in the inclusion bodies (Figure 12).

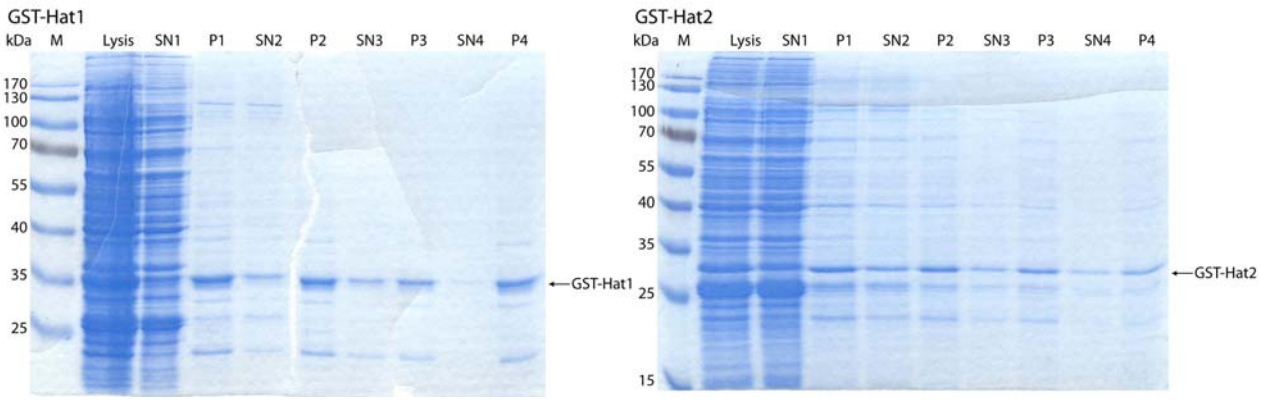


**Figure 12: Inclusion body preparation of GST-Hat1 and GST-Hat2.** BL21 cells harboring pGEX-5X-2 or pGEX-5X-2_Hat1-Antigen were induced to express the GST-fusion proteins (GST-Hat1 36.2kDa, GST-Hat2 33.3kDa) by addition of 1mM IPTG and incubated at 30°C for 240 minutes. Cells were lysed by lysozyme treatment and sonication (Lysis). Soluble (SN1) and insoluble fractions (P1) were separated by centrifugation. The pellet was washed with lysis buffer + 1% NP-40 (SN2, P2), lysis buffer + 2M urea (SN3, P3) and finally with only lysis buffer (SN4, P4). 0.15 $OD_{600}$ equivalents were separated through a 12% SDS-PAGE gel and stained with Coomassie Blue.

### 3.1.2. C-terminal Antigen

Since the fusion protein of GST with the N-terminal region of Hat1 and Hat2 did not produce a soluble protein, a second antigenic region was chosen. This time the C-terminal region of Hat1 and Hat2 was used. Amino acids 365 to 413 of Hat1 and 363 to 382 of Hat2 were selected. These regions were PCR-amplified using primers HAT1-antig2_fwd and HAT1-antig2_rev for Hat1 and HAT2-antig2_fwd and HAT2-antig2_rev for Hat2. The fragments were cloned in frame with GST into pGEX-5X-2 with BamHI and EcoRI resulting in the plasmids pGEX-5X-2_Hat1-Antigen2 and pGEX-5X-2_Hat2-Antigen2 (Figure 13).

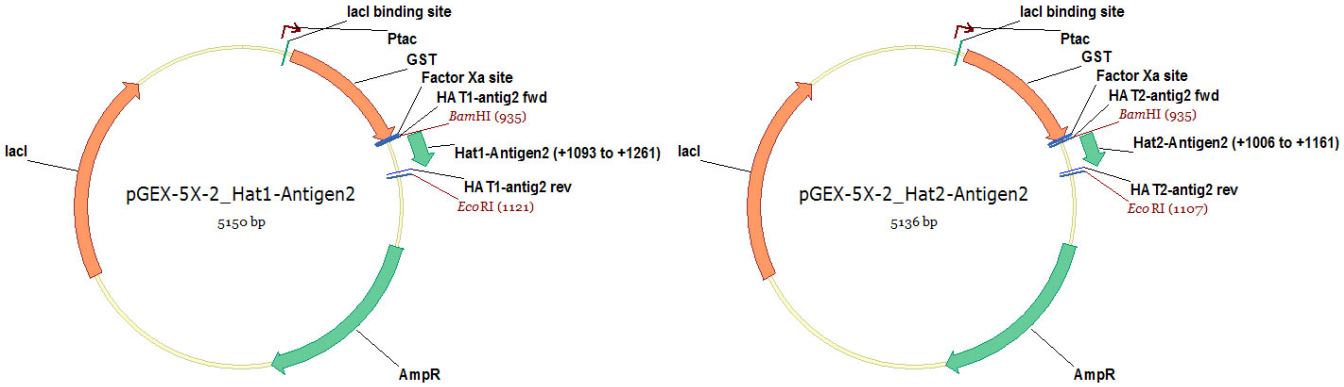


**Figure 13: Plasmids to express the C-terminal antigen of Hat1 and Hat2.** The C-terminal part of the coding sequence of Hat1 and Hat2 was cloned in frame after GST into pGEX-5X-2.

The plasmids were transformed into BL21 cells and the induction of fusion protein expression with 1mM IPTG was tested. Aliquots were taken at several time points to determine the optimal induction time and 0.2 $OD_{600}$ equivalents were separated through 12% SDS-PAGE gel followed by staining with Coomassie Blue. An induction time of 2 hours for GST-Hat1 and 4 hours for GST-Hat2 was found to be satisfactory and was used for all further experiments.

Subsequently, the solubility of the fusion protein was tested. After induction with 1mM IPTG and incubation for 2 hours for GST-Hat1 and 4 hours for GST-Hat2 at 30°C cells were lysed by sonication. Soluble and insoluble fractions were separated by centrifugation. Aliquots of the insoluble fraction and the soluble fraction were separated through a 12% SDS-PAGE gel and stained with Coomassie Blue. A significant amount of fusion protein was found in the soluble fraction (Figure 14).

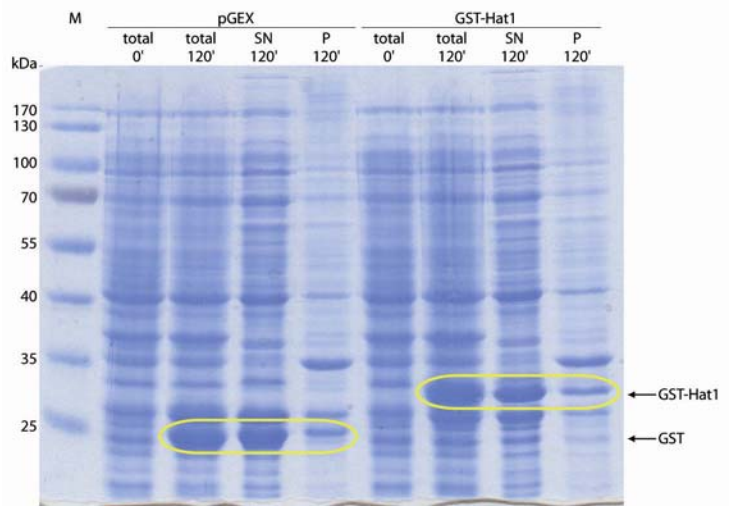


**Figure 14: Solubility of GST-Hat1 Antigen 2.** BL21 cells harboring pGEX-5X-2 or pGEX-5X-2_Hat1-Antigen2 were induced to express the GST-fusion protein (GST 27.5kDa, GST-Hat1 32.8kDa) by addition of 1mM IPTG and incubated at 30°C for 120 minutes. 0.2 $OD_{600}$ equivalents of total extracts, 0.5 $OD_{600}$ equivalents of the insoluble fraction and 8µl of the soluble fraction were separated through a 12% SDS-PAGE gel and stained with Coomassie Blue.

Expression of the fusion proteins was repeated in a larger volume to increase the yield of purified fusion proteins. Purification of the GST-fusion proteins used glutathione sepharose beads as described in section 2.4.5. Therefore, cells were lysed by sonication. The soluble fraction was incubated with glutathione sepharose beads overnight. Finally, the GST-Hat1 and GST-Hat2 fusion proteins were eluted from the sepharose beads with glutathione. Samples were taken at every step, separated through a 12% SDS-PAGE gel and stained with Coomassie Blue (Figure 15).

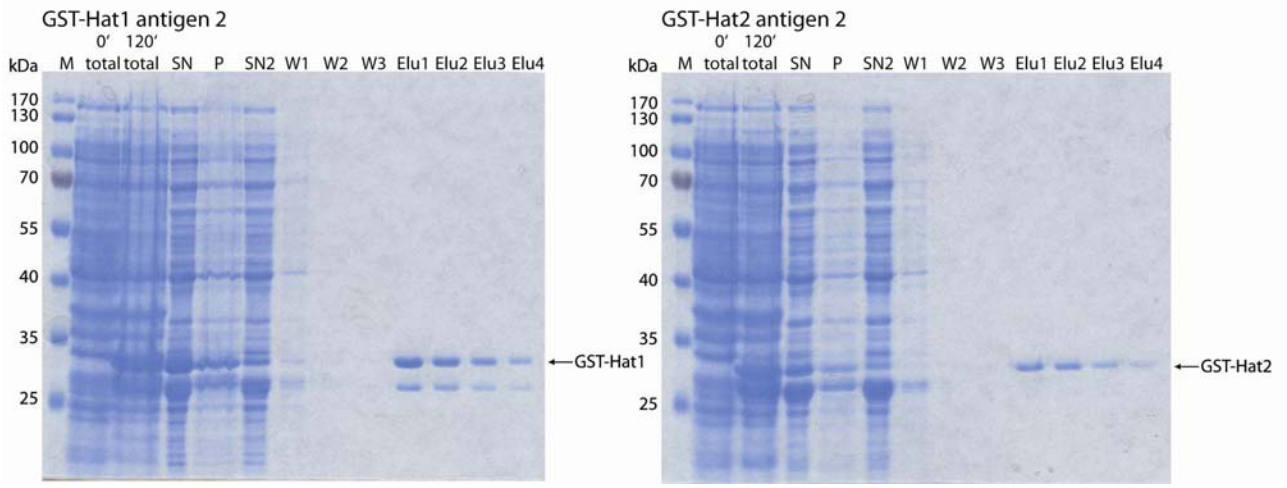


**Figure 15: Elution of Antigen.** 500ml LB were inoculated with BL21 cells harboring pGEX-5X-2_Hat1-Antigen2 or pGEX-5X-2_Hat2-Antigen2 and grown for 120 minutes for Hat1 and 240 minutes for Hat2 at 30°C. Cells were lysed by sonication. Sepharose glutathione beads were added to the soluble fraction. The GST-fusion protein (GST-Hat1 32.8kDa, GST-Hat2 32.0kDa) was eluted from the beads using glutathione buffer. 0.25 $OD_{600}$ equivalents from each step were separated through a 12% SDS-PAGE gel and stained with Coomassie Blue.

The concentration of the purified protein was determined using the BCA assay as described in section 2.4.12. The purification of the GST-fusion protein was repeated several times to yield enough antigen for immunization of the rabbits. The purified GST-fusion proteins were loaded on an Amicon Ultra 10k to exchange the buffer to PBS. In total, about 5mg of GST-Hat1 antigen 2 and 4mg of GST-Hat2 antigen 2 were purified (Figure 16).

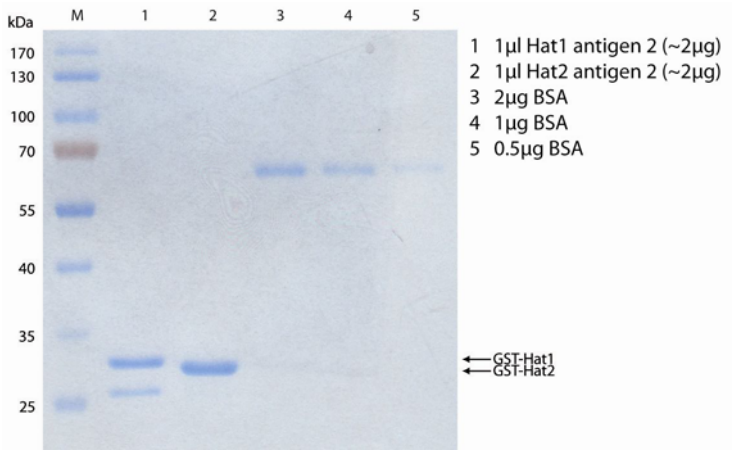


**Figure 16: Purified C-terminal antigen.** 1µl (conc. ~2mg/ml) of the purified GST-Hat1 (lane 1, 32.8kDa) and GST-Hat2 (lane 2, 32.0kDa) fusion protein in PBS were loaded onto a 12% SDS-PAGE gel and separated. Lane 3, 4 and 5 show 2µg, 1µg and 0.5µg BSA, respectively. The gel was stained with Coomassie Blue.

### 3.1.3. Antiserum Testing

The purified Hat1 and Hat2 antigens were used to immunize New Zealand White rabbits. Before the rabbits were injected with antigen for the first time their blood was tested for already present antibodies reacting with *Candida albicans* proteins as described in section 2.4.7. Blood was drawn and left at room temperature for several hours to coagulate and was then centrifuged. The cleared serum supernatant was used as the antiserum. TCA-extracts of wild type *Candida albicans* strain SC5314 were prepared as described in section 2.2.2, separated through a 12% SDS-PAGE gel and blotted onto nitrocellulose membranes as described in section 2.4.4. The blot was incubated with various antiserum dilutions overnight at 4°C. Antibodies reacting with *Candida albicans* proteins were detected with a secondary IRDye labeled antibody (Figure 17). As this pre-immune serum seemed clear at higher dilutions, the rabbits were injected with antigen according to the schedule described in section 2.4.7.

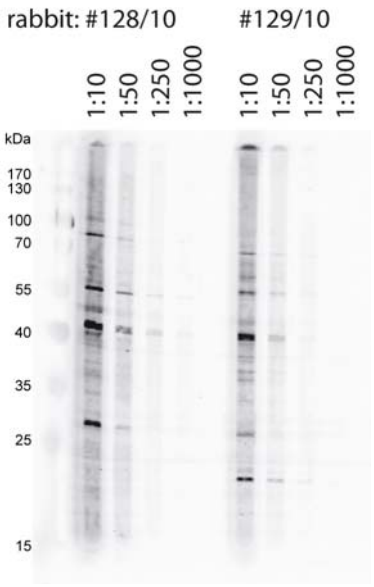


**Figure 17: Pre-immune serum control.** Wildtype TCA-extract was separated through a 12% SDS-PAGE gel and blotted onto a nitrocellulose membrane. The blot was incubated with 1:10, 1:50, 1:250 and 1:1000 dilutions of antiserum from rabbits #128 and #129. Reacting antibodies were detected with an anti-rabbit IRDye800CW labeled secondary antibody.

Approximately 2 weeks after each antigen injection boosting the rabbits' immune reaction their blood was drawn and tested for specific antibodies against Hat1 and Hat2, respectively. Antisera were prepared as described before. TCA-extracts from wild type, *hat1*Δ/Δ and *hat2*Δ/Δ strains were prepared, 0.4 $OD_{600}$ equivalents were separated through a 12% SDS-PAGE gel and blotted onto a nitrocellulose membrane. The blot was incubated with several dilutions of the antiserum overnight at 4°C. Antibodies were detected with a secondary IRDye labeled antibody.

Figure 18 shows that the Hat2-antiserum from the 6$^{th}$ and 7$^{th}$ bleed recognized a protein with the molecular mass of Hat2 in the wild type extract while this band was missing in the *hat2*Δ/Δ extract. Thus, a functional Hat2-specific antibody was obtained.

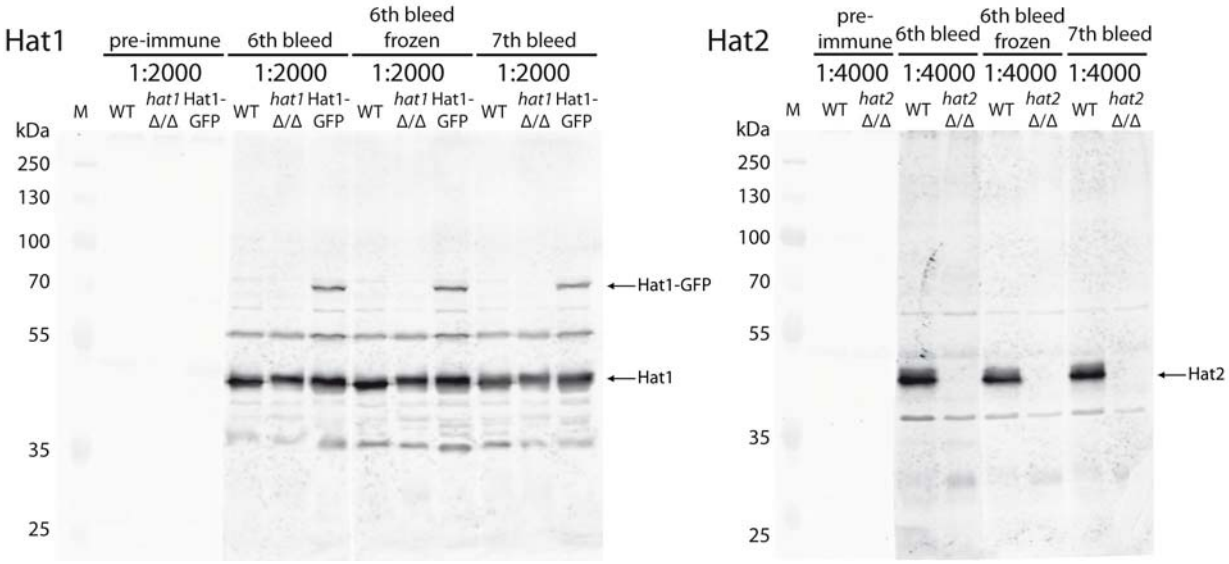


**Figure 18: Hat1 and Hat2 6th and 7th bleed.** TCA-extracts of indicated strains were separated through a 12% SDS-PAGE gel and blotted onto a nitrocellulose membrane. The membrane was cut and incubated with dilutions of pre-immune serum, 6th bleed and 7th bleed. An aliquot of the 6th bleed was frozen at -80°C before using it for the Western blot to test stability of the antibody. Bands were detected using IRDye800CW labeled secondary antibody. For Hat1, a strong cross reaction at the same molecular mass as Hat1 (48.4kDa) was detected. Therefore, the Hat1 band was not visible. Hat1-GFP (75.2kDa), however, is recognized. A strong signal for Hat2 (42.9kDa) was detected, which is missing in the *hat2*Δ/Δ control.

The Hat1-antiserum gave a signal at approximately 48kDa which would correspond to the calculated mass of Hat1. Unfortunately, this signal was present in the wild type as well as in the *hat1*Δ/Δ extract. To test whether the Hat1-antiserum really recognizes Hat1, a GFP-tagged Hat1 was used as a control. This protein is about 75.2kDa and can easily be distinguished from the unspecific bands detected with the Hat1-antiserum. Hat1-GFP was recognized by the Hat1-antiserum, indicating that a functional Hat1-antibody was present in the antiserum. The signal at 48kDa in the *hat1*Δ/Δ extract seems to come from another protein of this size which is recognized as well.

### 3.1.4. Purification of α-Hat1-Antiserum

Since the Hat1-antiserum also recognized another protein of the same mobility as Hat1, purification of the specific Hat1-antibody was necessary. In the first step, the 4th bleed was used for affinity purification of the antibody as described in section 2.4.9. 50µg purified GST-Hat1 antigen was spotted onto a membrane and incubated with 300µl antiserum overnight. Bound antibodies were eluted by incubating in 100mM glycine pH 2.5 for 2, 5, 10 and 15 minutes. A blot with wildtype and *hat1*Δ/Δ TCA-extracts was incubated with dilutions of the elutions overnight. Antibodies were detected with a secondary IRDye labeled antibody. As Figure 19 shows, in the third and fourth elution step (10min and 15min) a

protein of 48kDa, the size of Hat1, was recognized in the wild type but not in the *hat1*Δ/Δ extracts, suggesting that a pure, Hat1-specific antibody could be obtained this way.

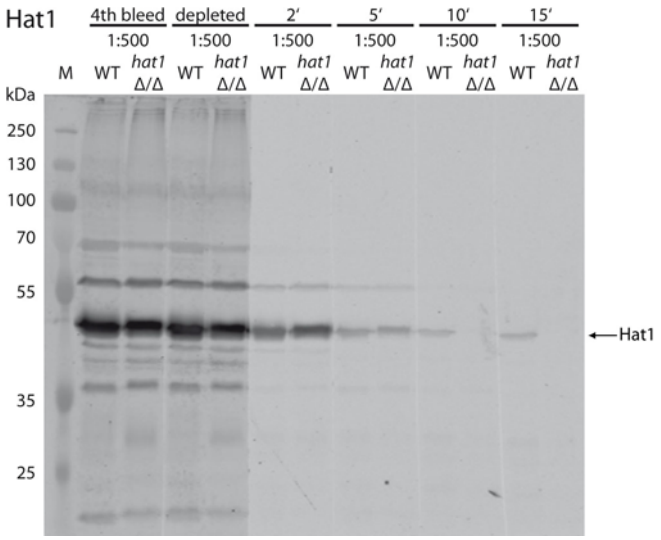


**Figure 19: Purification of Hat1-antiserum 4th bleed.** 0.4 $OD_{600}$ equivalents TCA-extract of wild type (WT) (Hat1 48.4kDa) and *hat1*Δ/Δ strains were separated through a 12% SDS-PAGE gel and blotted onto a nitrocellulose membrane. The membrane was cut and incubated with 1:500 dilutions of antiserum, Hat1-antibody depleted antiserum and eluted Hat1-antibody after 2, 5, 10 and 15 minutes elution.

The purification was repeated with the 6th bleed. 100µg purified GST-Hat1 antigen was spotted on a membrane and incubated with 5ml antiserum overnight. Elution and testing was performed as described above. Even in the last elution step, a signal at 48kDa remained in the *hat1*Δ/Δ extracts. The purification procedure was repeated with varying amounts of spotted antigen and antiserum, as well as different elution times. However, attempts to produce a pure Hat1-antibody solution from the 6th bleed failed.

In order to purify Hat1-antibody from the 6th bleed an additional purification step was introduced before affinity purification. Antibody IgG precipitation was performed as described in section 2.4.8. Saturated ammonium sulfate solution was added to 975µl antiserum at a final saturation of 35% and incubated on a rotation shaker overnight. After centrifugation, the pellet was redisolved in PBS. The remaining salt was removed by buffer exchange to PBS. This antibody solution was then used for affinity purification. It was incubated with 50µg GST-Hat1 spotted onto a membrane. Antibodies were eluted for 5, 10, 15 and 20 minutes. Unfortunately the Western blot revealed that even after this additional purification step the unspecific signal at 48kDa remained (Figure 20).

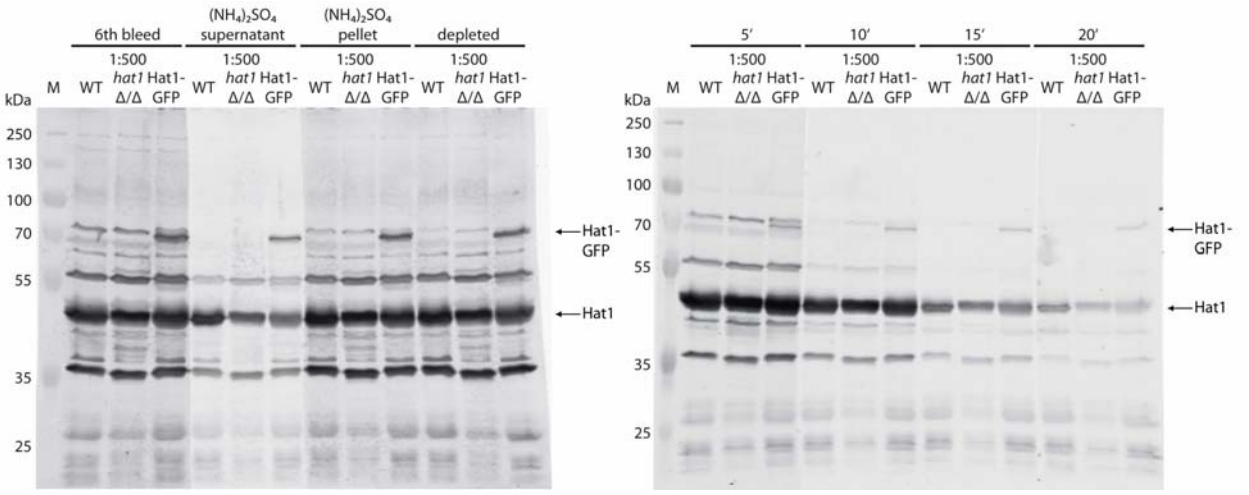


**Figure 20: Purification of Hat1-antiserum 6th bleed.** 0.4 $OD_{600}$ equivalents TCA-extract of the wildtype (WT) (Hat1 48.4kDa), *hat1*Δ/Δ strain and Hat1-GFP (75.2kDa) expressing strain were separated through a 12% SDS-PAGE gel and blotted onto a nitrocellulose membrane. The membrane was cut and incubated with 1:500 dilutions of antiserum aliquots taken during the purification of the Hat1-antiserum.

The purification was repeated with the remaining 4th bleed: 450µg GST-Hat1 was spotted onto a membrane and incubated with 3.8ml antiserum overnight. The antibody was eluted for 7, 10 and 15 minutes with 100mM glycine pH 2.5. Testing by immunoblotting revealed the last elution step to be pure Hat1-specific antibody (Figure 21). For storage the buffer of this fraction was exchanged to PBS over an Amicon Ultra 10k. About 3ml of pure Hat1-antibody solution for use in Western blots and immunoprecipitation experiments was obtained this way.

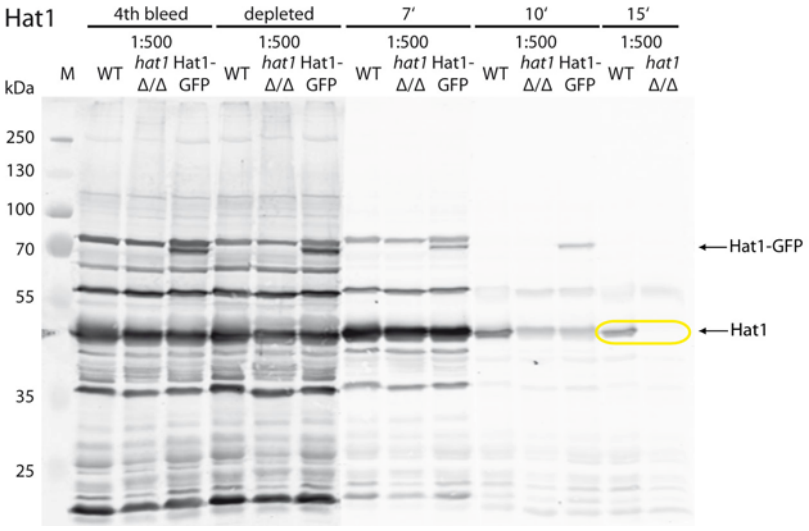


**Figure 21: Purification of remaining Hat1-antiserum 4th bleed.** 0.4 $OD_{600}$ equivalents TCA-extract of wildtype (WT) (Hat1 48.4kDa) *hat1*Δ/Δ strain and Hat1-GFP (75.2kDa) expressing strain were separated through a 12% SDS-PAGE gel and blotted onto a nitrocellulose membrane. The membrane was cut and incubated with 1:500 dilutions of antiserum, Hat1-antibody depleted antiserum and eluted Hat1-antibody after 7, 10 and 15 minutes elution.

### 3.1.5. Immunoprecipitation of Hat1 and Hat2

To investigate the interaction of Hat1 with Hat2, the raised antibodies were used to immunoprecipitate Hat1 and Hat2, respectively. The goal was to confirm a suspected interaction between Hat1 and Hat2 by co-precipitating one with the other. Furthermore, a possible interaction of Hat1/Hat2 with histone H4, the substrate of Hat1, should be tested.

Hat2-immunoprecipitation

Hat2 was immunoprecipitated as described in section 2.4.10. Two hundred $OD_{600}$ equivalents of wild type and Hat2-deficient cells were broken with glass beads in the FastPrep. Protein extracts were incubated with 50µl of the Hat2-antiserum overnight. Antibodies and bound proteins were precipitated by binding to magnetic beads for 4 hours. Finally, 0.01 $OD_{600}$ equivalents of the input and the supernatant after immunoprecipitation and half of the immunoprecipitated material were separated through a 15% SDS-PAGE gel and visualized by silver staining. At about 43kDa, the predicted mobility of Hat2, a protein band was visible which was missing in the *hat2*Δ/Δ strain. The IP was then analyzed by immunoblotting. Therefore, 1 $OD_{600}$ equivalent of the input and the supernatant after immunoprecipitation and half of the immunoprecipitated material was separated through a 15% SDS-PAGE gel and blotted onto a nitrocellulose membrane. Hat2 was detected in the precipitated fraction of the wild type. Unfortunately, no Hat1 or histone H4 was detectable in the IP (Figure 22).

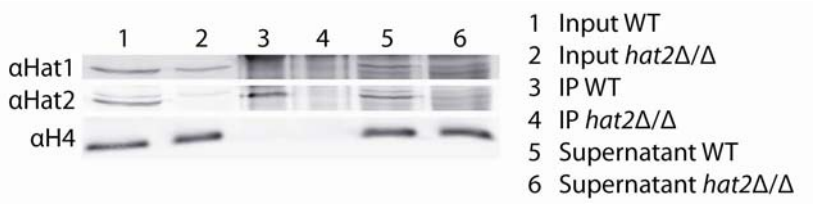


**Figure 22: Hat2 immunoprecipitation.** Wild type and *hat2*Δ/Δ strains were grown to an $OD_{600}$ of 2, harvested and broken with glass beads in breaking buffer A. 50µl Hat2-antiserum was added to protein extracts and incubated overnight at 4°C. Antibodies were precipitated by binding to magnetic beads. 1 $OD_{600}$ equivalent of input and supernatant after immunoprecipitation, and half of the immunoprecipitated material, was separated through a 15% SDS-PAGE gel and blotted onto a nitrocellulose membrane. Hat1 (48.4kDa), Hat2 (42.9kDa) and histone H4 (11.6kDa) were detected with specific antibodies.

The immunoprecipitation was repeated as described above with 10µl Hat2-antiserum. This time 0.1 $OD_{600}$ equivalents of the input and the supernatant after immunoprecipitation and half of the immunoprecipitated material were separated through a 12% SDS-PAGE gel and visualized by silver staining. Again a band corresponding to Hat2 was visible in the immunoprecipitated fraction of the wild type. However, in the Western blot analysis, no Hat1 was detectable in the IP.

Therefore, the immunoprecipitation was repeated with a less stringent breaking buffer (10mM Tris-HCl pH 8.0, 150mM NaCl, 0.1% Nonidet P40) to increase the binding of Hat1 to Hat2. This time 3µl Hat2-antiserum were used to precipitate Hat2. Again, 0.1 $OD_{600}$ equivalents of the input and the supernatant after immunoprecipitation and half of the immunoprecipitated material were separated through a 12% SDS-PAGE gel and visualized by silver staining. Hat2 was visible in the immunoprecipitated fraction of the wild type. However, in the Western blot, no Hat1 was detectable in the precipitated fraction (Figure 23).

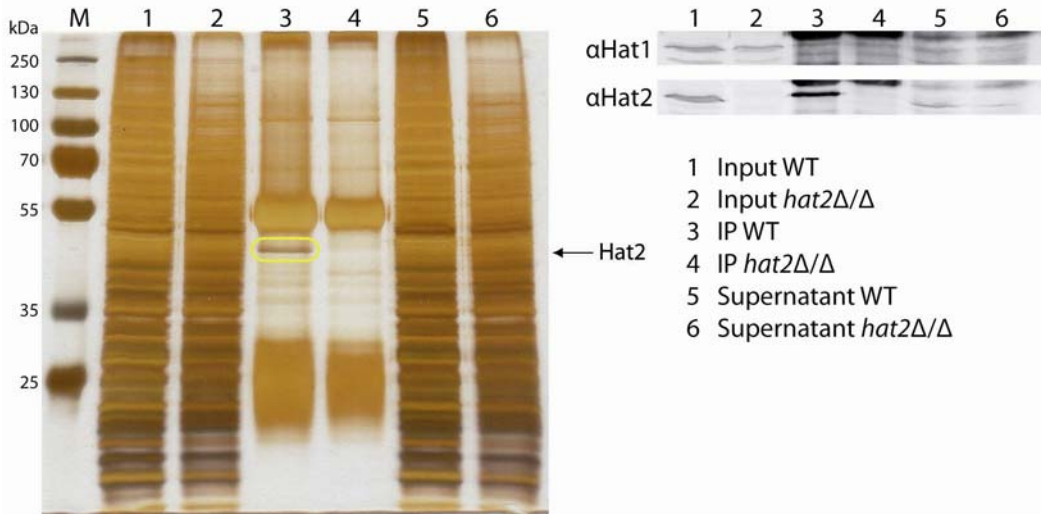


**Figure 23: Hat2 immunoprecipitation.** Wild type and *hat2*Δ/Δ strains were grown to an $OD_{600}$ of 2, harvested and broken up with glass beads in 10mM Tris-HCl pH 8.0, 150mM NaCl, 0.1% Nonidet P40. 3µl Hat2-antiserum was added to protein extracts and incubated overnight at 4°C. Antibodies were precipitated by binding to magnetic beads. For silver staining, 0.1 $OD_{600}$ equivalents of input and supernatant after immunoprecipitation and half of the immunoprecipitated material was separated through a 12% SDS-PAGE gel and stained. For Western blotting, 1 $OD_{600}$ equivalent of input and supernatant and half of the immunoprecipitated material was separated through a 12% SDS-PAGE gel and blotted onto a nitrocellulose membrane. Hat1 (48.4kDa) and Hat2 (42.9kDa) were detected with specific antibodies.

Hat1-immunoprecipitation

Hat1 was immunoprecipitated as described in section 2.4.10 using the purified Hat1-antibodies from the 4$^{th}$ bleed. Two hundred $OD_{600}$ equivalents of wild type and Hat1-deficient cells were disrupted with glass beads in breaking buffer A in the FastPrep. Protein extracts were incubated with 25µl of the purified Hat1-antibodies overnight. Antibodies and bound proteins were precipitated by binding to magnetic beads. Subsequently, 0.1 $OD_{600}$ equivalents of the input and the supernatant after immunoprecipitation and half of the immunoprecipitated material were separated through a 12% SDS-PAGE gel. Silver staining revealed no bands that were only present in the immunoprecipitated fraction of the wild type but not in extracts from *hat1*Δ/Δ cells. Immunoblotting of 1 $OD_{600}$ equivalent of the

input and the supernatant after immunoprecipitation and half of the IP showed no Hat1 in the precipitated fraction of the wild type (Figure 24).

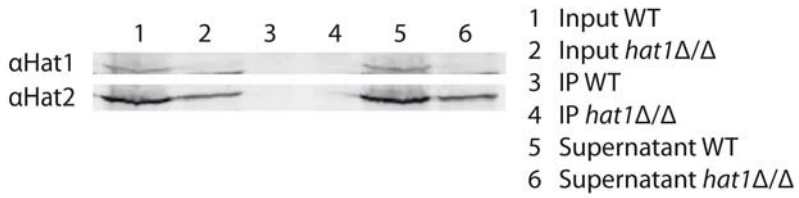


**Figure 24: Hat1 immunoprecipitation.** Wild type and *hat1*Δ/Δ strains were grown to an $OD_{600}$ of 2, harvested and disrupted with glass beads in breaking buffer A. 25µl purified Hat1-antibodies was added to protein extracts and incubated overnight at 4°C. Antibodies were precipitated by binding to magnetic beads. 1 $OD_{600}$ equivalent of input and supernatant after immunoprecipitation and half of the immunoprecipitated material was separated through a 12% SDS-PAGE gel and blotted onto a nitrocellulose membrane. Hat1 (48.4kDa) and Hat2 (42.9kDa) were detected with specific antibodies.

The immunoprecipitation was repeated several times under different conditions. The buffer was changed to a less stringent buffer (10mM Tris-HCl pH 8.0, 150mM NaCl, 0.1% Nonidet P40), and the amount of antibodies used was increased to up to 100µl, but precipitating Hat1 remained impossible.

To see if the Hat1-epitope recognized by the Hat1-antibodies may be hidden in its native conformation, SDS was added to the breaking buffer at a final concentration of 2%. Still no Hat1 was detected.

The immunoprecipitation was repeated, this time coupling 100µl of purified α-Hat1-antibodies to the beads first by incubating them with 50µl beads for 10 minutes at room temperature and then adding the cell extract of 200 $OD_{600}$ equivalents, using 10mM Tris-HCl pH 8.0, 100mM NaCl as breaking buffer. Hat1 was not detectable in the precipitated fraction. The amount of Hat1-antibody was increased to 200µl without any success of precipitating Hat1 (Figure 25).

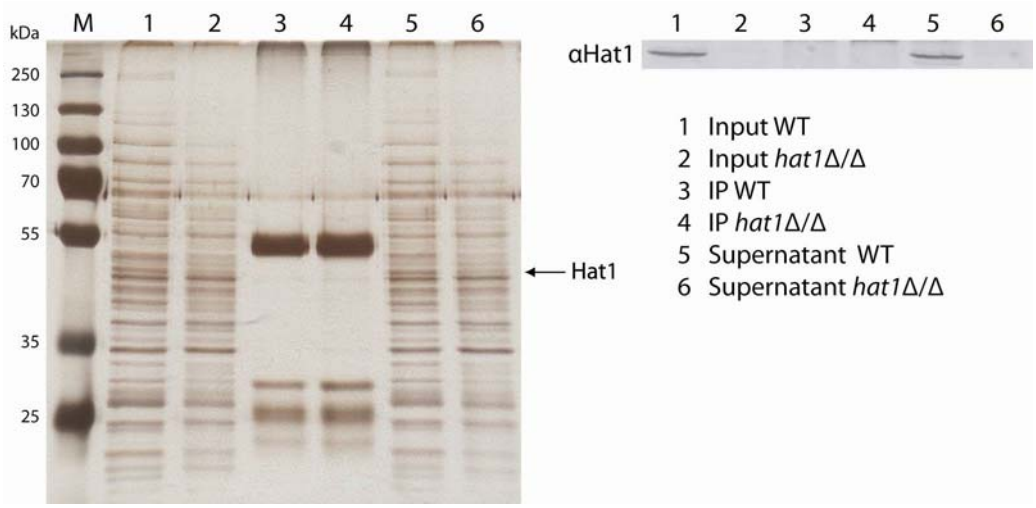


**Figure 25: Hat1 immunoprecipitation.** Wild type and *hat1*Δ/Δ strains were grown to an $OD_{600}$ of 2, harvested and disrupted with glass beads in 10mM Tris-HCl pH 8.0, 100mM NaCl. 200µl purified Hat1-antibody was bound to magnetic beads which were then added to protein extracts and incubated overnight at 4°C. For silver staining, 0.1 $OD_{600}$ equivalents of input and supernatant after immunoprecipitation and half of the immunoprecipitated material was separated through a 12% SDS-PAGE gel and stained. For Western blotting, 1 $OD_{600}$ equivalent of input and supernatant and half of the immunoprecipitated material was separated through a 12% SDS-PAGE gel and blotted onto a nitrocellulose membrane. Hat1 (48,4kDa) was detected with the purified Hat1 antibodies.

## 3.2. Hat2-Tagging

In *Saccharomyces cerevisiae*, Hat1 and Hat2 are mainly located in the nucleus (Poveda *et al.*, 2004). The nuclear localization of *Sc*Hat1 depends on *Sc*Hat2 but localization of *Sc*Hat2 is independent of *Sc*Hat1. In *Candida albicans*, GFP-tagged Hat1 localizes to the nucleus independently of Hat2 (Michael Tscherner, unpublished data). To investigate the subcellular localization of Hat2, it was epitope-tagged with a fluorescent protein.

### 3.2.1. Hat2-YFP Tagging in WT and *hat1*Δ/Δ Background

The YFP coding sequence was PCR-amplified from Yep532-YFP and cloned into the plasmids pFA6a and pSFS3b using SmaI AscI and KpnI ApaI, respectively, giving rise to the plasmids pFA6a-YFP and pSFS3b-YFP. Both plasmids carry the *Candida albicans* selection marker *NAT1*. pSFS3b contains the flippase *FLP* and the corresponding flippase recognition targets (FRTs), which can be used to excise the selection marker after integration of the tagging cassette into the genome (Reuss et al., 2004).
A Hat2-YFP tagging cassette was constructed by fusion PCR as described in section 2.3.7. The 3' part of the coding region and the downstream region of *HAT2* were PCR-amplified from genomic DNA and a fragment containing the YFP coding sequence and the marker was amplified from the plasmid pFA6a-YFP. However, amplifying and fusion of all three fragments in one PCR-reaction to obtain the tagging cassette did not work. Therefore, intermediate fragments were constructed: one fragment consisting of the 3' part of the *HAT2* coding region and YFP, the other of the YFP-marker and the downstream region of *HAT2*. These two fragments were then combined by fusion PCR (Figure 26). This cassette was used to insert the YFP coding sequence in frame with the coding sequence of Hat2, resulting in a C-terminally tagged Hat2-YFP fusion protein. After transformation by electroporation integration at the correct locus was verified by colony PCR.

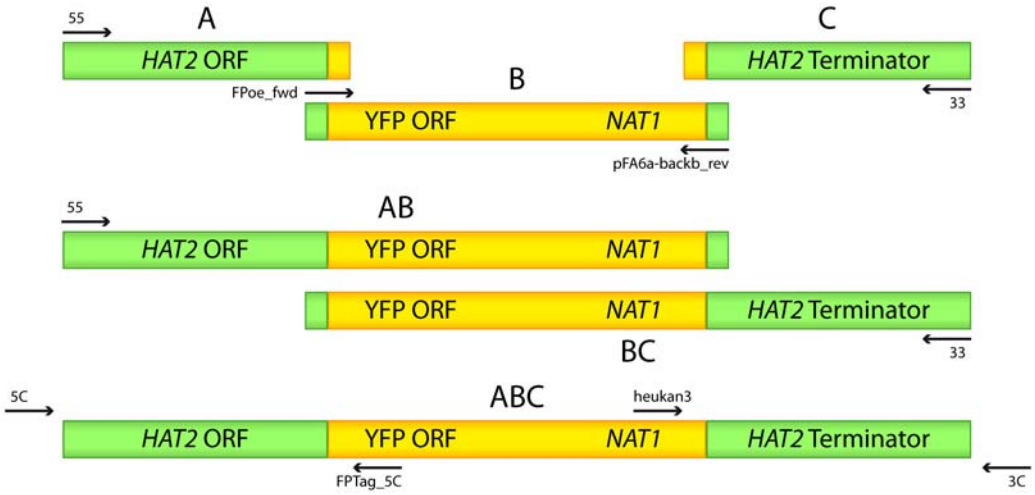


**Figure 26: Hat2-YFP tagging cassette generated by fusion PCR.** Fragments A and C were PCR-amplified from genomic DNA with primers 55_CA2146_FPTag and 53_HAT2-FPTag for fragment A and primers 35_HAT2-pFA and 33_Ca2146 for fragment C. Fragment B was PCR-amplified from plasmid pFA6a-YFP with primers FPoe_fwd and pFA6a-backb_rev. Fragment AB was generated by mixing fragment A with fragment B in one PCR reaction and amplifying with primers 55_CA2146_FPTag and pFA6a-backb_rev. Fragment BC was generated by mixing fragment B with fragment C in one PCR-reaction and amplifying with primers FPoe_fwd and 33_Ca2146. The whole tagging cassette (fragment ABC) was generated by mixing fragment AB with fragment BC in one PCR-reaction and amplifying with primers 55_CA2146_FPTag and 33_Ca2146. Integration of the cassette at the correct genomic locus was verified with primers 5C_HAT2_FPTag and FPTag_5C at the 5' side and heukan3 and 3C_Ca2146 at the 3' side.

Hat2-deficient *Candida albicans* cells form wrinkled colonies under yeast-promoting conditions, indicating constitutive filamentous growth. Moreover, cells are sensitive to genotoxic agents (Michael Tscherner, unpublished data). To confirm the functionality of the C-terminally tagged Hat2-YFP fusion protein, the tagging cassette was transformed into a heterozygous *HAT2* knock-out strain, resulting in a *HAT2*-YFP/*hat2*Δ strain. If the tagged Hat2-YFP protein was not functional, the strain would show the phenotype of a *hat2*Δ/Δ deletion strain. Integration of the tagging cassette at the correct locus was confirmed by colony PCR as described in section 2.2.5 using primer-pairs with one primer binding outside and one within the tagging cassette. Expression of Hat2-YFP was also checked by immunoblotting. In transformed strains, a signal at 69.8kDa was detected consistent with the expected molecular mass of Hat2-YFP. On YPD, the Hat2-YFP strain formed smooth colonies, indicating yeast-form growth (Figure 27 (A)). This was confirmed by inspection of single cells in the microscope (Figure 28). Examining its sensitivity to genotoxic agents, we found that it showed the same sensitivity to MMS and NQO as the wild type (Figure 27 (B)), demonstrating that Hat2-YFP is indeed functional.

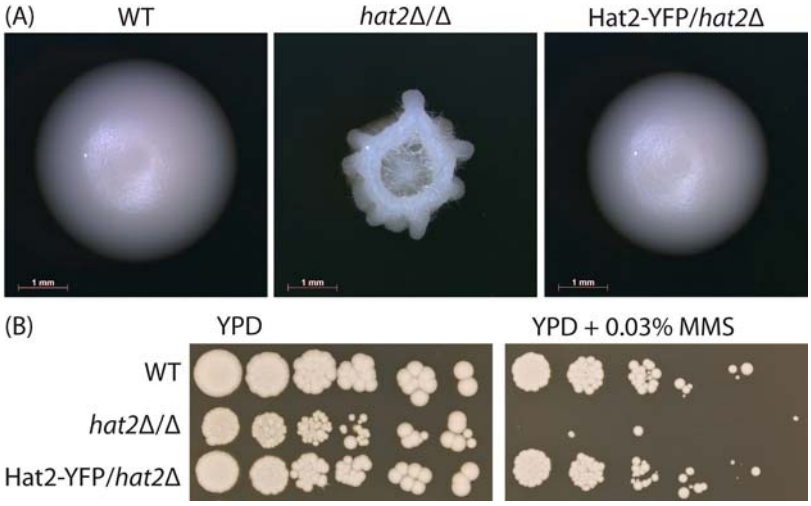


**Figure 27: Functionality of Hat2-YFP.** (A) Wild type, *hat2*Δ/Δ cells and Hat2-YFP expressing cells were plated on YPD and photographed after 3 days at 30°C. The Hat2-YFP expressing strain forms smooth colonies, indicating yeast-form growth. (B) To investigate sensitivity to genotoxic agents cells were spotted in serial dilutions (1:5) on plates containing 0.03% methyl methane sulfonate (MMS) and incubated at 30°C for 3 days. The Hat2-YFP strain has wild type sensitivity to MMS.

To visualize the subcellular localization of Hat2-YFP, cells were stained with Hoechst33342 and the samples were analyzed by fluorescence microscopy. Hat2-YFP was found to be localized mainly in the nucleus (Figure 28).

To further characterize the localization of Hat2, we asked whether Hat2 localization depends on Hat1. For transformation of Hat2-YFP into a Hat1-deficient strain, another tagging cassette was used. The cassette was constructed as described above, except using the plasmid pSFS3b-YFP instead of pFA6a-YFP as a template for the YFP and marker fragment. This way, thanks to the flipper construct, the *NAT1* marker could be recycled. The Hat2-YFP tagging cassette was transformed into a *hat1*Δ/Δ *hat2*Δ/*HAT2* strain, and the integration was confirmed by colony PCR. Again expression of Hat2-YFP was checked by immunoblotting. In transformed strains, a signal at 69.8kDa was detected consistent with the expected molecular mass of Hat2-YFP.

Cells were examined in the microscope to determine the localization of Hat2-YFP. Interestingly, in *hat1*Δ/Δ cells the nuclear localization of Hat2-YFP was lost and the Hat2-YFP-signal was distributed throughout the cell (Figure 28). To confirm that the loss of the nuclear localization was in fact due to the deletion of *HAT1*, *HAT1* was reintegrated into its original locus (reintegration cassette kindly provided by Michael Tscherner). The reintegration of *HAT1* was checked by colony PCR. Inspection of these cells in the microscope revealed that the nuclear localization of Hat2-YFP was fully restored by *HAT1* reintegration, confirming that in *Candida albicans* nuclear localization of Hat2 requires Hat1.

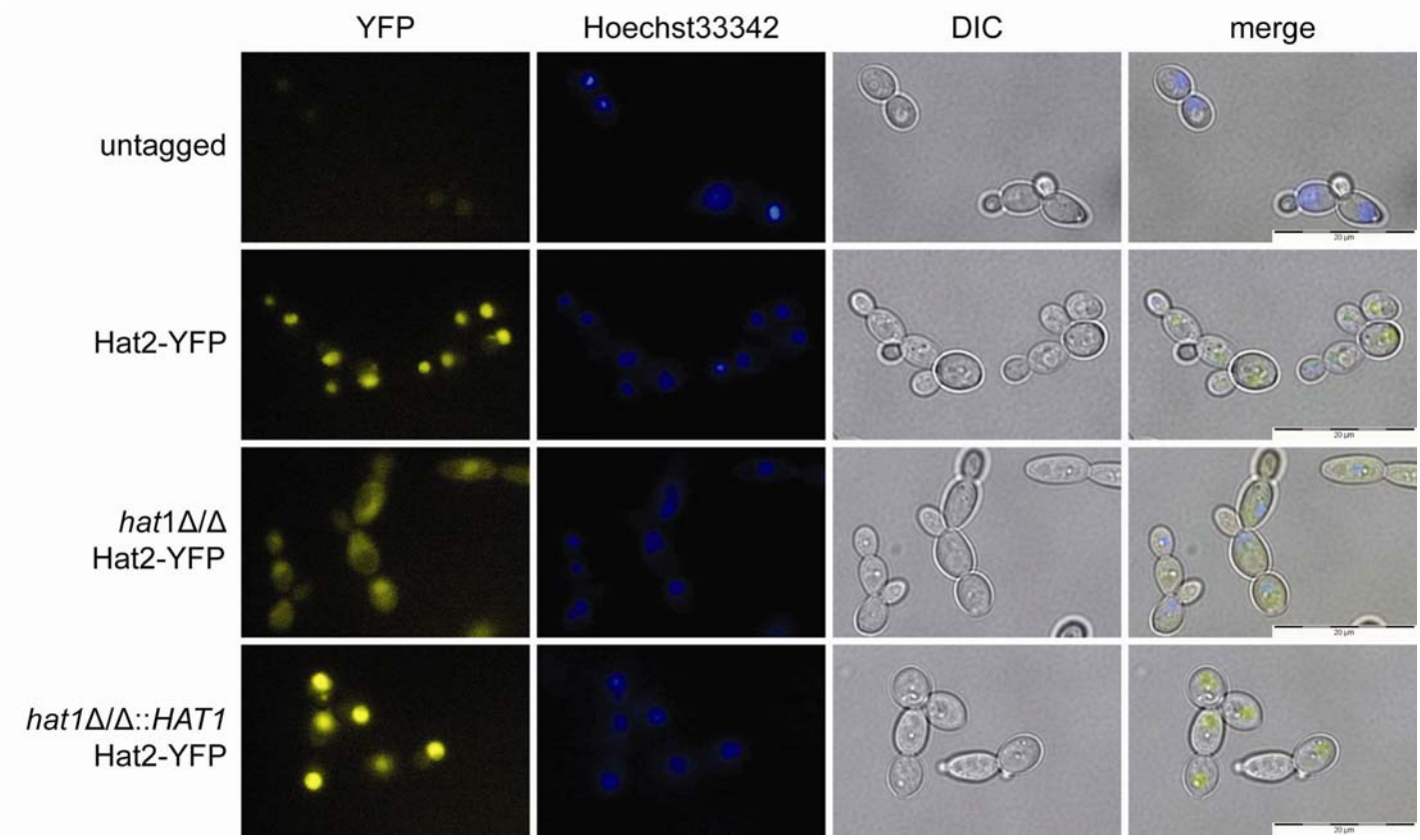


**Figure 28: Hat2-YFP localization.** Cells in the logarithmic phase grown in YPD at 30°C were stained with Hoechst33342. Hat2-YFP is localized in the nucleus. In the *hat1*Δ/Δ background the nuclear localization is lost and the signal is distributed throughout the cell. Reintegration of *HAT1* restores the nuclear localization of Hat2-YFP.

The Hat1/Hat2 complex is involved in DNA damage repair (Michael Tscherner, unpublished data). To investigate the effect of DNA-damaging agents on the Hat2-localization, the Hat2-YFP-expressing strain was treated with MMS and stained with Hoechst33342. Samples were analyzed by fluorescence microscopy. In untreated cells the nuclear Hat2-YFP signal was relatively low. After treatment with MMS the signal intensity in the nucleus increased dramatically (Figure 29).

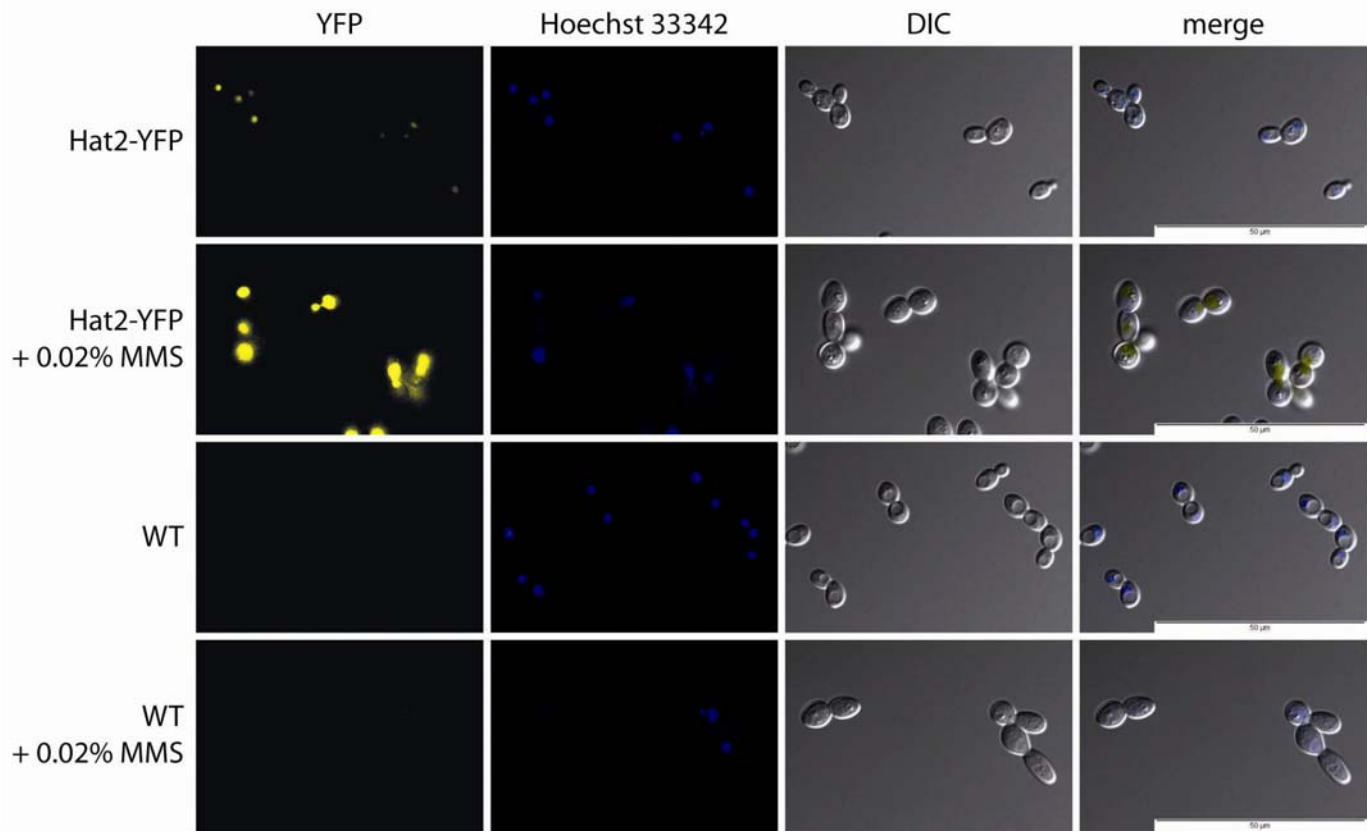


**Figure 29: Nuclear Hat2-YFP signal increases after MMS treatment.** Cells in the logarithmic phase grown in YPD at 30°C were treated with 0.02% MMS for 4 hours and stained with Hoechst33342.

### 3.2.2. Hat2-RFP and Hat2-mCherry Tagging

To investigate the localization of Hat1 and Hat2 in the same strain, we decided to construct a double-tagged strain. Using the already present Hat1-GFP and Hat2-YFP was not possible due to a significant spectral overlap of GFP and YFP. Therefore, we decided to use Hat1-GFP and attached a red fluorescent protein to Hat2.

The DsRFP gene from the plasmid pMG2160, obtained from the FGSC (Gerami-Nejad *et al.*, 2009) was PCR-amplified and cloned into plasmids pFA6a and pSFS3b using SmaI AscI and KpnI ApaI, respectively, giving rise to the plasmids pFA6a-RFP and pSFS3b-RFP. Both plasmids were sequenced to ensure the integration of the correct fragment.

Since generating a tagging cassette with YFP by overlap PCR proved to be difficult, the construction of the RFP-tagging cassette was done by cloning. The downstream region of *HAT2* was cloned into pSFS3b-RFP using SacI and NotI, resulting in the plasmid pSFS3b-3'HAT2_RFP. Next, the 3' coding region of *HAT2* was cloned into pSFS3b-3'HAT2_RFP using XmaI, resulting in the plasmid pSFS3b-HAT2_RFP. This plasmid was linearized using PvuI and used as Hat2-RFP tagging cassette. Hat2-RFP was integrated into a *HAT1/hat1*Δ *HAT2/hat2*Δ strain, to check the functionality of the tagged Hat1 and Hat2 proteins. Integration of the cassette at the correct genomic locus was checked by colony PCR. Expression of Hat2-RFP was confirmed by immunoblotting. Western blot analysis showed a protein at the expected mobility corresponding to Hat2-RFP. Cells were stained with Hoechst33342 and inspected in the microscope. However, no RFP-signal was detectable

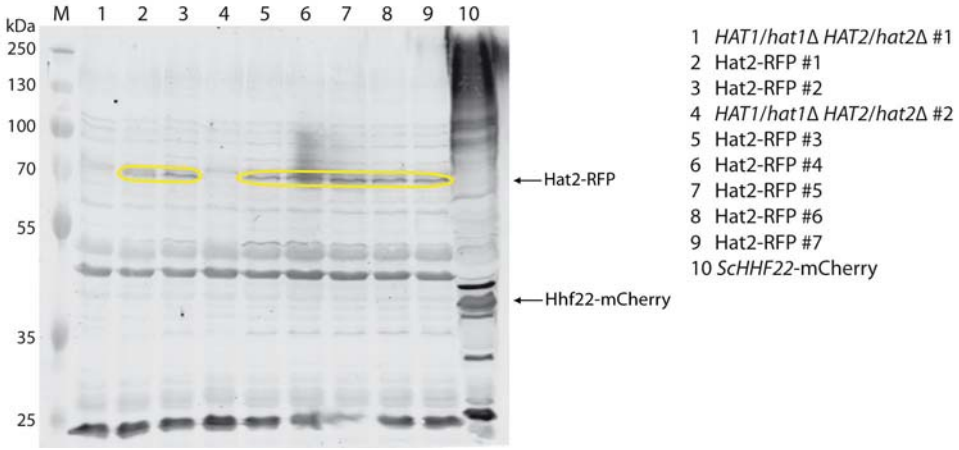


**Figure 30: Expression of Hat2-RFP.** 0.4 $OD_{600}$ equivalents TCA-extract of the indicated strains were separated through a 12% SDS-PAGE gel and blotted onto a nitrocellulose membrane. Hat2-RFP (68.6kDa) was detected with α-RFP-antibodies (1:1000). The *HAT1/hat1*Δ *HAT2/hat2*Δ strains (lane 1 and 4) served as negative controls, the *ScHHF22*-mCherry strain (lane 10) as positive control (38.1kDa).

To check the functionality to the RFP in *Candida albicans*, it was placed under the control of the *ACT1* promoter. This was done by integrating the RFP coding sequence into the *ACT1* locus. The upstream and downstream regions of *ACT1* were PCR-amplified from genomic DNA. RFP and the selection marker were amplified from pFA6a-RFP. The three fragments were then combined in a fusion PCR to generate the RFP cassette. This cassette was transformed into the wild type strain SC5314. Integration of the cassette at the correct genomic locus was verified by colony PCR. Expression of RFP was confirmed by immunoblotting. Only a very weak signal was detected at 25kDa, which would correspond to the mobility of RFP. Cells were also examined in the microscope but no RFP signal was visible.

The Hat2-tagging was repeated with another red fluorescent protein: mCherry. The mCherry gene from the plasmid pMG2254 (obtained from the FGSC (Gerami-Nejad *et al.*, 2009)) was PCR-amplified and cloned into plasmids pFA6a and pSFS3b using SmaI AscI and KpnI ApaI, respectively, giving rise to the plasmids pFA6a-mCherry and pSFS3b-mCherry.

The construction of the Hat2-mCherry tagging cassette was carried out as described for the Hat2-RFP tagging cassette. Western blot analysis of strains transformed with this cassette showed a protein at the expected mobility of 69.7kDa (Figure 31, lane 1, 3, 5, 6, 7 and 8), but no mCherry signal was detected in the microscope.

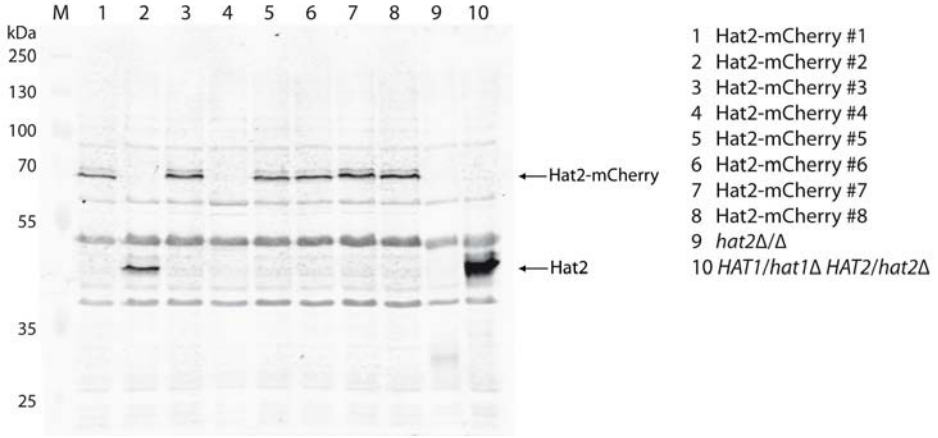


**Figure 31: Expression of Hat2-mCherry.** 0.4 $OD_{600}$ equivalents TCA-extract of the indicated strains were separated through a 12% SDS-PAGE gel and blotted onto a nitrocellulose membrane. Hat2-mCherry (69.7kDa) was detected with α-Hat2-antibodies (1:4000). The *hat2*Δ/Δ strain (lane 9) served as negative control, the *HAT1/hat1*Δ *HAT2/hat2*Δ strain (lane 10) as positive control (Hat2 42.9kDa).

## 3.3. Deletion of *RTT109* and *ASF1*

### 3.3.1. Deletion of *RTT109*

Deletion of *RTT109* was carried out using the flipper cassette from the plasmid pSFS3b (Figure 32). Upstream and downstream region of the *RTT109* ORF were PCR-amplified. The downstream region was cloned into pSFS3b behind the marker cassette using BglII and NotI yielding the plasmid pSFS3b-3'RTT109. The upstream region was then cloned in front of the marker region using KpnI and ApaI resulting in the plasmid pSFS3b-RTT109urdr. The plasmid was linearized with PvuII and used as the deletion cassette. The cassette was transformed into the wild type strain SC5314 by electroporation as described in section 2.2.4. Integration of the knock-out cassette was confirmed by colony PCR using primer pairs with one primer binding outside and one within the deletion construct. The *NAT1* marker was flipped out by incubating overnight in YP+2% maltose and selecting for colonies that had lost their nourseothricin resistance. The knock-out procedure was repeated with this strain to obtain a homozygous *rtt109*Δ/Δ strain. As a control, *RTT109* was also reintegrated into the homozygous *rtt109*Δ/Δ strain (Figure 33). Hence, the coding sequence plus the upstream and downstream region was PCR-amplified from genomic DNA and cloned into pSFS3b-3'RTT109 using KpnI and ApaI, resulting in the plasmid pSFS3b-CaRTT109-Rev. The plasmid was linearized with PvuII and used for transformation into the *rtt109*Δ/Δ strain. Integration at the correct genomic locus was verified by colony PCR.

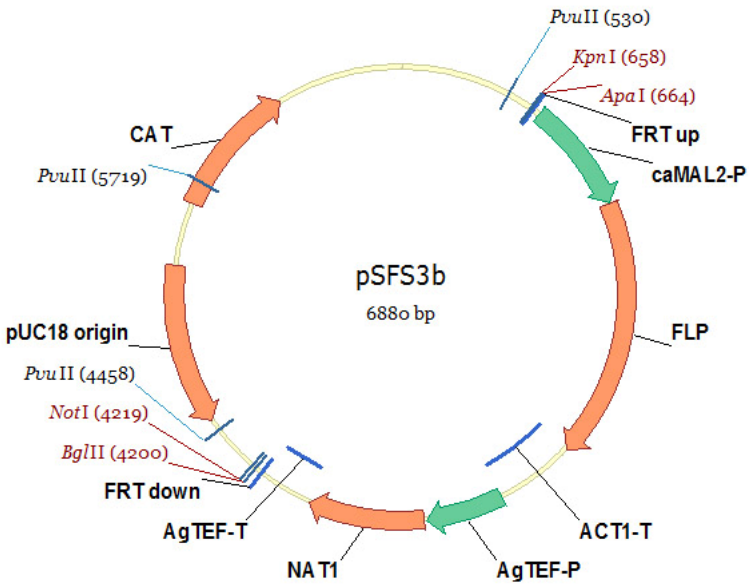


**Figure 32: Parental plasmid pSFS3b for construction of knock-out cassettes.**

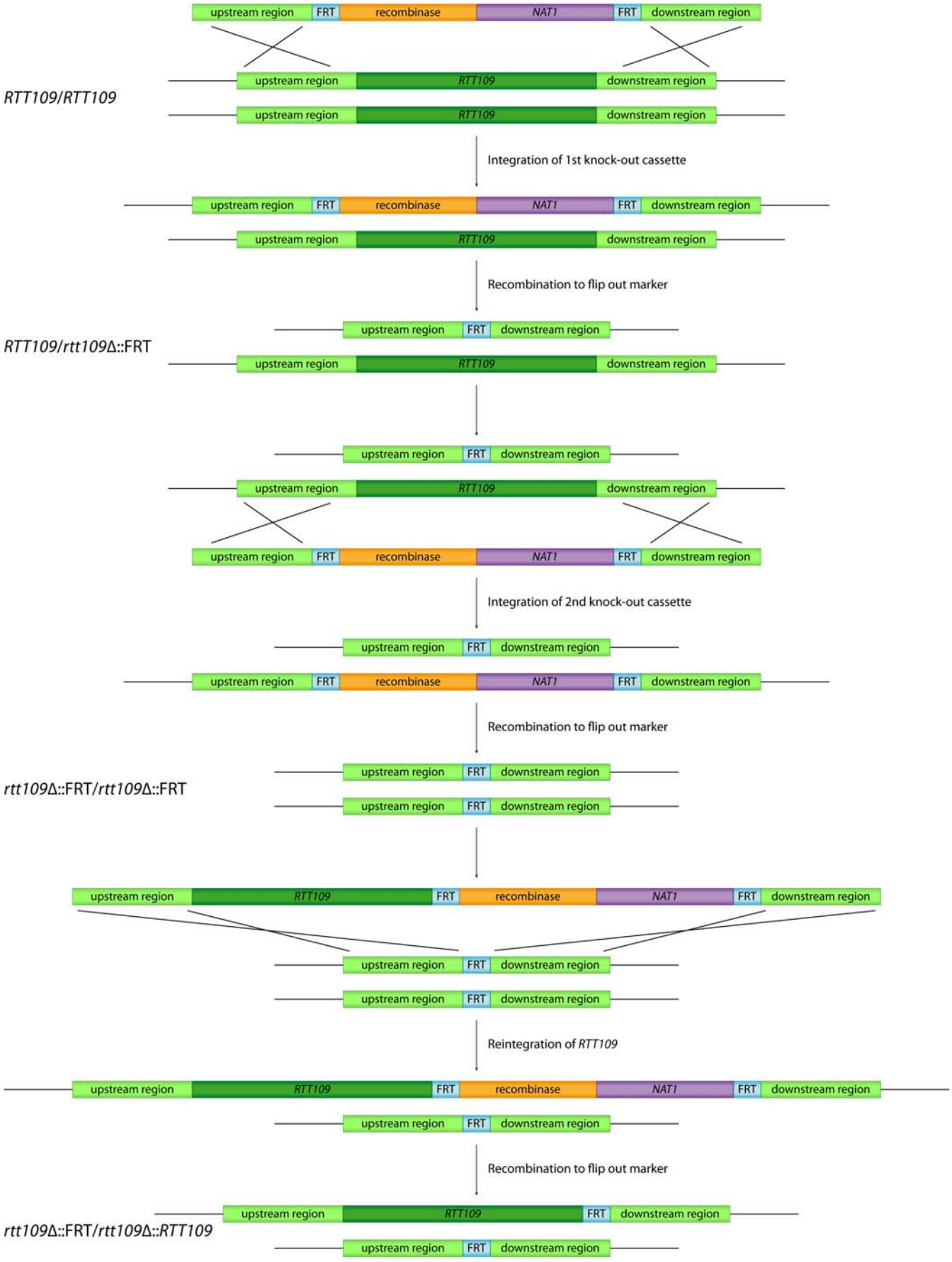


**Figure 33: Flowchart of *RTT109* knock-out construction.**

Filamentous growth in *Candida albicans* can be induced by several stimuli, one of which is DNA damage. Lack of Rtt109 mediated H3K56 acetylation in *S. cerevisiae* leads to spontaneous DNA damage (Han *et al.*, 2007). Therefore, we examined the morphology of cells lacking Rtt109. These cells showed a wrinkled colony morphology indicating filamentous growth under yeast-promoting conditions (Figure 34 (A)). This was confirmed by microscopic inspection of single cells, which showed elongated cell morphologies (Figure 34 (B)).

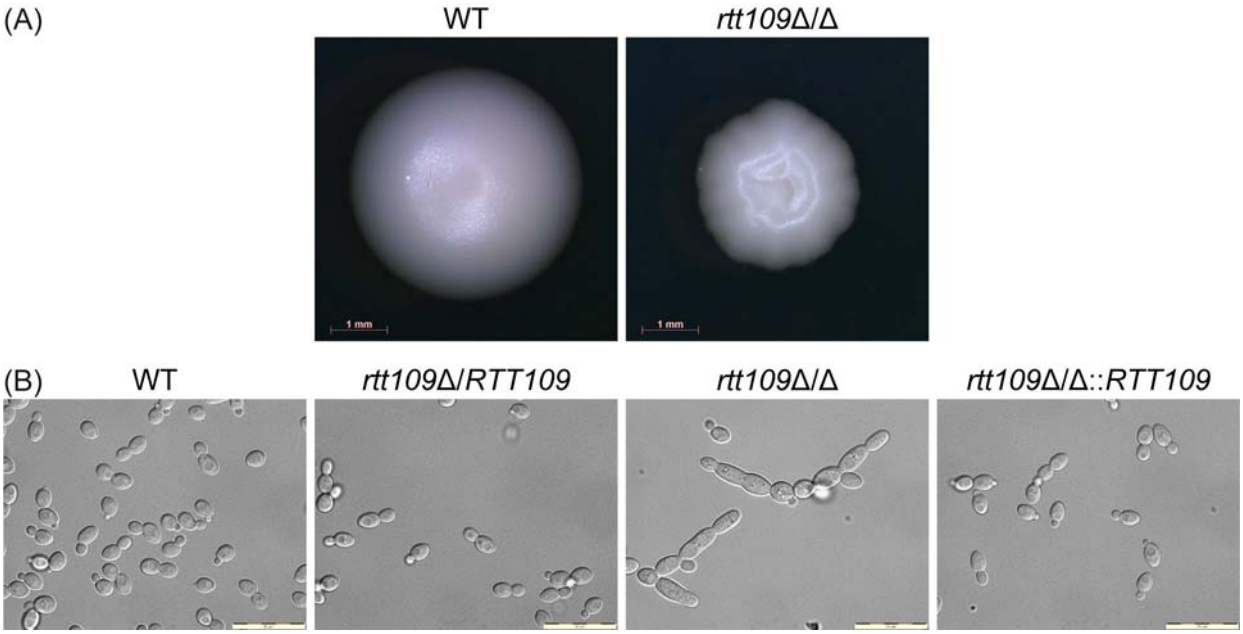


**Figure 34: Morphology of the *rtt109*Δ/Δ strain.** (A) Wild type (WT) and *rtt109*Δ/Δ cells were plated on YPD and incubated at 30°C for 3 days. (B) Cells in logarithmic phase grown in YPD at 30°C.

To test the sensitivity of Rtt109-deficient cells to DNA-damaging agents, cells were spotted onto YPD plates containing methyl methane sulfonate (MMS), ethyl methane sulfonate (EMS) and 4-nitroquinoline 1-oxide (NQO). The homozygous *rtt109*Δ/Δ strain was hypersensitive to all three substances, whereas the heterozygous *rtt109*Δ/*RTT109* strain showed the same sensitivity as the wild type. Reintegration of *RTT109* into the corresponding locus in the knock-out strain fully restored the wild type phenotype (Figure 35).

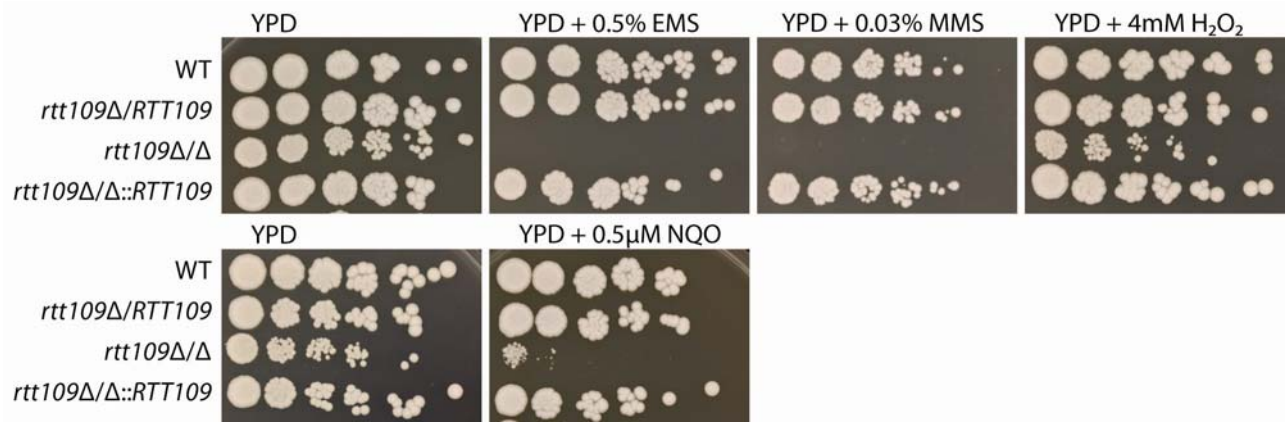


**Figure 35: Sensitivity of *rtt109*Δ/Δ to DNA-damaging agents and $H_2O_2$.** Cells were spotted in serial dilutions (1:5) on YPD plates containing 0.5% ethyl methane sulfonate (EMS), 0.03% methyl methane sulfonate (MMS), 4mM hydrogen peroxide ($H_2O_2$) or 0.5µM 4-nitroquinoline 1-oxide (NQO) and incubated at 30°C for 3 days.

Furthermore, the *rtt109*Δ/Δ strain also showed some sensitivity to hydrogen peroxide ($H_2O_2$), a reactive oxygen species.

Next, a *hat1*Δ/Δ *rtt109*Δ/Δ double knock-out strain was constructed. Both alleles of *HAT1* were sequentially deleted in the homozygous *rtt109*Δ/Δ strain using the *HAT1* knock-out cassette (kindly provided by Michael Tscherner) using the *SAT1* flipper.
Sensitivity of the *hat1*Δ/Δ *rtt109*Δ/Δ double knock-out strain to MMS, NQO and $H_2O_2$ was tested in spot assays (Figure 36). The *hat1*Δ/Δ strain as well as the *rtt109*Δ/Δ strain was sensitive to MMS and NQO, though the *rtt109*Δ/Δ strain had an increased sensitivity to MMS compared to the *hat1*Δ/Δ strain. Cells lacking Hat1 and Rtt109, showed the same sensitivities to MMS as the *rtt109*Δ/Δ strain. Hat1-deficient cells, but not Rtt109-deficient cells showed an increased resistance to $H_2O_2$. The *hat1*Δ/Δ *rtt109*Δ/Δ double knock-out exhibited the same hyperresistance as the *hat1*Δ/Δ strain.

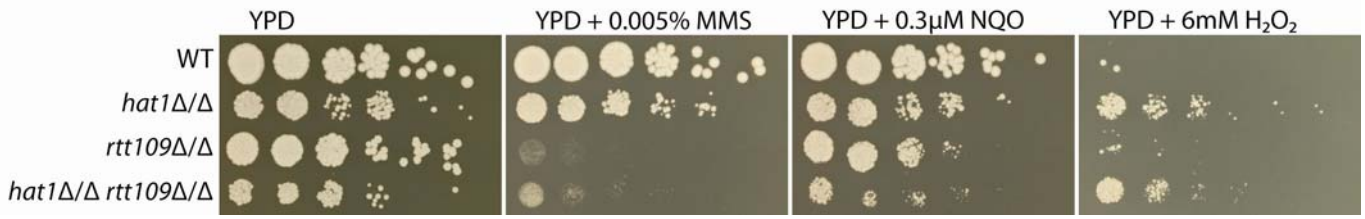


**Figure 36: Sensitivity of *hat1*Δ/Δ *rtt109*Δ/Δ to DNA-damaging agents and $H_2O_2$.** Cells were spotted in serial dilutions (1:5) on YPD plates containing 0.005% methyl methane sulfonate (MMS), 0.3µM 4-nitroquinoline 1-oxide (NQO) or 6mM hydrogen peroxide ($H_2O_2$) and incubated at 30°C for 2 days.

### 3.3.2. Deletion of *ASF1*

For the deletion of *ASF1*, we constructed a knock-out cassette following the same scheme as described for *RTT109* in Figure 33. The flanking regions of the *ASF1* coding sequence were cloned into pSFS3b using BglII and NotI for the downstream region (pSFS3b-3'ASF1), and ApaI and KpnI for the upstream region resulting in the plasmid pSFS3b-ASF1urdr. The plasmid was linearized with PvuII and used as knock-out cassette. The *ASF1* knock-out cassette was transformed into the wild type strain SC5314 by electroporation. Integration at the correct genomic locus was verified by colony PCR. The *NAT1* marker was flipped out by incubating cells overnight in YP+2% maltose and selecting for colonies that had lost their nourseothricin resistance.

The knock-out procedure was repeated with the *ASF1* knock-out cassette but no clones lacking both alleles of *ASF1* were obtained. It seems that Asf1 is essential (Davis *et al.*, 2002). Therefore, we decided to put one copy of *ASF1* under a repressible promoter after deleting the other allele. The *Candida albicans MET3* promoter was chosen. This promoter is repressed in the presence of 2.5mM methionine and 0.5mM cysteine (Care *et al.*, 1999). 1.4kb of the *MET3* promoter and the *ASF1*-ORF were PCR-amplified. A $P_{MET3}$-*ASF1* fragment was created by fusion PCR using the two outer primers MET3-P_SmaI_fwd and ASF1_AscI_rev. This fragment was cloned into pFA6a with SmaI and AscI resulting in the plasmid pFA6a-MET3-P_ASF1. The plasmid was linearized with BsaBI and AscI, thereby removing the last 215bp of the *ASF1* coding sequence. This cassette was then transformed into the heterozygous *asf1*Δ/*ASF1* strain. Integration into the *ASF1* CDS would disrupt the remaining wild type allele and place *ASF1* under the control of the *MET3* promoter. To ensure that no methionine or cysteine were present in the medium, which would repress the *MET3* promoter, minimal media was used in the transformation protocol. Since ammonium sulfate impairs the function of nourseothricin, 1g/l glutamic acid was used as nitrogen source instead (Tong and Boone, 2006). However, no positive clones able to grow in the absence but not in the presence of methionine and cysteine were obtained.

In *S. cerevisiae*, the C-terminally region of Asf1 is not required for functionality (Umehara *et al.*, 2002). Thus, it is possible that the truncated version, which remains in the genome after using the approach described above, is still functional. Therefore, the $P_{MET3}$-*ASF1* fragment was amplified using a primer that was binding in the middle of *ASF1* CDS (MET3-P_SmaI_fwd and ASF1_2_AscI_rev) giving rise to a fragment consisting of the *MET*-promoter and only the first 299bp of *ASF1*. This fragment was cloned into pFA6a using SmaI and AscI resulting in the plasmid pFA6a-MET3-P_ASF1_2. The cassette was then PCR-amplified with ASF1_int_fwd and ASF1_int_rev. This cassette was transformed into the heterozygous *asf1*Δ/*ASF1* strain. No positive clones able to grow in the absence but not in the presence of methionine and cysteine were obtained.

Since we were unable to obtain positive clones this way, we decided to replace the *ASF1*-promoter with the *MET3*-promoter. To do this a region upstream of the *ASF1*-promoter (ur_ASF1_fwd and ur_ASF1_rev), the *MET3*-promoter (MET3-P_KpnI_fwd and MET3-P_oe_rev) and full length *ASF1* (ASF1_oe_fwd and 33_ASF1_NotIApaI_rev) was PCR-amplified from genomic DNA. The $P_{MET3}$-*ASF1* fragment was created by fusion PCR using the two outer primers MET3-P_KpnI_fwd and 33_ASF1_NotIApaI_rev. This fragment was then cloned into pSFS3b-3'ASF1 with KpnI and ApaI resulting in the plasmid pSFS3b-MET3P-ASF1-drASF1. The upstream *ASF1* region was then cloned into this plasmid with KpnI giving rise to the plasmid pSFS3b-urASF1-MET3P-ASF1-drASF1. This plasmid was linearized with PvuII and transformed into the *asf1*Δ/*ASF1* strain. Integration at the correct genomic locus was verified by colony PCR. In all transformants, the cassette failed to integrate at the *ASF1* wild type allele, but integrated at the *asf1*Δ knock-out allele instead. The *NAT1* marker was flipped out by incubating cells overnight in YP+2% maltose and selecting colonies that had lost their nourseothricin resistance. The strain was then transformed by electroporation with the *ASF1* knock-out cassette to delete the remaining wild type allele. However, no positive clones, which had integrated the cassette at the correct locus, were obtained.

## 3.4. Histone H4 Mutants

### 3.4.1. Deletion of *HHF1* and *HHF22*

The *Candida albicans* genome contains two genes encoding histone H4: *HHF1* (orf19.1059) and *HHF22* (orf19.1854) (Zacchi et al., 2010). To introduce mutations mimicking the acetylated or deacetylated state of lysine 5 and 12, first the number of wild type histone H4 copies was reduced by sequentially deleting 2 copies of *HHF1* and one copy of *HHF22*. First, a knock-out cassette for *HHF1* was constructed. The upstream and downstream region of *HHF1* were PCR-amplified from genomic DNA and cloned into pSFS3b using BglII and NotI for the downstream region (pSFS3b-3'HHF1) and ApaI and KpnI for the upstream region, resulting in the plasmid pSFS3b-HHF1urdr. The plasmid was linearized with PvuII and transformed by electroporation into the wild type strain SC5314. Integration at the correct genomic locus was verified by colony PCR. The *NAT1* marker was flipped out by incubating cells overnight in YP+2% maltose and selecting colonies that had lost their nourseothricin resistance. To delete the second allele of *HHF1*, the knock-out procedure was repeated as described above. For deleting *HHF22*, a *HHF22* knock-out cassette was constructed. The flanking regions of *HHF22* were PCR-amplified from genomic DNA and cloned into pSFS3b using BglII and NotI for the downstream region (pSFS3b-3'HHF22) and ApaI and KpnI for the upstream region, resulting in the plasmid pSFS3b-HHF22urdr. The plasmid was linearized with PvuII and transformed by electroporation into the homozygous *hhf1*Δ/Δ strain. Integration at the correct genomic locus was verified by colony PCR. The *NAT1* marker was flipped out by incubating cells overnight in YP+2% maltose and selecting colonies that had lost their nourseothricin resistance.

Deletion of *HHF1* and *HHF22* was verified by Southern blotting. Genomic DNA was isolated from all strains as described in section 2.2.3. For the isolation 5ml overnight culture was harvested, resuspended in Yeast Lysis Buffer and PCI (phenol-chlorophorm-isoamyl alcohol) and glass beads were added. Cells were broken up in the FastPrep and TE was added. RNA was digested with RNase A. DNA was precipitated and resuspended in 50µl $dH_2O$. For *HHF1*, 25µg genomic DNA was digested with HindIII. For *HHF22*, 40µg genomic DNA was digested with BglII. DNA was separated in an agarose gel and blotted onto a nylon membrane. Fragments containing *HHF1* or *HHF22* were detected with a digoxigenin labeled probe and an anti-digoxigenin antibody. All strains showed bands at the expected sizes.

Since it is known that low dosage of histone H4 can lead to chromosome duplication (Zacchi *et al.*, 2010), the histone H4 copy number was checked by quantitative PCR as described in section 2.3.9. For each reaction, 7.5ng genomic DNA was used. *RIP1* and

*ECE1* were chosen as reference genes. Copy number was calculated relative to the wild type which harbors 4 copies of histone H4. All knock-out strains had the expected copy number of histone H4 (Figure 37).

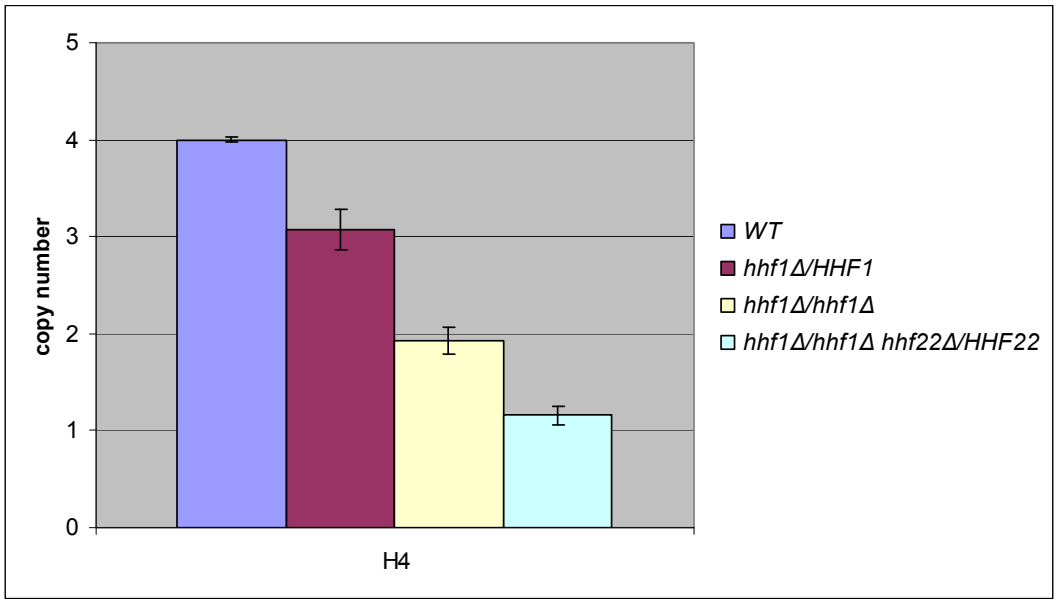


**Figure 37: Quantitative PCR showing histone H4 copy number.** qPCR was performed with 7.5ng genomic DNA per reaction and *RIP1* and *ECE1* as reference genes. Signals were normalized to the mean of the reference genes and to the WT signal.

Next the sensitivity of the histone H4 knock-out strains to Caspofungin, methyl methane sulfonate (MMS), hydrogen peroxide ($H_2O_2$), Itraconazole and Voriconazole was tested (Figure 38). Knock-out strains with one or two copies of histone H4 deleted behaved as the wild type. However, the knock-out strain harboring only copy left showed increased sensitivity to Caspofungin. Notably, this could be rescued by addition of vitamin C. It was also sensitive to MMS, similar to the *hat1*Δ/Δ strain. Another similarity was that both strains showed an increased resistance to $H_2O_2$. Resistance to Itraconazole and Voriconazole was slightly elevated in the one histone H4 copy strain compared to the wildtype, but not as pronounced as in the *hat1*Δ/Δ strain (Figure 38).

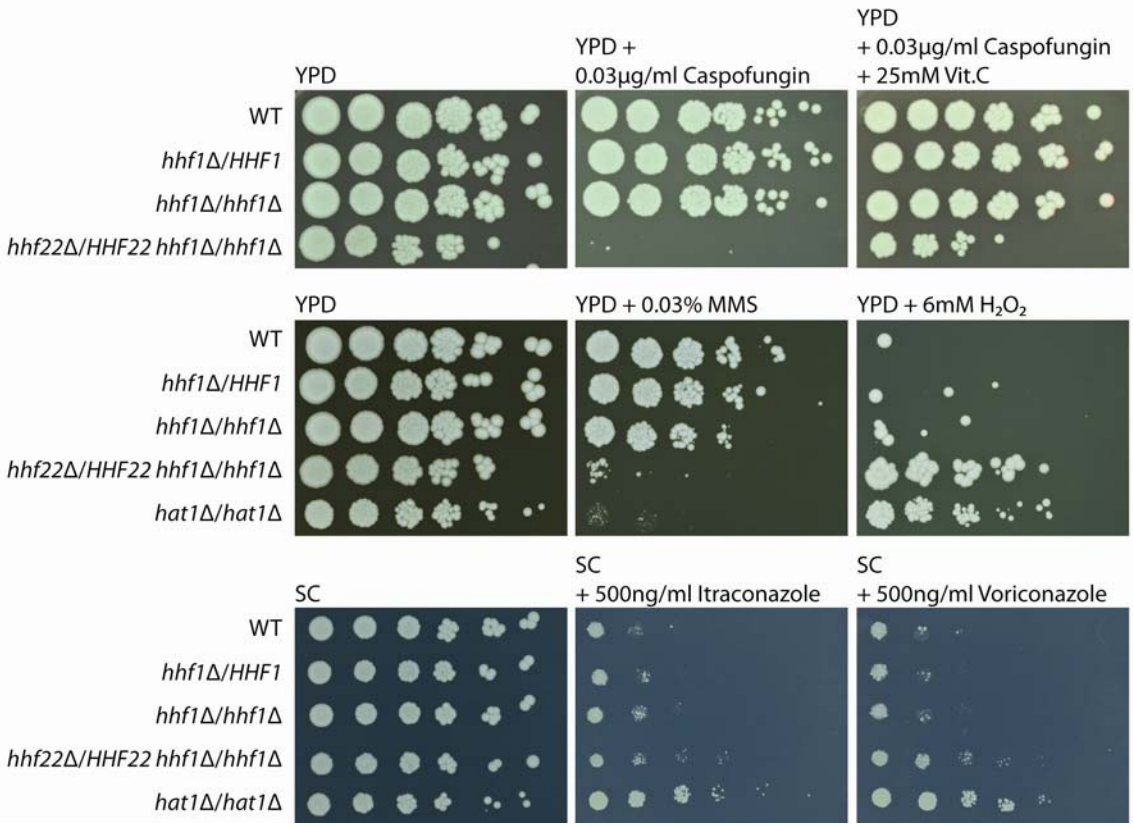


**Figure 38: Sensitivity of histone H4 knock-out strains.** Cells were spotted in serial dilutions (1:5) on YPD plates containing 0.03µg/ml Caspofungin, 0.03µg/ml Caspofungin and 25mM vitamin C, 0.03% methyl methane sulfonate (MMS), 6mM hydrogen peroxide ($H_2O_2$) or on SC-plates containing 500ng/ml Itraconazole or 500ng/ml Voriconazole and incubated at 30°C for 3 days.

The next step was to integrate a mutated version of *HHF1* into the *HHF1* locus. First, the coding sequence of *HHF1* was PCR-amplified (55_CaHHF1 and 33_CaHHF1) and cloned into pSFS3b-3'HHF1 using PvuI and ApaI giving rise to the plasmid pSFS3b-CaHHF1-Rev. Lysine 5 and 12 were mutated to glutamine to mimic the acetylated state, and to arginine to mimic the unacetylated state, as described in section 2.3.8. Therefore, primers with one point mutation were designed changing lysine to glutamine or arginine. pSFS3b-CaHHF1-Rev was PCR-amplified using these primers (HHF1 K12Q_fwd + HHF1 K12Q_rev, HHF1 K12R_fwd + HHF1 K12R_rev). After the amplification, the template plasmid pSFS3b-CaHHF1-Rev was digested with DpnI which cuts only methylated DNA, leaving behind the PCR-amplified and therefore unmethylated mutated version of the plasmid. The resulting plasmids were named pSFS3b-CaHHF1 K12Q and pSFS3b-CaHHF1 K12R and transformed into competent DH5α cells. To ensure the correct mutations were present in all plasmids, sequencing was carried out. The plasmids were linearized with PvuII and transformed into the histone H4 knock-out strain with only one wild type histone H4 copy left. As a control the non-mutagenized *HHF1* was reintegrated as well.

It has already been shown that altering the histone H4 dosage in *Candida albicans* leads to a growth defect (Zacchi *et al.*, 2010). Therefore, a growth curve was taken for all of the

histone H4 knock-out strains (Figure 39). Deletion of one or two copies of histone H4 did not affect the growth rate. Both strains grew at about the same rate as the wild type. However, the knock-out strain with only one histone H4 copy left grew considerably slower than the others. Unfortunately, reintegration of *HHF1* failed to restore the phenotype of the strain harboring two histone H4 copies. All strains with a reintegrated copy of *HHF1* with or without mutation of lysine 12 grew at the same rate as the one copy strain. It is possible that this strain acquired some mutation during the transformation procedure. Therefore, the construction of a one-copy strain was repeated.

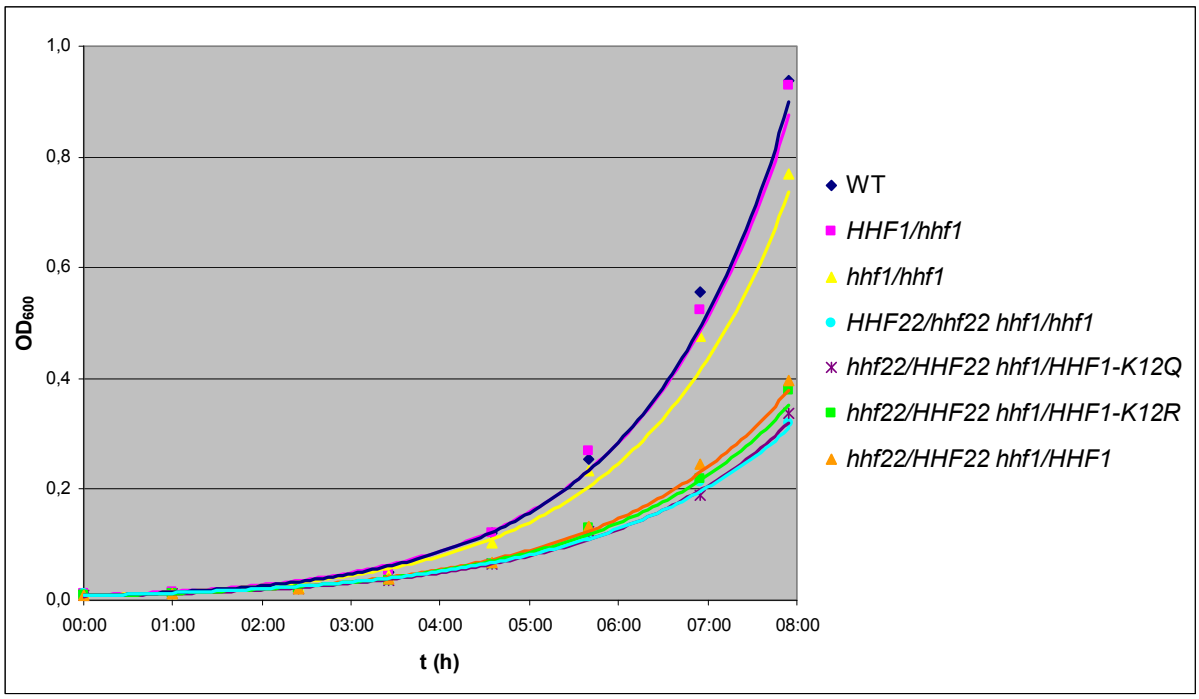


**Figure 39: Growth of histone H4 mutant strains.** Overnight cultures were diluted to $OD_{600}$ 0.05 and grown in YPD at 30°C. $OD_{600}$ was measured at the indicated time points.

For the previous knock-outs, only *HHF1* and *HHF22* were deleted. This changes the histone H3 / histone H4 ratio which may have potentially harmful effects (Castillo *et al.*, 2007; Clark-Adams *et al.*, 1988). To reduce these effects, a knock-out cassette that would delete *HHF22* and *HHT2*, which encodes histone H3, was constructed (Figure 40).

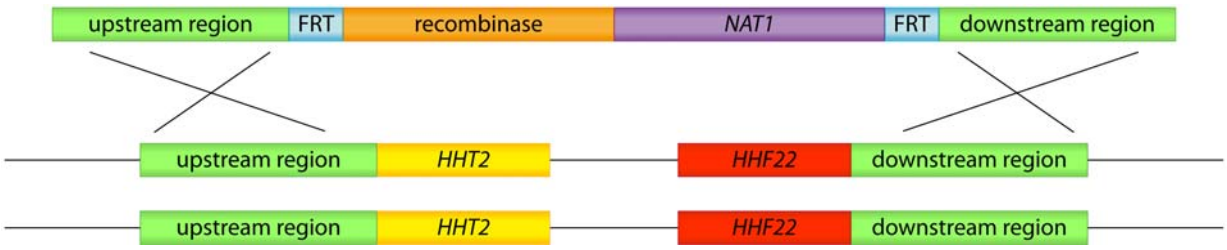


**Figure 40: *HHT2* and *HHF22* locus.**

The upstream region of *HHT2* was PCR-amplified from genomic DNA and cloned into pSFS3b-3'HHF22 with KpnI and ApaI giving rise to pSFS3b-5'HHT2-3'HHF22. The plasmid was linearized with PvuII and transformed into a strain lacking one copy of *HHF1*. Integration at the correct genomic locus was verified by colony PCR. Recombination was induced by incubation in YP + 2% maltose overnight. Colonies that had lost their nourseothricin resistance were selected and the transformation procedure was repeated. Several clones with integration into the correct locus were obtained. To check the histone H4 copy number, quantitative PCR was performed on genomic DNA isolated from all strains. About 7.5ng DNA was used for each reaction. *RIP1* was chosen as a reference gene. Copy number was calculated relative to the wild type, which has 4 copies of histone H4. Even though colony PCR indicated integration of the knock-out cassette into the right locus, leaving only one histone H4 copy, qPCR indicated that in all tested strains there were still 2 remaining copies of histone H4 (Figure 41). While the transformation was repeated several times, a strain with only one copy of *HHF1* and no copy of *HHF22* left was not obtained.

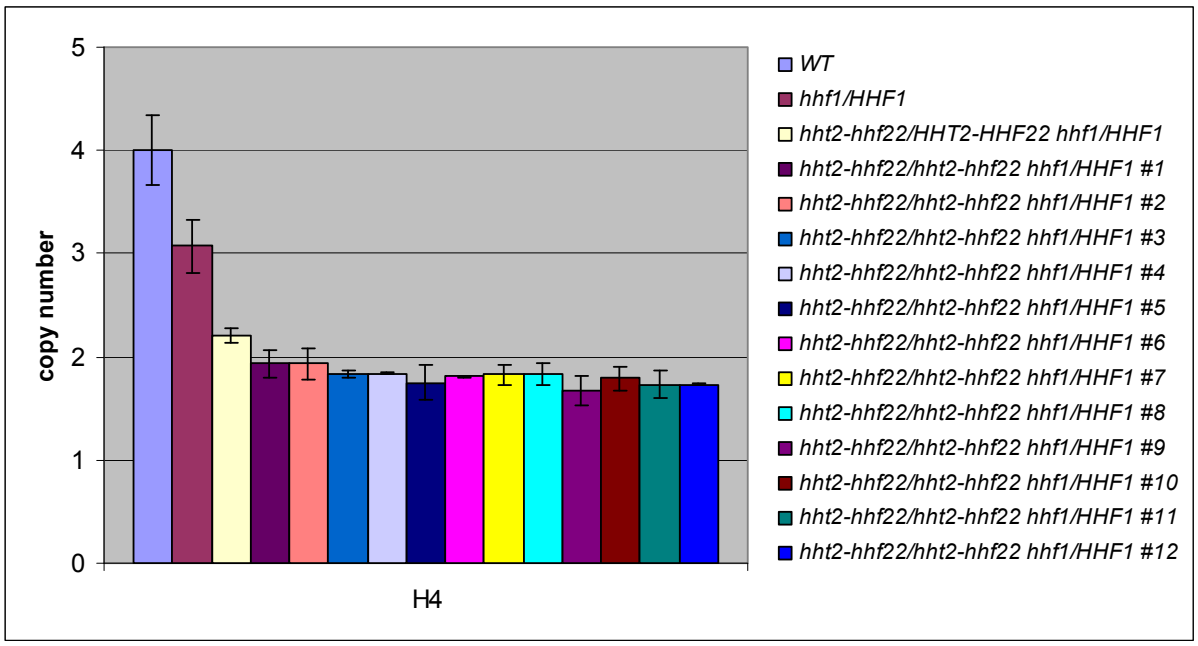


**Figure 41: Histone H4 copy number of *HHT2-HHF22* knock-outs.** qPCR was performed with 7.5ng genomic DNA per reaction and *RIP1* as reference gene. Signals were normalized to the reference gene and to the WT signal.

### 3.4.2. Mimicking Histone H4 K5 and K12 Acetylation in a *hat1*Δ/Δ Background

Hat1-deficient cells show elongated cell morphologies and are hypersensitive to genotoxic agents (Michael Tscherner, unpublished data). Since Hat1 acetylates histone H4K5 and H4K12, we wanted to see if mutating these residues to glutamate mimicking the acetylated state can reverse the phenotype.

First, one copy of *HHF1* was deleted in a *hat1*Δ/Δ strain using the knock-out cassette described above (linearized pSFS3b-HHF1urdr). Deletion of *HHF1* was verified by colony PCR. The *NAT1* marker was flipped out by incubating cells overnight in YP+2% maltose and selecting colonies that had lost their nourseothricin resistance. Linearized pSFS3b-CaHHF1 K12Q was transformed into this strain by electroporation to introduce the *HHF1* variant carrying the K12Q mutation. As a control, the wild type *HHF1* was reintegrated as well. Integration at the correct genomic locus was verified by colony PCR. To ensure the strain was carrying the mutation, *HHF1* was PCR-amplified and sequenced.

Colonies and cellular morphologies of the H4K12Q strain were inspected (Figure 42). Colonies showed a wrinkled morphology indicating filamentous growth. This was confirmed by inspection of single cells. Integration of one K12Q mutated version of *HHF1* did not change the phenotype of the *hat1*Δ/Δ strain.

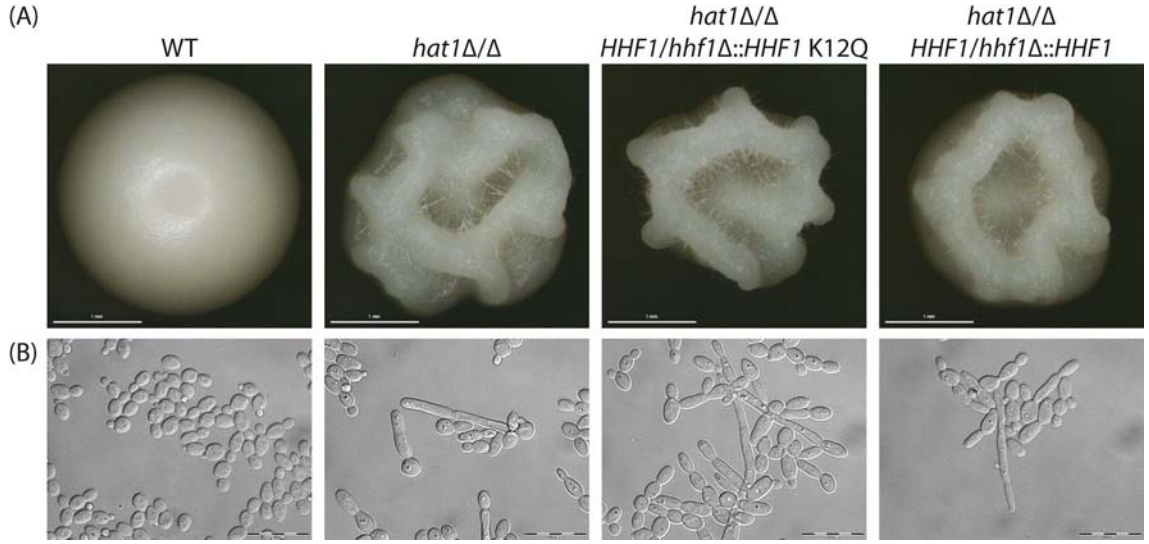


**Figure 42: Morphology of *hat1*Δ/Δ strains with H4K12Q.** (A) Cells were plated on YPD and incubated at 30°C for 3 days. (B) Cells in logarithmic phase grown in YPD at 30°C.

To see if the H4K12Q mutation had any effect on the sensitivity to genotoxic agents, the strains were spotted onto MMS-containing YPD plates. The *HHF1* K12Q strain showed the same sensitivity to MMS as the *hat1*Δ/Δ background strain (data not shown).

Since Hat1 can also acetylate H4K5, primers with one point mutation changing lysine 5 to glutamine were designed. pSFS3b-CaHHF1-Rev and pSFS3b-CaHHF1 K12Q were PCR-amplified using these primers (HHF1 K5Q_fwd + HHF1 K5Q_rev). After the PCR, the parental plasmid was digested with DpnI. The plasmids were then transformed into competent DH5α cells. The resulting plasmids were named pSFS3b-CaHHF1 K5Q and pSFS3b-CaHHF1 K5Q K12Q and were sequenced to ensure they were carrying the correct mutations. The plasmids were linearized with PvuII and transformed by electroporation into the *hat1*Δ/Δ *hhf1*Δ/*HHF1* strain. Integration at the correct genomic locus was verified by colony PCR. The cassette did not integrate at the knock-out allele but instead, replaced the wild type allele. Since it was planed to reduce the number of wild type H4 copies anyway, these strains were used for further experiments. To ensure the strains were carrying the mutations, *HHF1* was PCR-amplified and sequenced.

Colony and cell morphologies of the H4K5QK12Q strains were further investigated (Figure 43). The wrinkled colony morphology indicated filamentous growth. This was confirmed by inspection of single cells. Having one mutated histone H4 copy did not change the phenotype when compared to the *hat1*Δ/Δ background strain.

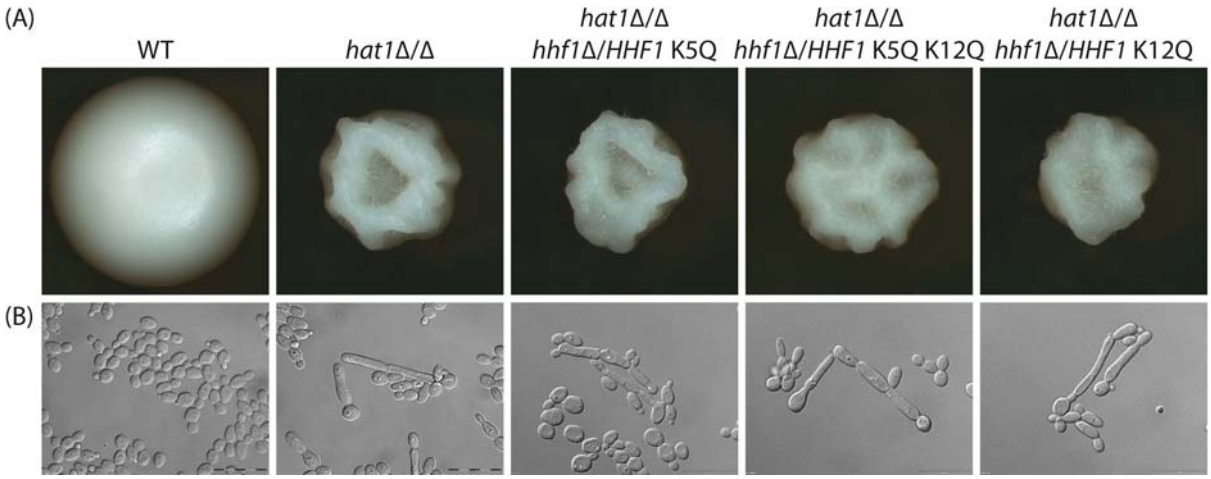


**Figure 43: Morphology of *hat1*Δ/Δ strains with mutated H4.** (A) Cells were plated on YPD and incubated at 30°C for 3 days. (B) Cells in logarithmic phase grown in YPD at 30°C.

To see if mimicking histone H4 K5 or K12 acetylation has any effect on sensitivity to genotoxic agents, the strains were spotted on MMS-containing YPD plates. All strains showed the same sensitivities to MMS as the *hat1*Δ/Δ background strain (Figure 44).

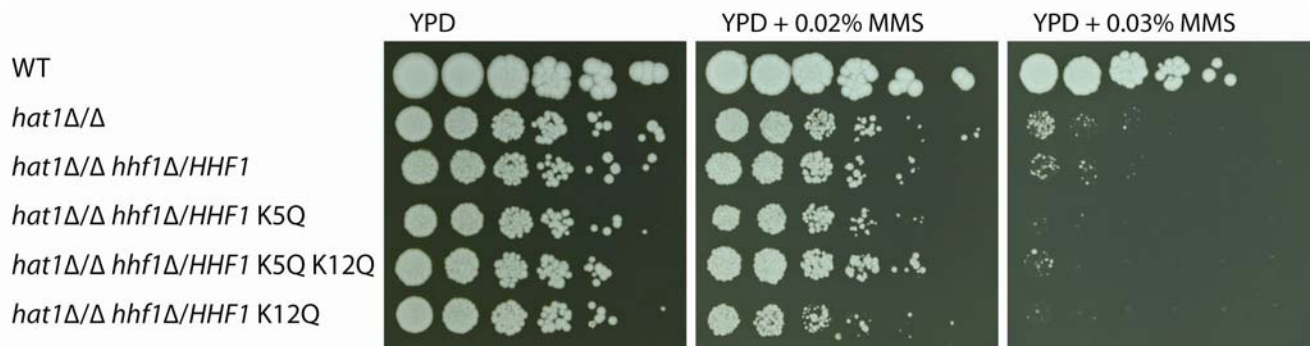


**Figure 44: Sensitivity of *hat1*Δ/Δ strains with mutated H4 to MMS.** Cells were spotted in serial dilutions (1:5) on YPD plates containing 0.02% or 0.03% methyl methane sulfonate (MMS) and incubated at 30°C for 3 days.

# 4. Discussion

## 4.1. α-Hat1 and α-Hat2 Antibodies

Polyclonal antibodies against *Ca*Hat1 and *Ca*Hat2 were raised to be used in immunoblotting and immunoprecipitation experiments. Functional antibodies against both proteins could be obtained. However, only the α-Hat2 antibodies could be used successfully to precipitate their target protein in immunoprecipitation experiments.

Antibodies can be a useful tool in the characterization of protein function. They allow for determination of protein levels via immunoblotting or can be used in immunoprecipitation experiments to identify binding partners.
To raise antibodies against *Ca*Hat1 and *Ca*Hat2, the N-terminal regions of these proteins were expressed as GST-fusion proteins and used as antigen for immunization of rabbits. Unfortunately, both initial GST-fusion proteins were insoluble. Therefore, we fused other antigenic regions consisting of the C-terminal parts of Hat1 and Hat2 to GST. Since these fusion proteins were soluble, the new antigens were then purified and used to immunize rabbits.
The antibodies raised against Hat2 work very well and can be used without further purification in dilutions up to 1:4000 in Western blot analysis. The Hat1 antiserum recognizes Hat1 as well as another protein of similar mobility as Hat1. To obtain specific α-Hat1 antibodies, the purification of the antiserum became necessary. Affinity purification was first tested using the 4$^{th}$ bleed. Pure α-Hat1 antibodies were obtained. Since the 4$^{th}$ bleed was only a test bleed during the immunization, only a limited amount of antiserum was available for purification. Therefore, the 6$^{th}$ bleed, of which larger amounts of antiserum were present, was used for purification. However, even though functional Hat1-antibodies were present in the 6$^{th}$ bleed, the affinity purification failed to yield pure α-Hat1 antibodies. Even after an additional purification step of IgG precipitation, no pure α-Hat1 antibodies were obtained. It may be that the cross-reacting protein of the same mass as Hat1 is recognized by IgG antibodies, and was therefore not removed during the IgG purification. Thus, the affinity purification was successful for the 4$^{th}$ bleed but not for the 6$^{th}$ bleed, most likely because the affinity of the cross-reacting antibody increased between the 4$^{th}$ and 6$^{th}$ bleed and could therefore no longer be removed during the purification steps.

The interaction of Hat1 and Hat2 was previously demonstrated by immunoprecipitation using tagged versions of the proteins (Michael Tscherner, unpublished data). Notably, these results were not reproduced using the polyclonal α-Hat1 and α-Hat2 antibodies.

Immunoprecipitation of Hat2 was successful, but Hat1 was not coprecipitating. One reason why Hat1 could not be coprecipitated with Hat2, may be that the epitope recognized by the α-Hat2 antibodies lies within the region that binds to Hat1. In this scenario, antibody binding would block the interaction of Hat1 with Hat2 and therefore prevent coprecipitation.
Unfortunately, the immunoprecipitation of Hat1 did not work. Even using very low stringency conditions Hat1 failed to precipitate. The antibodies work fine in Western blot analysis but are not useful in immunoprecipitation experiments. Thus, it is possible that the affinity of the antibodies is too low to perform immunoprecipitations or that the antibodies lost their functionality during the purification procedure. Furthermore, since the antibodies work fine in Western blot experiments but are unable to precipitate the native protein, the epitope might not be accessible in the extracts with native Hat1.

## 4.2. Intracellular Localization of Hat2

Hat1 is classified as type B histone acetyltransferase, which is defined as a cytoplasmic enzyme acetylating free but not nucleosomal histones. Thus, one would expect to find the Hat1/Hat2 complex primarily in the cytoplasm. However, the Hat1/Hat2 complex has been detected in the nucleus in several species (Imhof and Wolffe, 1999; Lusser *et al.*, 1999; Poveda *et al.*, 2004; Verreault *et al.*, 1998). In *Saccharomyces cerevisiae*, the nuclear localization of Hat1 depends on Hat2 but the localization of Hat2 is independent of Hat1 (Poveda *et al.*, 2004). Interestingly, in *Candida albicans* this scenario is reversed. While Hat1 is localized in the nucleus independently of the presence of Hat2 (Michael Tscherner, unpublished data), Hat2 requires Hat1 for its nuclear localization.
The Hat1/Hat2 complex is involved in DNA damage repair, as cells lacking either one of the components are hypersensitive to DNA-damaging agents (Michael Tscherner, unpublished data). We used our Hat2-YFP tagged strain to investigate the localization of Hat2 after inducing DNA-damage. In cells treated with the DNA-alkylating agent methyl methane sulfonate (MMS), the intensity of the nuclear Hat2-YFP signal was dramatically increased, mirroring the results obtained with a Hat1-GFP strain (Michael Tscherner, unpublished data). It is, however, not clear how this is achieved, since mRNA levels of *HAT1* and *HAT2* after MMS treatment remain unchanged (Michael Tscherner, unpublished data). It is possible that cytoplasmatic Hat1/Hat2, previously dispersed throughout the cell, is imported into the nucleus, becoming more concentrated and therefore detectable by microscopy. However, it is questionable if an increase of this magnitude could be caused solely by this mechanism, since no Hat2-YFP is detectable by microscopy in the cytoplasm. Another way of increasing the amount of Hat2-YFP, even though not as quickly, could be increased translation of its mRNA.

To investigate Hat1 and Hat2 localization within a single cell it would have been useful to construct a strain in which both proteins are labeled with different fluorescent proteins. Unfortunately, I was not able to tag Hat2 with a red fluorescent protein. Even though a protein of the expected molecular mass of Hat2-RFP could be detected by Western blotting, RFP signals were not detectable when cells were examined in the fluorescence microscope. The same result was obtained with another RFP variant, mCherry. It is possible that in both cases signals were too weak to be detectable. Another explanation would be that the fluorescent proteins were not folded correctly in the Hat2-RFP fusion protein and therefore did not fluoresce. Thus, the functionality of RFP in *Candida albicans* was tested by transforming cells with the RFP coding sequence under a constitutive active promoter. The expression level of RFP was very low and no signal could be detected in the fluorescence microscope. It seems that the RFP is not functional in *Candida albicans*.

## 4.3. Histone Acetyltransferase Rtt109 and Chaperone Asf1

Rtt109 is the only histone acetyltransferase responsible for histone H3K56 acetylation, a modification that is important for DNA damage repair in *Saccharomyces cerevisiae* (Fillingham *et al.*, 2008). Deletion of *RTT109* in *Candida albicans* leads to constitutive filamentous growth, probably induced by impaired DNA damage repair due to the lack of H3K56ac. Furthermore, the *rtt109*Δ/Δ strain is hypersensitive to DNA-damaging agents. Cells lacking the histone acetyltransferase Hat1 are also sensitive to these substances, albeit to a different extent. Sensitivity to the DNA-alkylating agent MMS is strongly increased in the *rtt109*Δ/Δ strain compared to the *hat1*Δ/Δ strain, indicating that acetylation of histone H3 by Rtt109 is more important for DNA damage repair after double strand breaks than histone H4 acetylation by Hat1. The *hat1*Δ/Δ *rtt109*Δ/Δ double knock-out shows similar sensitivities to MMS as the *rtt109*Δ/Δ single knock-out.

Sensitivity to NQO, which typically induces DNA lesions corrected by nucleotide excision repair, is about the same in the *hat1*Δ/Δ strain and the *rtt109*Δ/Δ strain. By contrast, the *hat1*Δ/Δ *rtt109*Δ/Δ double knock-out seems to be more sensitive to NQO. Thus, both proteins may contribute to the repair of these lesions in parallel pathways.

During the course of this work, two publications appeared, describing the phenotype of *rtt109* deletion in *Candida albicans* (Lopes da Rosa *et al.*, 2010; Wurtele *et al.*, 2010). The published data were consistent with our results concerning the filamentation phenotype and DNA damage sensitivity. Furthermore, it was shown that Rtt109 is indeed responsible for H3K56 acetylation in *Candida albicans*. In addition, cells lacking Rtt109 show attenuated virulence in a mouse model of systemic infection (Lopes da Rosa *et al.*, 2010; Wurtele *et al.*, 2010).

Interestingly, the *hat1*Δ/Δ strain exhibits increased resistance to $H_2O_2$, whereas the *rtt109*Δ/Δ strain remains sensitive. In cells lacking Hat1, oxidative stress response genes such as *CAT1* are already upregulated, even in the absence of reactive oxygen species (ROS) (Michael Tscherner, unpublished data), explaining why these cells are able to detoxify high concentrations of $H_2O_2$. The *hat1*Δ/Δ *rtt109*Δ/Δ double knock-out strain behaves like the *hat1*Δ/Δ single knock-out strain, since it shows the same increase in $H_2O_2$ resistance. Thus, Hat1 may be in addition involved in a pathway other than the DNA damage repair-associated histone deposition. The latter influences the expression of oxidative stress response genes and is completely independent of Rtt109.

Asf1 is a histone chaperone interacting with Rtt109. Interestingly, Asf1 is required for the acetylation of H3K56 by Rtt109 in *Saccharomyces cerevisiae* (Fillingham *et al.*, 2008). In a *Candida albicans* insertional mutagenesis screen, *ASF1* was one of several genes from which no homozygous mutants could be obtained, indicating that it may be essential (Davis *et al.*, 2002). We tried to delete *ASF1* in a targeted approach, but were also unable to construct a homozygous *asf1*Δ/Δ strain. Therefore, *ASF1* was placed under a conditional promoter. Unfortunately, deletion of the remaining *ASF1* wild type allele was not possible. It is possible that the endogenous *ASF1* promoter is stronger than the inducible *MET3* promoter used here. Therefore, cells with only one copy of *ASF1* under the control of the *MET3* promoter might not express sufficient amounts of Asf1 to be viable.

## 4.4. Mimicking Histone H4 Acetylation

As in all other organisms investigated so far, the *Candida albicans* histone acetyltransferase Hat1 acetylates histone H4 on positions 5 and 12 (Michael Tscherner, unpublished data). In fact, the *Candida albicans* histone H4 N-terminus contains two additional amino acids when compared to *Saccharomyces cerevisiae*. Therefore, the lysine residues 5 and 12 are actually at position 7 and 14, respectively. Nevertheless, since these residues are based on the sequence homology equivalent to K5 and K12 in *Saccharomyces cerevisiae* and many other organisms the same description was used in this thesis for *Candida albicans* as well. To study the effect of lysine 5 and 12 acetylation on chromatin assembly and DNA damage repair, these residues were mutated to mimic the acetylated or unacetylated state. To reduce the number of wild type histone H4, 3 out of the 4 histone H4 genes were deleted before introducing a mutated histone H4 variant gene. As already published (Zacchi *et al.*, 2010), the strain harboring only one copy of histone H4 grows considerably slower than strains with 2, 3 or 4 copies. Furthermore, it shows increased sensitivity to Caspofungin and MMS, similar to the *hat1*Δ/Δ strain. The single

copy H4 strain exhibits additional similarities to the *hat1*Δ/Δ strain. For example, both strains are more resistant to $H_2O_2$. As mentioned before, oxidative stress response genes are upregulated in the *hat1*Δ/Δ strain. Whether $H_2O_2$ resistance in the single copy H4 strain is conferred by the same mechanism has to be determined. Furthermore, both strains show increased tolerance to Itraconazole and Voriconazole. However, resistance in the single copy H4 strain is only slightly elevated, whereas it is considerably stronger in the *hat1*Δ/Δ strain. The elevated resistance in this strain may be due to upregulation of several transporters, including the Mdr1 permease (Michael Tscherner, unpublished data). Possibly, a similar mechanism is active in the single copy H4 strain.

Unfortunately, the genomic reintegration of one histone H4 gene into the single copy H4 strain failed to restore the phenotype of the dual copy H4 strain concerning its growth defect. It is possible that the strain acquired some additional mutations during the transformation procedure. Another explanation could be that a low histone density due to the low histone dosage induces epigenetic changes that would not revert by reintegration of one histone H4 gene.

To rule out that additional mutations were causing the problems, the construction of the single copy strain was repeated. This time one copy of histone H4 and one copy of histone H3 were deleted simultaneously to avoid dramatic changes in the histone H3 / H4 ratio. A strain with only two histone H4 copies was constructed this way without any problems. However, deletion of the third histone H4 copy failed. Even though colony PCR suggested positive clones, all tested strains had 2 copies of histone H4. Notably, alterations in histone dosage can lead to segmental or whole chromosomal trisomies (Zacchi *et al.*, 2010), which would explain why, even though colony PCR verified integration at the correct genomic locus, quantitative PCR indicated two remaining copies of histone H4.

Since Hat1 mediates histone H4K5 and H4K12 acetylation, we wanted to see if mimicking the acetylated state of these residues can rescue the phenotypes of a *hat1*Δ/Δ strain. Thus, mutated variants of histone H4 were introduced into the *hat1*Δ/Δ strain. Unfortunately, strains carrying *HHF1* K5Q, K12Q or K5Q K12Q show no differences when compared to the *hat1*Δ/Δ background strain with respects to cell morphology. All strains exhibit filamentous growth. Furthermore, sensitivity to MMS is not influenced by any of the tested histone H4 mutations. In these strains, one mutated and two wild type histone H4 versions are present. Thus, only one out of three histone H4 copies carrying the mutation is not enough to reverse the *hat1*Δ/Δ phenotype. Thus, further reducing the histone H4 copy number in these strains may help to rescue the *hat1*Δ/Δ phenotype. Furthermore, the acetylation of histone H4 by Hat1 may only be a transient modification, which is rapidly removed after incorporation into chromatin. The mutation introduced to mimic acetylation is

a permanent mark that cannot be removed and might therefore cause additional pleiotropic effects. Furthermore, the absence of acetylated H4K5 and K12 may not be the only explanation for the defects observed in the *hat1*Δ/Δ strain. Hat1 may play a role in another pathway that cannot be rescued by mimicking acetylation of histone H4 lysine residues.

In summary, during this thesis antibodies against both Hat and Hat2 were raised successfully and the nuclear localization of Hat2 was elucidated by epitope tagging. Furthermore, the function of the histone acetyltransferase Rtt109 was investigated and it was shown that cells lacking Rtt109 exhibit a similar phenotype to those lacking Hat1. Additionally, to further investigate the role of histone acetylation by Hat1, strains mimicking these modifications were constructed. However, they could not rescue the *hat1*Δ/Δ phenotype.

# 5. References

Ahmad, A., Takami, Y., and Nakayama, T. (2000). Distinct regions of the chicken p46 polypeptide are required for its *in vitro* interaction with histones H2B and H4 and histone acetyltransferase-1. Biochem Biophys Res Commun *279*, 95-102.

Ai, X., and Parthun, M.R. (2004). The nuclear Hat1p/Hat2p complex: a molecular link between type B histone acetyltransferases and chromatin assembly. Mol Cell *14*, 195-205.

Annunziato, A.T., and Hansen, J.C. (2000). Role of histone acetylation in the assembly and modulation of chromatin structures. Gene Expr *9*, 37-61.

Bachewich, C., Nantel, A., and Whiteway, M. (2005). Cell cycle arrest during S or M phase generates polarized growth via distinct signals in *Candida albicans*. Mol Microbiol *57*, 942-959.

Bennett, R.J., and Johnson, A.D. (2003). Completion of a parasexual cycle in *Candida albicans* by induced chromosome loss in tetraploid strains. EMBO J *22*, 2505-2515.

Benson, L.J., Phillips, J.A., Gu, Y., Parthun, M.R., Hoffman, C.S., and Annunziato, A.T. (2007). Properties of the type B histone acetyltransferase Hat1: H4 tail interaction, site preference, and involvement in DNA repair. J Biol Chem *282*, 836-842.

Berman, J., and Sudbery, P.E. (2002). *Candida albicans*: a molecular revolution built on lessons from budding yeast. Nat Rev Genet *3*, 918-930.

Bienko, M., Green, C.M., Crosetto, N., Rudolf, F., Zapart, G., Coull, B., Kannouche, P., Wider, G., Peter, M., Lehmann, A.R.*, et al.* (2005). Ubiquitin-binding domains in Y-family polymerases regulate translesion synthesis. Science *310*, 1821-1824.

Biswas, S., Van Dijck, P., and Datta, A. (2007). Environmental sensing and signal transduction pathways regulating morphopathogenic determinants of *Candida albicans*. Microbiol Mol Biol Rev *71*, 348-376.

Brownell, J.E., and Allis, C.D. (1996). Special HATs for special occasions: linking histone acetylation to chromatin assembly and gene activation. Curr Opin Genet Dev *6*, 176-184.

Campos, E.I., Fillingham, J., Li, G., Zheng, H., Voigt, P., Kuo, W.H., Seepany, H., Gao, Z., Day, L.A., Greenblatt, J.F., and Reinberg, D. (2010). The program for processing newly synthesized histones H3.1 and H4. Nat Struct Mol Biol *17*, 1343-1351.

Care, R.S., Trevethick, J., Binley, K.M., and Sudbery, P.E. (1999). The *MET3* promoter: a new tool for *Candida albicans* molecular genetics. Mol Microbiol *34*, 792-798.

Castillo, A.G., Mellone, B.G., Partridge, J.F., Richardson, W., Hamilton, G.L., Allshire, R.C., and Pidoux, A.L. (2007). Plasticity of fission yeast CENP-A chromatin driven by relative levels of histone H3 and H4. PLoS Genet *3*, e121.

Celic, I., Masumoto, H., Griffith, W.P., Meluh, P., Cotter, R.J., Boeke, J.D., and Verreault, A. (2006). The sirtuins hst3 and Hst4p preserve genome integrity by controlling histone h3 lysine 56 deacetylation. Curr Biol *16*, 1280-1289.

Chang, B., Chen, Y., Zhao, Y., and Bruick, R.K. (2007). JMJD6 is a histone arginine demethylase. Science *318*, 444-447.

Chang, L., Loranger, S.S., Mizzen, C., Ernst, S.G., Allis, C.D., and Annunziato, A.T. (1997). Histones in transit: cytosolic histone complexes and diacetylation of H4 during nucleosome assembly in human cells. Biochemistry *36*, 469-480.

Chau, V., Tobias, J.W., Bachmair, A., Marriott, D., Ecker, D.J., Gonda, D.K., and Varshavsky, A. (1989). A multiubiquitin chain is confined to specific lysine in a targeted short-lived protein. Science *243*, 1576-1583.

Chen, C.C., Carson, J.J., Feser, J., Tamburini, B., Zabaronick, S., Linger, J., and Tyler, J.K. (2008). Acetylated lysine 56 on histone H3 drives chromatin assembly after repair and signals for the completion of repair. Cell *134*, 231-243.

Clark-Adams, C.D., Norris, D., Osley, M.A., Fassler, J.S., and Winston, F. (1988). Changes in histone gene dosage alter transcription in yeast. Genes Dev *2*, 150-159.

Cuthbert, G.L., Daujat, S., Snowden, A.W., Erdjument-Bromage, H., Hagiwara, T., Yamada, M., Schneider, R., Gregory, P.D., Tempst, P., Bannister, A.J., and Kouzarides, T. (2004). Histone deimination antagonizes arginine methylation. Cell *118*, 545-553.

Davis, D.A., Bruno, V.M., Loza, L., Filler, S.G., and Mitchell, A.P. (2002). *Candida albicans* Mds3p, a conserved regulator of pH responses and virulence identified through insertional mutagenesis. Genetics *162*, 1573-1581.

Driscoll, R., Hudson, A., and Jackson, S.P. (2007). Yeast Rtt109 promotes genome stability by acetylating histone H3 on lysine 56. Science *315*, 649-652.

Eberharter, A., Lechner, T., Goralik-Schramel, M., and Loidl, P. (1996). Purification and characterization of the cytoplasmic histone acetyltransferase B of maize embryos. FEBS Lett *386*, 75-81.

Ernst, J.F. (2000). Transcription factors in *Candida albicans* - environmental control of morphogenesis. Microbiology *146 ( Pt 8)*, 1763-1774.

Escargueil, A.E., Soares, D.G., Salvador, M., Larsen, A.K., and Henriques, J.A. (2008). What histone code for DNA repair? Mutat Res *658*, 259-270.

Fan, Y., Nikitina, T., Morin-Kensicki, E.M., Zhao, J., Magnuson, T.R., Woodcock, C.L., and Skoultchi, A.I. (2003). H1 linker histones are essential for mouse development and affect nucleosome spacing *in vivo*. Mol Cell Biol *23*, 4559-4572.

Felsenfeld, G., and Groudine, M. (2003). Controlling the double helix. Nature *421*, 448-453.

Fidel, P.L., Jr. (2007). History and update on host defense against vaginal candidiasis. Am J Reprod Immunol *57*, 2-12.

Fillingham, J., Recht, J., Silva, A.C., Suter, B., Emili, A., Stagljar, I., Krogan, N.J., Allis, C.D., Keogh, M.C., and Greenblatt, J.F. (2008). Chaperone control of the activity and specificity of the histone H3 acetyltransferase Rtt109. Mol Cell Biol *28*, 4342-4353.

Garcea, R.L., and Alberts, B.M. (1980). Comparative studies of histone acetylation in nucleosomes, nuclei, and intact cells. Evidence for special factors which modify acetylase action. J Biol Chem *255*, 11454-11463.

Ge, Z., Wang, H., and Parthun, M.R. (2011). Nuclear Hat1p complex (NuB4) components participate in DNA repair-linked chromatin reassembly. J Biol Chem.

Geetha, T., Jiang, J., and Wooten, M.W. (2005). Lysine 63 polyubiquitination of the nerve growth factor receptor TrkA directs internalization and signaling. Mol Cell *20*, 301-312.

Gerami-Nejad, M., Dulmage, K., and Berman, J. (2009). Additional cassettes for epitope and fluorescent fusion proteins in *Candida albicans*. Yeast *26*, 399-406.

Gow, N.A., Brown, A.J., and Odds, F.C. (2002). Fungal morphogenesis and host invasion. Curr Opin Microbiol *5*, 366-371.

Grunstein, M. (1990). Histone function in transcription. Annu Rev Cell Biol *6*, 643-678.

Gupta-Rossi, N., Six, E., LeBail, O., Logeat, F., Chastagner, P., Olry, A., Israel, A., and Brou, C. (2004). Monoubiquitination and endocytosis direct gamma-secretase cleavage of activated Notch receptor. J Cell Biol *166*, 73-83.

Han, J., Zhou, H., Horazdovsky, B., Zhang, K., Xu, R.M., and Zhang, Z. (2007). Rtt109 acetylates histone H3 lysine 56 and functions in DNA replication. Science *315*, 653-655.

Happel, N., and Doenecke, D. (2009). Histone H1 and its isoforms: contribution to chromatin structure and function. Gene *431*, 1-12.

He, H., and Lehming, N. (2003). Global effects of histone modifications. Brief Funct Genomic Proteomic *2*, 234-243.

Henikoff, S., and Shilatifard, A. (2011). Histone modification: cause or cog? Trends Genet.

Hicke, L. (2001). Protein regulation by monoubiquitin. Nat Rev Mol Cell Biol *2*, 195-201.

Hicke, L., and Riezman, H. (1996). Ubiquitination of a yeast plasma membrane receptor signals its ligand-stimulated endocytosis. Cell *84*, 277-287.

Higashi, M., Inoue, S., and Ito, T. (2010). Core histone H2A ubiquitylation and transcriptional regulation. Exp Cell Res *316*, 2707-2712.

Hull, C.M., Raisner, R.M., and Johnson, A.D. (2000). Evidence for mating of the "asexual" yeast *Candida albicans* in a mammalian host. Science *289*, 307-310.

Imhof, A., and Wolffe, A.P. (1999). Purification and properties of the *Xenopus* Hat1 acetyltransferase: association with the 14-3-3 proteins in the oocyte nucleus. Biochemistry *38*, 13085-13093.

Ito, T. (2007). Role of histone modification in chromatin dynamics. J Biochem *141*, 609-614.

Jackson, V., Shires, A., Tanphaichitr, N., and Chalkley, R. (1976). Modifications to histones immediately after synthesis. J Mol Biol *104*, 471-483.

Jenuwein, T., and Allis, C.D. (2001). Translating the histone code. Science *293*, 1074-1080.

Johnson, E.S. (2004). Protein modification by SUMO. Annu Rev Biochem *73*, 355-382.

Kannouche, P.L., Wing, J., and Lehmann, A.R. (2004). Interaction of human DNA polymerase eta with monoubiquitinated PCNA: a possible mechanism for the polymerase switch in response to DNA damage. Mol Cell *14*, 491-500.

Kelly, T.J., Qin, S., Gottschling, D.E., and Parthun, M.R. (2000). Type B histone acetyltransferase Hat1p participates in telomeric silencing. Mol Cell Biol *20*, 7051-7058.

Kolling, R., and Hollenberg, C.P. (1994). The ABC-transporter Ste6 accumulates in the plasma membrane in a ubiquitinated form in endocytosis mutants. EMBO J *13*, 3261-3271.

Kouzarides, T. (2007). Chromatin modifications and their function. Cell *128*, 693-705.

Kuo, M.H., Brownell, J.E., Sobel, R.E., Ranalli, T.A., Cook, R.G., Edmondson, D.G., Roth, S.Y., and Allis, C.D. (1996). Transcription-linked acetylation by Gcn5p of histones H3 and H4 at specific lysines. Nature *383*, 269-272.

Kurdistani, S.K., and Grunstein, M. (2003). Histone acetylation and deacetylation in yeast. Nat Rev Mol Cell Biol *4*, 276-284.

Li, Q., Zhou, H., Wurtele, H., Davies, B., Horazdovsky, B., Verreault, A., and Zhang, Z. (2008). Acetylation of histone H3 lysine 56 regulates replication-coupled nucleosome assembly. Cell *134*, 244-255.

Liu, H. (2001). Transcriptional control of dimorphism in *Candida albicans*. Curr Opin Microbiol *4*, 728-735.

Lopes da Rosa, J., Boyartchuk, V.L., Zhu, L.J., and Kaufman, P.D. (2010). Histone acetyltransferase Rtt109 is required for *Candida albicans* pathogenesis. Proc Natl Acad Sci U S A *107*, 1594-1599.

Lu, X., Wontakal, S.N., Emelyanov, A.V., Morcillo, P., Konev, A.Y., Fyodorov, D.V., and Skoultchi, A.I. (2009). Linker histone H1 is essential for *Drosophila* development, the establishment of pericentric heterochromatin, and a normal polytene chromosome structure. Genes Dev *23*, 452-465.

Luger, K., Mader, A.W., Richmond, R.K., Sargent, D.F., and Richmond, T.J. (1997). Crystal structure of the nucleosome core particle at 2.8 A resolution. Nature *389*, 251-260.

Lusser, A., Eberharter, A., Loidl, A., Goralik-Schramel, M., Horngacher, M., Haas, H., and Loidl, P. (1999). Analysis of the histone acetyltransferase B complex of maize embryos. Nucleic Acids Res *27*, 4427-4435.

Ma, X.J., Wu, J., Altheim, B.A., Schultz, M.C., and Grunstein, M. (1998). Deposition-related sites K5/K12 in histone H4 are not required for nucleosome deposition in yeast. Proc Natl Acad Sci U S A *95*, 6693-6698.

Magee, B.B., and Magee, P.T. (2000). Induction of mating in *Candida albicans* by construction of MTLa and MTLalpha strains. Science *289*, 310-313.

Masumoto, H., Hawke, D., Kobayashi, R., and Verreault, A. (2005). A role for cell-cycle-regulated histone H3 lysine 56 acetylation in the DNA damage response. Nature *436*, 294-298.

Messner, S., Altmeyer, M., Zhao, H., Pozivil, A., Roschitzki, B., Gehrig, P., Rutishauser, D., Huang, D., Caflisch, A., and Hottiger, M.O. (2010). PARP1 ADP-ribosylates lysine residues of the core histone tails. Nucleic Acids Res *38*, 6350-6362.

Millar, C.B., and Grunstein, M. (2006). Genome-wide patterns of histone modifications in yeast. Nat Rev Mol Cell Biol *7*, 657-666.

Mukhopadhyay, D., and Riezman, H. (2007). Proteasome-independent functions of ubiquitin in endocytosis and signaling. Science *315*, 201-205.

Nelson, C.J., Santos-Rosa, H., and Kouzarides, T. (2006). Proline isomerization of histone H3 regulates lysine methylation and gene expression. Cell *126*, 905-916.

Parthun, M.R. (2007). Hat1: the emerging cellular roles of a type B histone acetyltransferase. Oncogene *26*, 5319-5328.

Parthun, M.R., Widom, J., and Gottschling, D.E. (1996). The major cytoplasmic histone acetyltransferase in yeast: links to chromatin replication and histone metabolism. Cell *87*, 85-94.

Pfaffl, M.W. (2001). A new mathematical model for relative quantification in real-time RT-PCR. Nucleic Acids Res *29*, e45.

Pfaller, M.A., and Diekema, D.J. (2004). Rare and emerging opportunistic fungal pathogens: concern for resistance beyond *Candida albicans* and *Aspergillus fumigatus*. J Clin Microbiol *42*, 4419-4431.

Pfaller, M.A., and Diekema, D.J. (2007). Epidemiology of invasive candidiasis: a persistent public health problem. Clin Microbiol Rev *20*, 133-163.

Poveda, A., Pamblanco, M., Tafrov, S., Tordera, V., Sternglanz, R., and Sendra, R. (2004). Hif1 Is a Component of Yeast Histone Acetyltransferase B, a Complex Mainly Localized in the Nucleus. Journal of Biological Chemistry *279*, 16033-16043.

Qin, S., and Parthun, M.R. (2002). Histone H3 and the histone acetyltransferase Hat1p contribute to DNA double-strand break repair. Mol Cell Biol *22*, 8353-8365.

Qin, S., and Parthun, M.R. (2006). Recruitment of the type B histone acetyltransferase Hat1p to chromatin is linked to DNA double-strand breaks. Mol Cell Biol *26*, 3649-3658.

Reuss, O., Vik, A., Kolter, R., and Morschhauser, J. (2004). The SAT1 flipper, an optimized tool for gene disruption in *Candida albicans*. Gene *341*, 119-127.

Ruiz-Garcia, A.B., Sendra, R., Galiana, M., Pamblanco, M., Perez-Ortin, J.E., and Tordera, V. (1998). HAT1 and HAT2 proteins are components of a yeast nuclear histone acetyltransferase enzyme specific for free histone H4. J Biol Chem *273*, 12599-12605.

Sandman, K., Pereira, S.L., and Reeve, J.N. (1998). Diversity of prokaryotic chromosomal proteins and the origin of the nucleosome. Cell Mol Life Sci *54*, 1350-1364.

Shepherd, M.G., Yin, C.Y., Ram, S.P., and Sullivan, P.A. (1980). Germ tube induction in *Candida albicans*. Can J Microbiol *26*, 21-26.

Shi, Q.M., Wang, Y.M., Zheng, X.D., Lee, R.T., and Wang, Y. (2007). Critical role of DNA checkpoints in mediating genotoxic-stress-induced filamentous growth in *Candida albicans*. Mol Biol Cell *18*, 815-826.

Shi, Y., Lan, F., Matson, C., Mulligan, P., Whetstine, J.R., Cole, P.A., and Casero, R.A. (2004). Histone demethylation mediated by the nuclear amine oxidase homolog LSD1. Cell *119*, 941-953.

Shi, Y., and Whetstine, J.R. (2007). Dynamic regulation of histone lysine methylation by demethylases. Mol Cell *25*, 1-14.

Sobel, R.E., Cook, R.G., Perry, C.A., Annunziato, A.T., and Allis, C.D. (1995). Conservation of deposition-related acetylation sites in newly synthesized histones H3 and H4. Proc Natl Acad Sci U S A *92*, 1237-1241.

Staib, P., and Morschhauser, J. (2007). Chlamydospore formation in *Candida albicans* and *Candida dubliniensis*--an enigmatic developmental programme. Mycoses *50*, 1-12.

Sterner, D.E., and Berger, S.L. (2000). Acetylation of histones and transcription-related factors. Microbiol Mol Biol Rev *64*, 435-459.

Strahl, B.D., and Allis, C.D. (2000). The language of covalent histone modifications. Nature *403*, 41-45.

Sudbery, P., Gow, N., and Berman, J. (2004). The distinct morphogenic states of *Candida albicans*. Trends Microbiol *12*, 317-324.

Thrower, J.S., Hoffman, L., Rechsteiner, M., and Pickart, C.M. (2000). Recognition of the polyubiquitin proteolytic signal. EMBO J *19*, 94-102.

Tong, A.H., and Boone, C. (2006). Synthetic genetic array analysis in *Saccharomyces cerevisiae*. Methods Mol Biol *313*, 171-192.

Tsubota, T., Berndsen, C.E., Erkmann, J.A., Smith, C.L., Yang, L., Freitas, M.A., Denu, J.M., and Kaufman, P.D. (2007). Histone H3-K56 acetylation is catalyzed by histone chaperone-dependent complexes. Mol Cell *25*, 703-712.

Umehara, T., Chimura, T., Ichikawa, N., and Horikoshi, M. (2002). Polyanionic stretch-deleted histone chaperone cia1/Asf1p is functional both *in vivo* and *in vitro*. Genes Cells *7*, 59-73.

Verreault, A., Kaufman, P.D., Kobayashi, R., and Stillman, B. (1998). Nucleosomal DNA regulates the core-histone-binding subunit of the human Hat1 acetyltransferase. Curr Biol *8*, 96-108.

Whiteway, M., and Bachewich, C. (2007). Morphogenesis in *Candida albicans*. Annu Rev Microbiol *61*, 529-553.

Woodcock, C.L., and Ghosh, R.P. (2010). Chromatin higher-order structure and dynamics. Cold Spring Harb Perspect Biol *2*, a000596.

Wurtele, H., Tsao, S., Lepine, G., Mullick, A., Tremblay, J., Drogaris, P., Lee, E.H., Thibault, P., Verreault, A., and Raymond, M. (2010). Modulation of histone H3 lysine 56 acetylation as an antifungal therapeutic strategy. Nat Med *16*, 774-780.

Xhemalce, B., Miller, K.M., Driscoll, R., Masumoto, H., Jackson, S.P., Kouzarides, T., Verreault, A., and Arcangioli, B. (2007). Regulation of histone H3 lysine 56 acetylation in *Schizosaccharomyces pombe*. J Biol Chem *282*, 15040-15047.

Ye, J., Ai, X., Eugeni, E.E., Zhang, L., Carpenter, L.R., Jelinek, M.A., Freitas, M.A., and Parthun, M.R. (2005). Histone H4 lysine 91 acetylation a core domain modification associated with chromatin assembly. Mol Cell *18*, 123-130.

Zacchi, L.F., Selmecki, A.M., Berman, J., and Davis, D.A. (2010). Low dosage of histone H4 leads to growth defects and morphological changes in *Candida albicans*. PLoS One *5*, e10629.

# Danke

Da mein Studium nun zu Ende geht, möchte ich mich hier bei all den Menschen bedanken, die mich in dieser Zeit unterstützt haben. Zuallererst bei meiner Familie, besonders bei meiner Mutter, die immer an mich geglaubt hat und auch bei meinem Vater, der meinen Abschluss leider nicht mehr miterleben kann.

Weiters möchte ich mich bei meinem Chef Karl Kuchler bedanken, dafür dass er mir einen Platz in seinem Labor gegeben hat und für seine Unterstützung während meiner Diplomarbeit.

Ein großes Danke an alle KaKus, die für eine angenehme Arbeitsatmosphäre im Labor gesorgt haben. Ganz besonders an Michi, der meine Fragen immer geduldig beantwortet hat und mir bei meinen Experimenten weiter geholfen hat.

Abschließend möchte ich mich auch noch bei meinen Freunden bedanken, die mich durchs Studium begleitet haben und immer wieder für Abwechslung zwischen Prüfungen und Laboralltag gesorgt haben.

# Curriculum Vitae

## Personal Information


| | |
|---|---|
| Name: | Eva Stappler |
| E-mail: | eva.stappler@gmail.com |
| Date of Birth: | 15.09.1985 |
| Place of Birth: | Vienna, Austria |
| Citizenship: | Austria |


## Education

| | |
|---|---|
| since 12/2009 | Diploma Thesis at the University of Vienna, Group Kuchler, Department of Medical Biochemistry |
| 07 – 08/2009 | Practicum Molecular Medicine, Group Schneider, Department of Medical Biochemistry, University of Vienna<br>Topic: AADA (Arylacetamide Deacetylase) in Chicken |
| 02/2009 | Practicum Cellbiology, Group Hilberg, Boehringer Ingelheim, Vienna<br>Topic: Effect of Angiogenesis Inhibitors on Tumor Celllines |
| 01/2009 | Practicum Biochemistry, Group Skern, Department of Medical Biochemistry, University of Vienna<br>Topic: Specificity of the 2A Protease of Human Rhinoviruses |
| 11/2008 | Practicum Cellbiology, Group Propst, Department for Biochemistry and Cellbiology, University of Vienna<br>Topic: Regulation of the Cytoskeleton in Neurons |
| 01/2008 | Practicum Biochemistry, Group Brocard, Department for Biochemistry and Cellbiology, University of Vienna<br>Topic: Peroxisomal Proliferation |
| 2004 – 2011 | Studies of Molecular Biology at the University of Vienna |
| 1996 – 2004 | Secondary School, Realgymnasium GRG13 Wenzgasse, Vienna<br>Graduation with distinction |
| 1992 – 1996 | Elementary School, Rohrwassergasse, Vienna |

## Conferences:

| | |
|---|---|
| 09/2010 | Poster presentation at the 44. Wissenschaftliche Tagung der Deutschsprachigen Mykologischen Gesellschaft e. V. |
| 06/2010 | Poster presentation at the 6$^{th}$ PhD Symposium of the Young Scientist Association of the Medical University of Vienna |